Supplementary file

Article's Title;

A new intestinal model for analysis of drug absorption and interactions considering physiological translocation of contents

Authors;

Satoshi Asano, Aoi Yoshitomo, Shizuka Hozuki, Hiromi Sato, Yasuhiro Kazuki, and Akihiro Hisaka

Journal Title;

Drug Metabolism and Disposition

Supplementary text 1

Model construction in esophagus, stomach, enterocytes, lamina propria, portal vein, central and peripheral compartment

In ATOM, the concentration profiles of drugs in the tissues except for the intestine are expressed by the following differential equations S1-8.

Esophagus:

$$\frac{dC_{es}}{dt} = -k_{es}C_{es} \quad \text{(S1)}$$

Stomach:

$$\frac{dC_{sto}}{dt} = k_{es}C_{es}V_{es}/V_{sto} - k_{sto}C_{sto} \quad \text{(S2)}$$

where C_{es}, C_{sto}, k_{es}, k_{sto}, V_{es}, and V_{sto} represent drug concentrations, elimination rate constants, and volumes for the esophagus and stomach, respectively. At the initial condition, all doses and drinking water were located in the esophagus. It was assumed that the drinking water does not change the volumes in the esophagus and stomach and moves with the drug in accordance with equations S1 and S2. k_{es} and k_{sto} were used in both drugs and water simulations because their movements were assumed to be the same in the esophagus and stomach.

Enterocytes and lamina propria:

$$\frac{\partial C_{ent,z}}{\partial t} = PS_{a,in,z}\frac{f_{lum}C_{lum,z}V_{lum}}{V_{water}+V_{lum}} - \left(PS_{a,out,z} + CL_{ent,z} + PS_{b,out,z}\right)f_{ent}C_{ent,z} + f_{pro}PS_{b,in,z}C_{pro,z} \quad \text{(S3)}$$

$$\frac{\partial C_{pro,z}}{\partial t} = PS_{b,in,z}f_{ent}C_{ent,z} - \left(\frac{Q_{pro,z}}{f_b} + f_{pro}PS_{b,in,z}\right)C_{pro,z} \quad \text{(S4)}$$

where $C_{pro,z}$ is the drug concentration in the lamina propria, including blood capillaries at location z. $PS_{b,in,z}$ and $PS_{b,out,z}$ are the permeability clearance of reuptake from the lamina propria to enterocytes and of efflux from enterocytes to lamina propria, respectively, via the basolateral membrane at location z. $CL_{ent,z}$ represents intestinal intrinsic clearance in enterocytes at location z. $Q_{pro,z}$ represents blood flow of the blood capillaries in the lamina propria at location z. f_{ent} and f_{pro} represent the unbound fraction of the drug in the enterocytes and lamina propria, respectively. f_{pro} was assumed to be 1. In this study, f_{ent} values were tentatively assumed to be equal to f_b. However, it does not affect the availability as shown in a sensitivity analysis of f_{ent} values on availability of midazolam in a linear condition (Supplemental Fig. 5).

Portal vein and liver:

$$V_{pv}\frac{dC_{pv}}{dt} = \sum_z \frac{Q_{pro,z}}{f_b} C_{pro,z} - Q_{pv}C_{pv} \quad \text{(S5)}$$

$$V_{liver}\frac{dC_{liver}}{dt} = R_B(Q_{pv}C_{pv} + Q_{ha}C_p) - \left(\frac{R_B(Q_{pv}+Q_{ha})}{K_{p,liver}} + f_h CL_{int}\right)C_{liver} \quad \text{(S6)}$$

where C_p, C_{pv}, V_{pv}, and Q_{pv} represent plasma concentration in systemic circulation, plasma concentration, volume , and blood flow in the portal vein, respectively. C_{liver}, V_{liver}, and Q_{ha} represent drug concentration, volume, and blood flow in the liver and blood flow in the hepatic artery, respectively. R_B, $K_{p,liver}$, f_h, and CL_{int} represent the blood/plasma partition coefficient, liver/plasma partition coefficient, unbound fraction in the liver and hepatic intrinsic clearance, respectively.

Central and peripheral compartments:

$$V_d \frac{dC_p}{dt} = \frac{R_B(Q_{pv}+Q_{ha})}{K_{p,liver}} C_{liver} + \sum_{i=1}^{n} k_{i1} X_{peri,i} - \left(R_B Q_{ha} + \sum_{i=1}^{n} k_{1i} + CL_R\right) C_p \quad \text{(S7)}$$

$$\frac{dX_{peri,i}}{dt} = k_{1i} V_d C_p - k_{i1} X_{peri,i}$$

(i = 0 for itraconazole, i = 1 for midazolam and clarithromycin, i = 2 for digoxin) (S8).

where V_d and CL_R represent the distribution volume in the central compartment (rapid equilibrium is assumed between plasma concentration) and renal plasma clearance, respectively. For peripheral compartments, $X_{peri,i}$ is the drug amount in the i-th peripheral compartment, and k_{1i} and k_{i1} represent distribution constants from the central to peripheral compartment and peripheral to central compartment, respectively. CL_R is the sum of renal clearance mediated by P-gp ($CL_{R,Pgp}$) and that by other mechanisms ($CL_{R,nonPgp}$).

Model structure of the intestine in ATOM and CAT

CYP3A and P-gp expression levels in each location, pH changes in the lumen, surface area in enterocytes, volume of enterocytes and lamina propria, and blood flow in the lamina propria were shown using equations S9-15. The relative P-gp expression level in each location was shown because the absolute P-gp amount was not reported. Blood flow in the lamina propria (Q_{pro}) was assumed to be 18,000 mL/h, which assumes that the blood flow into the superior mesenteric artery is 37,200 mL/h accounting for 10% of the cardiac output, and 80 % of the blood flow of the superior mesenteric artery flows into the mucosa, and then 60% of the mucosal blood flows into the epithelial cells of the villi (Jamei et al., 2009)

CYP3A expression:

$$Exp_{CYP3A,z} = \frac{Exp_{CYP3A,whole}}{L_{si}}(1 - \frac{z}{L_{si}}) \quad (S9)$$

Relative P-gp expression:

$$Exp_{Pgp,z} = \frac{Exp_{Pgp,whole}}{L_{si}}(\frac{z}{L_{si}}) \quad (S10)$$

pH changes in the lumen:

$$pH_{lumen,z} = 5.85 + pH_{grad}\frac{z}{L_{si}} \quad (S11)$$

Surface area in enterocytes:

$$S_{ent,z} = \pi(r_{in} + r_z)\sqrt{(r_{in} - r_z)^2 + L_z^2}\ PE\ VE \quad (S12)$$

Volume of enterocytes:

$$V_{ent,z} = S_{ent,z}\ T_{ent} \quad (S13)$$

Volume of lamina propria:

$$V_{lam,z} = \frac{S_{ent}H_{villi}}{VE} - V_{ent,z} \quad (S14)$$

Blood flow in lamina propria:

$$Q_{pro,z} = Q_{pro}\ \frac{S_{ent,z}}{S_{ent,whole}} \quad (S15)$$

where L_{si}, $Exp_{CYP3A,whole}$, $Exp_{Pgp,whole}$, and r_{in} represent the total normalized length of the intestine ($L_{si} = 1$), the total expression level of CYP3A and P-gp in the intestine, and radius in the inlet of the small intestine, respectively. z is within the range of 0 and L_{si} ($0 \leqq z \leqq L_{si} = 1$).

PE, VE, H_{villi}, $S_{ent,whole}$, T_{ent}, and ME represent plicate expansion, villi expansion, height of villi, total surface area of enterocytes, height of enterocytes, and microvilli expansion, respectively. The absolute expression level of P-gp has not been clearly reported; therefore, it was expressed as a relative expression level and the whole expression level was set to 1. The values of these parameters were obtained from the previous report by Ando et al. (2015).

Membrane permeability model between *in vitro* and *in vivo*

Equations S16-19 were used to calculate *in vivo* permeability coefficients from *in vitro* permeability using the concept shown in Supplemental Fig. 4, which was same with TLM (Ando et al., 2015). Apparent permeability in Caco-2 cells ($P_{app,Caco-2}$) was transferred into the permeability of a single membrane ($P_{s,Caco-2}$) using equation S16 from the previous report by Gertz et al. (2010).

$$P_{s,Caco-2} = \frac{1+ME_{Caco-2}}{ME_{Caco-2}} P_{app,Caco-2} \quad \text{(S16)}$$

where ME_{Caco-2} represents the surface area ratio in apical and basolateral membranes in Caco-2 cells and was set as 4 based on a previous report by Ohura et al. (2011).

Then, *in vivo* membrane permeability ($P_{in\ vivo}$) was calculated from $P_{s,Caco-2}$ using equation S17.

$$P_{in\ vivo} = P_{s,Caco-2}\ psf_{passive} \quad \text{(S17)}$$

where $psf_{passive}$ represents a scaling factor regarding the difference in passive transport between *in vitro* and *in vivo*, which was obtained from approximation of the simulated and reported F_A, and $psf_{passive}$ was set as 2.23 based on the previous report by Ando et al. (2015).

According to the definition of membrane permeability clearance in apical and basolateral membranes (Supplemental Fig. 4), $P_{in\ vivo}$ is equal to the passive permeability from cells to apical side (P_2), from cells to basolateral side (P_3), and from basolateral side to cells (P_4) (equation S18).

$$P_{in\ vivo} = P_2 = P_3 = P_4 \quad \text{(S18)}$$

On the other hand, pH values in the lumen are lower than those in the enterocytes (pH 7.4), which leads to changes in the ionized fraction of the drug, depending on pKa values. In this study, it was assumed that the drug transported by passive diffusion is nonionic. Therefore, for P_1, the membrane permeation coefficient depending on the pKa values of the drug and the pH gradients in both the lumen and enterocytes was calculated according to equation S19.

$$P_{1,z} = P_{in\ vivo} \frac{1+10^{pH_{Caco-2}-pKa_{acid}}+10^{pKa_{base}-pH_{Caco-2}}}{1+10^{pH_{lumen,z}-pKa_{acid}}+10^{pKa_{base}-pH_{lumen,z}}} \quad \text{(S19)}$$

where $P_{1,z}$, pH_{Caco-2}, pKa_{acid}, and pKa_{base} represent P_1 at position z, pH in Caco-2, acid pKa, and base pKa of the drug, respectively. In this study, pH_{Caco-2} was assumed to be 7.4.

Permeability on the apical ($P_{1,z}$, and P_2) and basolateral sides (P_3 and P_4) can be transferred into permeability clearance (PS) using equations S20-24.

$$PS_{a,in,z} = P_{1,z}S_{abs,api} \quad \text{(S20)}$$

$$PS_{a,out,z} = P_2 S_{abs,api} + PS_{a,Pgp,z} \quad \text{(S21)}$$

$$PS_{b,in,z} = P_3 S_{abs,bas} \quad \text{(S22)}$$

$$PS_{b,out,z} = P_4 S_{abs,bas} \quad \text{(S23)}$$

$$S_{abs,api} = ME_{in\ vivo} S_{abs,bas} \quad \text{(S24)}$$

where $S_{abs,api}$, $S_{abs,bas}$, $PS_{a,Pgp,z}$, and $ME_{in\ vivo}$ represent the surface area on the apical side, surface area on the basolateral side, transport clearance by P-gp, and surface area ratio between apical and basolateral side in humans, respectively. In this study, $ME_{in\ vivo}$ was set to 20. $PS_{a,Pgp,z}$, and intrinsic clearance by CYP3A ($CL_{ent,z}$) in enterocytes were calculated using equations S25 and S26.

$$PS_{a,Pgp,z} = \frac{V_{max,Pgp} Exp_{Pgp,z} psf_{Pgp}}{K_{m,Pgp,u} + C_{ent,z}} \quad \text{(S25)}$$

$$CL_{ent,z} = \frac{V_{max,CYP3A} Exp_{CYP3A,z} psf_{CYP3A}}{K_{m,CYP3A,u} + C_{ent,z}} \quad \text{(S26)}$$

where $V_{max,Pgp}$, $V_{max,CYP3A}$, $K_{m,Pgp,u}$, $K_{m,CYP3A,u}$, psf_{Pgp}, and psf_{CYP3A} represent V_{max} for P-gp and CYP3A, K_m values based on unbound concentrations for P-gp and CYP3A, the scaling factor for transport clearance by P-gp, and intrinsic clearance by CYP3A between *in vitro* and *in vivo*, respectively. In this study, psf_{CYP3A} was assumed to be 1. Therefore, the scaling factors used in ATOM are only $psf_{passive}$ and psf_{Pgp}. The values of these parameters above were obtained from a previous report by Ando et al. (2015).

Parameter estimation of water distribution in the stomach and intestine

Water distribution was simulated in both ATOM and ACAT models by optimizing the secretion clearance and absorption rate using the reported water distribution in the stomach and small intestine after water intake by Mudie et al. (2014). Equations S27-29 were used for the simulation of water movement. The initial water volume was also obtained from the same report.

Esophagus:

$$\frac{dX_{water,es}}{dt} = -k_{es}X_{water,es} \tag{S27}$$

Stomach:

$$\frac{dX_{water,sto}}{dt} = k_{es}X_{water,es}V_{es}/V_{sto} - k_{sto}X_{water,sto} - k_{water,sto}X_{water,z} + Se_{water,sto} \tag{S28}$$

Lumen:

$$\frac{\partial X_{lum,z}}{\partial t} = D_z\frac{\partial^2 X_{lum,z}}{\partial z^2} - M_t\frac{\partial X_{lum,z}}{\partial z} - k_{water,abs}X_{water,z} + Se_{water,abs} \tag{S29}$$

where $X_{water,es}$, $X_{water,sto}$, and $X_{water,z}$ represent the amount of inflating water in the esophagus, stomach, and lumen at position z, respectively. k_{es}, k_{sto}, V_{es}, and V_{sto} represent the transit rate of drug (or water) from the esophagus to the stomach, from the stomach to the small intestine, and volume of the esophagus and stomach, respectively. $k_{water,sto}$ and $k_{water,abs}$ are the water absorption rates in the stomach and lumen, respectively. $Se_{water,sto}$ and $Se_{water,abs}$ are water secretion clearances in the stomach and lumen, respectively. The transit rate from the esophagus to the stomach (k_{es}), water absorption rate ($k_{water,sto}$ and k_{water}), and secretion clearance ($Se_{water,sto}$ and $Se_{water,z}$) were optimized using reported luminal water volume after oral intake of 240 mL water as reported by Mudie et al. (2014). The simulated water distribution and estimated parameters are shown in Supplemental Fig. 1 and Table S1, respectively.

Sensitivity analysis of f_{ent} on the accumulation of midazolam into the portal vein in a linear condition

Sensitivity analysis of f_{ent} on drug accumulation into the portal vein was performed using pharmacokinetic parameters of midazolam with different f_{ent} values (f_{ent} = 1, 0.5, 0.1 and 0.01) at 0.001 mg. Simulation conditions were same with the ones in Fig. 6. In the simulation, the optimized dispersion numbers and intestinal flow rates determined using the ^{99m}Tc-DTPA distribution of subject A (Haruta et al., 2002) were used shown in Fig. 2A.

Estimation of pharmacokinetic parameters of midazolam, digoxin, itraconazole and clarithromycin

Distribution constants between central and peripheral compartments (k_{12} and k_{21}), distribution volume in the central compartment ($V_{central}$) and hepatic intrinsic clearance (CL_{int}) were optimized using the plasma concentration profile of midazolam after intravenous injection as reported by Link et al. (2008).

Regarding digoxin, V_{max} for P-gp ($V_{max,Pgp}$) was optimized by a fitting analysis to the reported F_A value in a previous report by Elmeliegy et al. (2020). Distribution constants (k_{12},

k_{13}, k_{21}, k_{31}) were optimized using the reported plasma concentration profile of digoxin after intravenous injection as reported by Ding et al. (2004).

Regarding itraconazole, no peripheral compartment model was applied, according to the previous report by Kudo et al. (2013). The optimization process for obtaining pharmacokinetic parameters was not conducted because all parameters were obtained from the previous reports or in silico software. Observed plasma concentration profile of itraconazole was not shown in the DI study with midazolam (Templeton et al., 2010). Therefore, the reported plasma concentration profile of itraconazole 3 days after oral administration of 100 mg twice daily in another study (Jakkola et al., 2015) was adopted for verification for predicting plasma concentration of itraconazole (Supplemental Fig. 6A).

Distribution volume in central compartment ($V_{central}$) were optimized using reported plasma concentration profile of clarithromycin after intravenous injection (Lappin et al., 2011). Distribution constants and intrinsic clearance of clarithromycin (k_{12}, k_{21}, CL_{int}) in oral administration were thought to be independent of that in intravenous administration because the distribution and elimination phase could not be reproduced using optimized parameters using the plasma concentration profile of clarithromycin in intravenous dosing as reported by Lappin et al. (2011). Hence, in this study, these parameters were directly optimized using the plasma concentration of clarithromycin after oral dosing. Unbound fraction in the liver (f_h) was calculated using equations S30 and S31 according to the previous reports by Kudo et al. (2013) and Poulin et al. (2002).

$$K_{p,liver} = \frac{0.02289*P + 0.72621}{0.001719*P + 0.960581} * f_p/f_h \quad \text{(S30)}$$

$$P = 10^{LogP} \quad \text{(S31)}$$

where $K_{p,liver}$ and LogP represent liver/plasma partition coefficient and logarithm partition coefficient, respectively. Reported plasma concentration profile of clarithromycin 2 days after oral administration of 250 mg twice daily (Rengelshausen et al., 2003) was adopted for verification for predicting plasma concentration of clarithromycin (Supplemental Fig. 6B).

References for Supplementary text

1. Jamei M, Turner D, Yang J, Neuhoff S, Polak S, Rostami-Hodjegan A, Tucker G (2009) Population-based mechanistic prediction of oral drug absorption. *AAPS J*. **11**(2):225-237.
2. Ando H, Hisaka A, Suzuki H (2015) A new physiologically based pharmacokinetic model for the prediction of gastrointestinal drug absorption: translocation model. *Drug Metab Dispos*. **43**(4):590-602.
3. Asaumi R, Toshimoto K, Tobe Y, Hashizume K, Nunoya KI, Imawaka H, Lee W, Sugiyama Y (2018) Comprehensive PBPK Model of Rifampicin for Quantitative Prediction of Complex Drug-Drug Interactions: CYP3A/2C9 Induction and OATP Inhibition Effects. *CPT Pharmacometrics Syst Pharmacol*. **7**(3):186-196.
4. Gertz M, Harrison A, Houston JB, Galetin A (2010) Prediction of human intestinal first-pass metabolism of 25 CYP3A substrates from in vitro clearance and permeability data. *Drug Metab Dispos*. **38**(7):1147-1158.
5. Link B, Haschke M, Grignaschi N, Bodmer M, Aschmann YZ, Wenk M, Krähenbühl S (2008) Pharmacokinetics of intravenous and oral midazolam in plasma and saliva in humans: usefulness of saliva as matrix for CYP3A phenotyping. *Br J Clin Pharmacol*. **66**(4):473-484.
6. Lin X, Skolnik S, Chen X, Wang J (2011) Attenuation of intestinal absorption by major efflux transporters: quantitative tools and strategies using a Caco-2 model. *Drug Metab Dispos*. **39**(2):265-274.
7. Elmeliegy M, Vourvahis M, Guo C, Wang DD (2020) Effect of P-glycoprotein (P-gp) Inducers on Exposure of P-gp Substrates: Review of Clinical Drug-Drug Interaction Studies. *Clin Pharmacokinet.* **59**(6):699-714.

8. Collett A, Tanianis-Hughes J, Hallifax D, Warhurst G (2004) Predicting P-glycoprotein effects on oral absorption: correlation of transport in Caco-2 with drug pharmacokinetics in wild-type and mdr1a(-/-) mice in vivo. *Pharm Res*. **21**(5):819-826.
9. Neuhoff S, Yeo KR, Barter Z, Jamei M, Turner DB, Rostami-Hodjegan A (2013) Application of permeability-limited physiologically-based pharmacokinetic models: part I-digoxin pharmacokinetics incorporating P-glycoprotein-mediated efflux. *J Pharm Sci.* **102**(9):3145-60.
10. Ding R, Tayrouz Y, Riedel KD, Burhenne J, Weiss J, Mikus G, Haefeli WE (2004) Substantial pharmacokinetic interaction between digoxin and ritonavir in healthy volunteers. *Clin Pharmacol Ther*. **76**(1):73-84.
11. Rengelshausen J, Göggelmann C, Burhenne J, Riedel KD, Ludwig J, Weiss J, Mikus G, Walter-Sack I, Haefeli WE (2003) Contribution of increased oral bioavailability and reduced nonglomerular renal clearance of digoxin to the digoxin-clarithromycin interaction. *Br J Clin Pharmacol*. **56**(1):32-38.
12. Berben P, Brouwers J, Augustijns P (2018) Assessment of Passive Intestinal Permeability Using an Artificial Membrane Insert System. *J Pharm Sci*. **107**(1):250-256.
13. Isoherranen N, Kunze KL, Allen KE, Nelson WL, Thummel KE (2004) Role of itraconazole metabolites in CYP3A4 inhibition. *Drug Metab Dispos*. **32**(10):1121-1131.
14. Kudo T, Hisaka A, Sugiyama Y, Ito K (2013) Analysis of the repaglinide concentration increase produced by gemfibrozil and itraconazole based on the inhibition of the hepatic uptake transporter and metabolic enzymes. *Drug Metab Dispos*. **41**(2):362-371.
15. Nožinić D, Milić A, Mikac L, Ralić J, Padovan J, Antolović R (2010) Assessment of Macrolide Transport Using PAMPA, Caco-2 and MDCKII-hMDR1 Assays. *Croat Chem Acta*. **83**(3): 323-331.

16. Yoshikado T, Maeda K, Kusuhara H, Furihata KI, Sugiyama Y (2017) Quantitative Analyses of the Influence of Parameters Governing Rate-Determining Process of Hepatic Elimination of Drugs on the Magnitudes of Drug-Drug Interactions via Hepatic OATPs and CYP3A Using Physiologically Based Pharmacokinetic Models. *J Pharm Sci*. **106**(9):2739-2750.
17. Hanke N, Frechen S, Moj D, Britz H, Eissing T, Wendl T, Lehr T (2018) PBPK Models for CYP3A4 and P-gp DDI Prediction: A Modeling Network of Rifampicin, Itraconazole, Clarithromycin, Midazolam, Alfentanil, and Digoxin. *CPT Pharmacometrics Syst Pharmacol*. **7**(10):647-659.
18. Moj D, Hanke N, Britz H, Frechen S, Kanacher T, Wendl T, Haefeli WE, Lehr T (2017) Clarithromycin, Midazolam, and Digoxin: Application of PBPK Modeling to Gain New Insights into Drug-Drug Interactions and Co-medication Regimens. *AAPS J*. **19**(1):298-312.
19. Quinney SK, Zhang X, Lucksiri A, Gorski JC, Li L, Hall SD (2010) Physiologically based pharmacokinetic model of mechanism-based inhibition of CYP3A by clarithromycin. *Drug Metab Dispos*. **38**(2):241-248.
20. Lappin G, Shishikura Y, Jochemsen R, Weaver RJ, Gesson C, Brian Houston J, Oosterhuis B, Bjerrum OJ, Grynkiewicz G, Alder J, Rowland M, Garner C (2011) Comparative pharmacokinetics between a microdose and therapeutic dose for clarithromycin, sumatriptan, propafenone, paracetamol (acetaminophen), and phenobarbital in human volunteers. *Eur J Pharm Sci.* **43**(3):141-150.
21. Ohura K, Nozawa T, Murakami K, Imai T (2011) Evaluation of transport mechanism of prodrugs and parent drugs formed by intracellular metabolism in Caco-2 cells with modified carboxylesterase activity: temocapril as a model case. *J Pharm Sci.* **100**(9):3985-3994.

22. Mudie DM, Murray K, Hoad CL, Pritchard SE, Garnett MC, Amidon GL, Gowland PA, Spiller RC, Amidon GE, Marciani L (2014) Quantification of gastrointestinal liquid volumes and distribution following a 240 mL dose of water in the fasted state. *Mol Pharm*. **11**(9):3039-3047.
23. Poulin P, Theil FP (2002) Prediction of pharmacokinetics prior to in vivo studies. II. Generic physiologically based pharmacokinetic models of drug disposition. *J Pharm Sci*. **91**(5):1358-1370.
24. Rodrigues AD, Roberts EM, Mulford DJ, Yao Y, Ouellet D (1997) Oxidative metabolism of clarithromycin in the presence of human liver microsomes. Major role for the cytochrome P4503A (CYP3A) subfamily. *Drug Metab Dispos*. **25**(5):623-630.
25. Heikkinen AT, Baneyx G, Caruso A, Parrott N (2012) Application of PBPK modeling to predict human intestinal metabolism of CYP3A substrates - an evaluation and case study using GastroPlus. *Eur J Pharm Sci*. **47**(2):375-386.
26. Prueksaritanont T, Gorham LM, Ma B, Liu L, Yu X, Zhao JJ, Slaughter DE, Arison BH, Vyas KP (1997) In vitro metabolism of simvastatin in humans [SBT]identification of metabolizing enzymes and effect of the drug on hepatic P450s. *Drug Metab Dispos.* **25**(10):1191-1199.
27. Haruta S, Kawai K, Nishii R, Jinnouchi S, Ogawara Ki, Higaki K, Tamura S, Arimori K, Kimura T (2002) Prediction of plasma concentration-time curve of orally administered theophylline based on a scintigraphic monitoring of gastrointestinal transit in human volunteers. *Int J Pharm*. **21**;233(1-2):179-190.
28. Watari R, Kakiki M, Yamasaki C, Ishida Y, Tateno C, Kuroda Y, Ishida S, Kusano K (2019) Prediction of Human Hepatic Clearance for Cytochrome P450 Substrates via a New Culture Method Using the Collagen Vitrigel Membrane Chamber and Fresh Hepatocytes Isolated from Liver Humanized Mice. *Biol Pharm Bull.* **42**(3):348-353.

29. Jaakkola T, Backman JT, Neuvonen M, Neuvonen PJ (2005) Effects of gemfibrozil, itraconazole, and their combination on the pharmacokinetics of pioglitazone. *Clin Pharmacol Ther*. **77**(5):404-414.

30. Takano J, Maeda K, Bolger MB, Sugiyama Y (2016) The Prediction of the Relative Importance of CYP3A/P-glycoprotein to the Nonlinear Intestinal Absorption of Drugs by Advanced Compartmental Absorption and Transit Model. *Drug Metab Dispos*. **44**(11):1808-1818.

31. Schiller C, Fröhlich CP, Giessmann T, Siegmund W, Mönnikes H, Hosten N, Weitschies W (2005) Intestinal fluid volumes and transit of dosage forms as assessed by magnetic resonance imaging. *Aliment Pharmacol Ther*. **22**(10):971-979.

32. Poirier A, Cascais AC, Bader U, Portmann R, Brun ME, Walter I, Hillebrecht A, Ullah M, Funk C (2014) Calibration of in vitro multidrug resistance protein 1 substrate and inhibition assays as a basis to support the prediction of clinically relevant interactions in vivo. *Drug Metab Dispos*. **42**(9):1411-1122.

33. Templeton I, Peng CC, Thummel KE, Davis C, Kunze KL, Isoherranen N (2010) Accurate prediction of dose-dependent CYP3A4 inhibition by itraconazole and its metabolites from in vitro inhibition data. *Clin Pharmacol Ther*. **88**(4):499-505.

34. Heizmann P, Eckert M, Ziegler WH (1983) Pharmacokinetics and bioavailability of midazolam in man. *Br J Clin Pharmacol*. **16** Suppl 1(Suppl 1):43S-49S.

35. Prueksaritanont T, Gorham LM, Ma B, Liu L, Yu X, Zhao JJ, Slaughter DE, Arison BH, Vyas KP (1997) In vitro metabolism of simvastatin in humans [SBT]identification of metabolizing enzymes and effect of the drug on hepatic P450s. *Drug Metab Dispos*. **25**(10):1191-1199.

Legends for Supplementary Figures

Supplemental Fig. 1 Prediction of intestinal water profile in the stomach and small intestine after a water intake of 240 mL.

Open and closed circles represent the observed water volume in the stomach and whole intestine, respectively, as reported by Mudie et al. (2014). Initial values in the stomach and small intestine were also obtained from the same report. Optimized parameters in this analysis are shown in Supplemental Table S1.

Supplemental Fig. 2 Simulated movements of ^{99m}Tc-DTPA in the gastrointestinal tract by ATOM with fixed dispersion number.

In panel A, open circles, closed circles, open squares, and open triangles represent the observed distributions in the stomach, upper intestine, lower intestine, and caecum/colon, respectively. The observed ^{99m}Tc-DTPA distribution in the lumen was obtained from a previous report by Haruta et al. (2002), which reported its distribution in two subjects. In this analysis, the observed ^{99m}Tc-DTPA distribution in the small intestine of subject A in the fasted state was used. The lines represent the simulated ^{99m}Tc-DTPA distributions in each organ. In ATOM, distributions at 40 locations were simulated, and 24 segments were assigned in the upper intestine and the other 16 segments in the lower intestine corresponding to the CATmodel using the index of the length from the inlet in the intestine. In panel B, the fixed dispersion number was optimized by fitting analysis using the luminal ^{99m}Tc-DTPA distribution of subject A in the fasted condition. The fixed dispersion number was optimized as 0.812.

Supplemental Fig. 3 Simulated movements of ^{99m}Tc-DTPA in the gastrointestinal tract using CAT model with the reported transit times to the observed distribution.

Reported transit times were referenced from a previous report by Heikkinen et al. (2012), as shown in Supplemental Table S3. Open circles, closed circles, open squares and open triangles represent the observed ^{99m}Tc-DTPA distributions in the stomach, upper intestine, lower intestine and caecum/colon, respectively, as reported by Haruta et al. (2002). The lines represent the simulated ^{99m}Tc-DTPA distributions in each organ. CAT model assumes that the small intestine is divided into six portions.

Supplemental Fig. 4 Definitions of apical and basolateral permeability.
$S_{abs,api}$ and $S_{abs,bas}$ represent the surface areas of the apical and basolateral membranes, respectively. P_1, P_2, P_3, and P_4 represent the passive permeability from the lumen to enterocytes, enterocytes to the lumen, enterocytes to the lamina propria and blood capillaries, and blood capillaries to enterocytes, respectively. P_{Pgp} represents the active transport clearance of P-gp.

Supplemental Fig. 5 Effect of f_{ent} on the midazolam accumulation into the portal vein in linear conditions.
Red, blue, black and green lines represent the cumulative transfer of midazolam with $f_{ent} = 1$, 0.5, 0.1 and 0.01 into the portal vein simulated by ATOM with optimized transit times, respectively. Dose was set to 0.001 mg. The simulation was performed in the same condition with the one used in the analysis of Fig. 6.

Supplemental Fig. 6 Plasma concentration of itraconazole (A) and clarithromycin (B) in DI simulations.
In panel A, solid line represents the predicted blood concentration of itraconazole after oral administration of 100 mg twice daily. Solid circle symbol and error bars represent the mean

plasma concentration of itraconazole and the SDs reported by Jakkola et al. (2015). In panel B, solid line represents predicted plasma concentration of clarithromycin after oral administration of 250 mg twice daily. Solid circle symbol and error bars represent the mean plasma concentration of clarithromycin and the SDs reported by Rengelshausen et al. (2003).

Supplementary text 2

; Model equations used in ATOM

; Main model equation: Line 7 - 2252

; Preparative calculation equation: Line 2245 - 2845

@at 0:

; Initial water volume in the first location of the intestine

y1 = Wvol_int_up_r/3,

y2 = Wvol_int_up_r/3,

y3 =Wvol_int_up_r/3,

; Initial water volume in the second location of the intestine

y4=Wvol_int_up_l/11,

y5=Wvol_int_up_l/11,

y6=Wvol_int_up_l/11,

y7=Wvol_int_up_l/11,

y8=Wvol_int_up_l/11,

y9=Wvol_int_up_l/11,

y10=Wvol_int_up_l/11,

y11=Wvol_int_up_l/11,

y12=Wvol_int_up_l/11,

y13=Wvol_int_up_l/11,

y14=Wvol_int_up_l/11,

; Initial water volume in the third location of the intestine

y15=Wvol_int_low_l/18,

y16=Wvol_int_low_l/18,

y17=Wvol_int_low_l/18,

y18=Wvol_int_low_l/18,

y19=Wvol_int_low_l/18,

y20=Wvol_int_low_l/18,

y21=Wvol_int_low_l/18,

y22=Wvol_int_low_l/18,

y23=Wvol_int_low_l/18,

y24=Wvol_int_low_l/18,

y25=Wvol_int_low_l/18,

y26=Wvol_int_low_l/18,

y27=Wvol_int_low_l/18,

y28=Wvol_int_low_l/18,

y29=Wvol_int_low_l/18,

y30=Wvol_int_low_l/18,

y31=Wvol_int_low_l/18,

y32=Wvol_int_low_l/18,

; Initial water volume in the last location of the intestine

y33=Wvol_int_low_r/8,

y34=Wvol_int_low_r/8,

y35=Wvol_int_low_r/8,

y36=Wvol_int_low_r/8,

```
y37=Wvol_int_low_r/8,

y38=Wvol_int_low_r/8,

y39=Wvol_int_low_r/8,

y40=Wvol_int_low_r/8,


; Initial water volume in the colon/caecum

y41=Wvol_int_col,


; Initial water volume in the stomach

y43 = Wvol_int,


; Initial water volume in the whole small intetsine

y46=Wvol_int_low_l,


; Water intake volume

y50=Wvol_ini,


; Concentration of perpetorator in the esophagus

y320 = dose_inh/Ves,


; Concentration of substrate in the esophagus (administered at time=Lag)

@at Lag:

y100 = dose/Ves,


@from 0:
```

; Membrane permeability of substrate

Ppass_lum_a1 = P_invivo (1+10^(pH_Caco2-pKa_acid)+10^(pKa_base-pH_Caco2))/(1+10^(pH_lum1-pKa_acid)+10^(pKa_base-pH_lum1)),

PSpass_lum_a1= Ppass_lum_a1 ME Sent1,

PSpass_a1 = P_invivo ME Sent1,

PSpass_b1 = P_invivo Sent1,

PSap1 = PSpass_lum_a1,

PSbp1 = PSpass_b1,

PSbx1 = PSpass_b1,

PSpgp1 = psf_Pgp*Vmax_Pgp*Arel_Pgp1 /(Km_Pgp+fent*y101/Vent1),

PSax1 = (PSpass_a1+ PSpgp1),

CL1 = Vmax_3A4*Arel_3A4_1 /(Km_3A4+fent*y101/Vent1)/(1+(fent_inh*y231/Vent1)/Ki_3A4),

Ppass_lum_a2 = P_invivo (1+10^(pH_Caco2-pKa_acid)+10^(pKa_base-pH_Caco2))/(1+10^(pH_lum2-pKa_acid)+10^(pKa_base-pH_lum2)),

PSpass_lum_a2= Ppass_lum_a2 ME Sent2,

PSpass_a2 = P_invivo ME Sent2,

PSpass_b2 = P_invivo Sent2,

PSap2 = PSpass_lum_a2,

PSbp2 = PSpass_b2,

PSbx2 = PSpass_b2,

PSpgp2 = psf_Pgp*Vmax_Pgp*Arel_Pgp2 /(Km_Pgp+fent*y102/Vent2),

PSax2 = (PSpass_a2+ PSpgp2),

CL2 =   Vmax_3A4*Arel_3A4_2

/(Km_3A4+fent*y102/Vent2)/(1+(fent_inh*y232/Vent2)/Ki_3A4),

Ppass_lum_a3 = P_invivo (1+10^(pH_Caco2-pKa_acid)+10^(pKa_base-

pH_Caco2))/(1+10^(pH_lum3-pKa_acid)

+10^(pKa_base-pH_lum3)),

PSpass_lum_a3= Ppass_lum_a3 ME Sent3,

PSpass_a3 = P_invivo ME Sent3,

PSpass_b3 = P_invivo Sent3,

PSap3 = PSpass_lum_a3,

PSbp3 = PSpass_b3,

PSbx3 = PSpass_b3,

PSpgp3 = psf_Pgp Vmax_Pgp Arel_Pgp3 /(Km_Pgp+fent y103/Vent3),

PSax3 = (PSpass_a3+ PSpgp3),

CL3 =   Vmax_3A4 Arel_3A4_3 /(Km_3A4+fent

y103/Vent3)/(1+(fent_inh*y233/Vent3)/Ki_3A4),

Ppass_lum_a4 = P_invivo (1+10^(pH_Caco2-pKa_acid)+10^(pKa_base-

pH_Caco2))/(1+10^(pH_lum4-pKa_acid)+10^(pKa_base-pH_lum4)),

PSpass_a4 = P_invivo ME Sent4,

PSpass_b4 = P_invivo Sent4,

PSpass_lum_a4 = Ppass_lum_a4 ME Sent4,

PSap4 = PSpass_lum_a4,

PSbp4 = PSpass_b4,

PSbx4 = PSpass_b4,

PSpgp4 = psf_Pgp Vmax_Pgp Arel_Pgp4 /(Km_Pgp+fent y104/Vent4),

PSax4 = (PSpass_a4+ PSpgp4),

CL4 = Vmax_3A4 Arel_3A4_4 /(Km_3A4+fent y104/Vent4)/(1+(fent_inh*y234/Vent4)/Ki_3A4),

Ppass_lum_a5 = P_invivo (1+10^(pH_Caco2-pKa_acid)+10^(pKa_base-pH_Caco2))/(1+10^(pH_lum5-pKa_acid)+10^(pKa_base-pH_lum5)),

PSpass_a5 = P_invivo ME Sent5,

PSpass_b5 = P_invivo Sent5,

PSpass_lum_a5 = Ppass_lum_a5 ME Sent5,

PSap5 = PSpass_lum_a5,

PSbp5 = PSpass_b5,

PSbx5 = PSpass_b5,

PSpgp5 = psf_Pgp Vmax_Pgp Arel_Pgp5 /(Km_Pgp+fent y105/Vent5),

PSax5 = (PSpass_a5+ PSpgp5),

CL5 = Vmax_3A4 Arel_3A4_5 /(Km_3A4+fent y105/Vent5)/(1+(fent_inh*y235/Vent5)/Ki_3A4),

Ppass_lum_a6 = P_invivo (1+10^(pH_Caco2-pKa_acid)+10^(pKa_base-pH_Caco2))/(1+10^(pH_lum6-pKa_acid)+10^(pKa_base-pH_lum6)),

PSpass_a6 = P_invivo ME Sent6,

PSpass_b6 = P_invivo Sent6,

PSpass_lum_a6 = Ppass_lum_a6 ME Sent6,

PSap6 = PSpass_lum_a6,

PSbp6 = PSpass_b6,

PSbx6 = PSpass_b6,

PSpgp6 = psf_Pgp Vmax_Pgp Arel_Pgp6 /(Km_Pgp+fent y106/Vent6),

PSax6 = (PSpass_a6+ PSpgp6),

CL6 = Vmax_3A4 Arel_3A4_6 /(Km_3A4+fent y106/Vent6)/(1+(fent_inh*y236/Vent6)/Ki_3A4),

Ppass_lum_a7 = P_invivo (1+10^(pH_Caco2-pKa_acid)+10^(pKa_base-pH_Caco2))/(1+10^(pH_lum7-pKa_acid)+10^(pKa_base-pH_lum7)),

PSpass_a7 = P_invivo ME Sent7,

PSpass_b7 = P_invivo Sent7,

PSpass_lum_a7 = Ppass_lum_a7 ME Sent7,

PSap7 = PSpass_lum_a7,

PSbp7 = PSpass_b7,

PSbx7 = PSpass_b7,

PSpgp7 = psf_Pgp Vmax_Pgp Arel_Pgp7 /(Km_Pgp+fent y107/Vent7),

PSax7 = (PSpass_a7+ PSpgp7),

CL7 = Vmax_3A4 Arel_3A4_7 /(Km_3A4+fent y107/Vent7)/(1+(fent_inh*y237/Vent7)/Ki_3A4),

Ppass_lum_a8 = P_invivo (1+10^(pH_Caco2-pKa_acid)+10^(pKa_base-pH_Caco2))/(1+10^(pH_lum8-pKa_acid)+10^(pKa_base-pH_lum8)),

PSpass_a8 = P_invivo ME Sent8,

PSpass_b8 = P_invivo Sent8,

PSpass_lum_a8 = Ppass_lum_a8 ME Sent8,

PSap8 = PSpass_lum_a4,

PSbp8 = PSpass_b8,

PSbx8 = (PSpass_b8),

PSpgp8 = psf_Pgp Vmax_Pgp Arel_Pgp8 /(Km_Pgp+fent y108/Vent8),

PSax8 = (PSpass_a8+ PSpgp8),

CL8 = Vmax_3A4 Arel_3A4_8 /(Km_3A4+fent y108/Vent8)/(1+(fent_inh*y238/Vent8)/Ki_3A4),

Ppass_lum_a9 = P_invivo (1+10^(pH_Caco2-pKa_acid)+10^(pKa_base-pH_Caco2))/(1+10^(pH_lum9-pKa_acid)+10^(pKa_base-pH_lum9)),

PSpass_a9 = P_invivo ME Sent9,

PSpass_b9 = P_invivo Sent9,

PSpass_lum_a9 = Ppass_lum_a9 ME Sent9,

PSap9 = PSpass_lum_a9,

PSbp9 = PSpass_b9,

PSbx9 = PSpass_b9,

PSpgp9 = psf_Pgp Vmax_Pgp Arel_Pgp9 /(Km_Pgp+fent y109/Vent9),

PSax9 = (PSpass_a9+ PSpgp9),

CL9 = Vmax_3A4 Arel_3A4_9 /(Km_3A4+fent y109/Vent9)/(1+(fent_inh*y239/Vent9)/Ki_3A4),

Ppass_lum_a10 = P_invivo (1+10^(pH_Caco2-pKa_acid)+10^(pKa_base-pH_Caco2))/(1+10^(pH_lum10-pKa_acid)+10^(pKa_base-pH_lum10)),

PSpass_a10 = P_invivo ME Sent10,

PSpass_b10 = P_invivo Sent10,

PSpass_lum_a10 = Ppass_lum_a10 ME Sent10,

PSap10 = PSpass_lum_a10,

PSbp10 = PSpass_b10,

PSbx10 = PSpass_b10,

PSpgp10 = psf_Pgp Vmax_Pgp Arel_Pgp10 /(Km_Pgp+fent y110/Vent10),

PSax10 = (PSpass_a10+ PSpgp10),

CL10 = Vmax_3A4 Arel_3A4_10 /(Km_3A4+fent y110/Vent10)/(1+(fent_inh*y240/Vent10)/Ki_3A4),

Ppass_lum_a11 = P_invivo (1+10^(pH_Caco2-pKa_acid)+10^(pKa_base-pH_Caco2))/(1+10^(pH_lum11-pKa_acid)+10^(pKa_base-pH_lum11)),

PSpass_a11 = P_invivo ME Sent11,

PSpass_b11 = P_invivo Sent11,

PSpass_lum_a11 = Ppass_lum_a11 ME Sent11,

PSap11 = PSpass_lum_a11,

PSbp11 = PSpass_b11,

PSbx11 = PSpass_b11,

PSpgp11 = psf_Pgp Vmax_Pgp Arel_Pgp11 /(Km_Pgp+fent y111/Vent11),

PSax11 = (PSpass_a11+ PSpgp11),

CL11 = Vmax_3A4 Arel_3A4_11 /(Km_3A4+fent y111/Vent11)/(1+(fent_inh*y241/Vent11)/Ki_3A4),

Ppass_lum_a12 = P_invivo (1+10^(pH_Caco2-pKa_acid)+10^(pKa_base-pH_Caco2))/(1+10^(pH_lum12-pKa_acid)+10^(pKa_base-pH_lum12)),

PSpass_a12 = P_invivo ME Sent12,

PSpass_b12 = P_invivo Sent12,

PSpass_lum_a12 = Ppass_lum_a12 ME Sent12,

PSap12 = PSpass_lum_a12,

PSbp12 = PSpass_b12,

PSbx12 = PSpass_b12,

PSpgp12 = psf_Pgp Vmax_Pgp Arel_Pgp12 /(Km_Pgp+fent y112/Vent12),

PSax12 = (PSpass_a12+ PSpgp12),

CL12 = Vmax_3A4 Arel_3A4_12 /(Km_3A4+fent y112/Vent12)/(1+(fent_inh*y242/Vent12)/Ki_3A4),

Ppass_lum_a13 = P_invivo (1+10^(pH_Caco2-pKa_acid)+10^(pKa_base-pH_Caco2))/(1+10^(pH_lum13-pKa_acid)+10^(pKa_base-pH_lum13)),

PSpass_a13 = P_invivo ME Sent13,

PSpass_b13 = P_invivo Sent13,

PSpass_lum_a13 = Ppass_lum_a13 ME Sent13,

PSap13 = PSpass_lum_a13,

PSbp13 = PSpass_b13,

PSbx13 = PSpass_b13,

PSpgp13 = psf_Pgp Vmax_Pgp Arel_Pgp13 /(Km_Pgp+fent y113/Vent13),

PSax13 = (PSpass_a13+ PSpgp13),

CL13 = Vmax_3A4 Arel_3A4_13 /(Km_3A4+fent y113/Vent13)/(1+(fent_inh*y243/Vent13)/Ki_3A4),

Ppass_lum_a14 = P_invivo (1+10^(pH_Caco2-pKa_acid)+10^(pKa_base-pH_Caco2))/(1+10^(pH_lum14-pKa_acid)+10^(pKa_base-pH_lum14)),

PSpass_a14 = P_invivo ME Sent14,

PSpass_b14 = P_invivo Sent14,

PSpass_lum_a14 = Ppass_lum_a14 ME Sent14,

PSap14 = PSpass_lum_a14,

PSbp14 = PSpass_b14,

PSbx14 = PSpass_b14,

PSpgp14 = psf_Pgp Vmax_Pgp Arel_Pgp14 /(Km_Pgp+fent y114/Vent14),

PSax14 = (PSpass_a14+ PSpgp14),

CL14 = Vmax_3A4 Arel_3A4_14 /(Km_3A4+fent y114/Vent14)/(1+(fent_inh*y244/Vent14)/Ki_3A4),

Ppass_lum_a15 = P_invivo (1+10^(pH_Caco2-pKa_acid)+10^(pKa_base-pH_Caco2))/(1+10^(pH_lum15-pKa_acid)+10^(pKa_base-pH_lum15)),

PSpass_a15 = P_invivo ME Sent15,

PSpass_b15 = P_invivo Sent15,

PSpass_lum_a15 = Ppass_lum_a15 ME Sent15,

PSap15 = PSpass_lum_a15,

PSbp15 = PSpass_b15,

PSbx15 = PSpass_b15,

PSpgp15 = psf_Pgp Vmax_Pgp Arel_Pgp15 /(Km_Pgp+fent y115/Vent15),

PSax15 = (PSpass_a15+ PSpgp15),

CL15 = Vmax_3A4 Arel_3A4_15 /(Km_3A4+fent y115/Vent15)/(1+(fent_inh*y245/Vent15)/Ki_3A4),

Ppass_lum_a16 = P_invivo (1+10^(pH_Caco2-pKa_acid)+10^(pKa_base-pH_Caco2))/(1+10^(pH_lum16-pKa_acid)+10^(pKa_base-pH_lum16)),

PSpass_a16 = P_invivo ME Sent16,

PSpass_b16 = P_invivo Sent16,

PSpass_lum_a16 = Ppass_lum_a16 ME Sent16,

PSap16 = PSpass_lum_a16,

PSbp16 = PSpass_b16,

PSbx16 = PSpass_b16,

PSpgp16 = psf_Pgp Vmax_Pgp Arel_Pgp16 /(Km_Pgp+fent y116/Vent16),

PSax16 = (PSpass_a16+ PSpgp16),

CL16 = Vmax_3A4 Arel_3A4_16 /(Km_3A4+fent y116/Vent16)/(1+(fent_inh*y246/Vent16)/Ki_3A4),

Ppass_lum_a17 = P_invivo (1+10^(pH_Caco2-pKa_acid)+10^(pKa_base-pH_Caco2))/(1+10^(pH_lum17-pKa_acid)+10^(pKa_base-pH_lum17)),

PSpass_a17 = P_invivo ME Sent17,

PSpass_b17 = P_invivo Sent17,

PSpass_lum_a17 = Ppass_lum_a17 ME Sent17,

PSap17 = PSpass_lum_a17,

PSbp17 = PSpass_b17,

PSbx17 = PSpass_b17,

PSpgp17 = psf_Pgp Vmax_Pgp Arel_Pgp17 /(Km_Pgp+fent y117/Vent17),

PSax17 = (PSpass_a17+ PSpgp17),

CL17 = Vmax_3A4 Arel_3A4_17 /(Km_3A4+fent y117/Vent17)/(1+(fent_inh*y247/Vent17)/Ki_3A4),

Ppass_lum_a18 = P_invivo (1+10^(pH_Caco2-pKa_acid)+10^(pKa_base-pH_Caco2))/(1+10^(pH_lum18-pKa_acid)+10^(pKa_base-pH_lum18)),

PSpass_a18 = P_invivo ME Sent18,

PSpass_b18 = P_invivo Sent18,

PSpass_lum_a18 = Ppass_lum_a18 ME Sent18,

PSap18 = PSpass_lum_a18,

PSbp18 = PSpass_b18,

PSbx18 = PSpass_b18,

PSpgp18 = psf_Pgp Vmax_Pgp Arel_Pgp18 /(Km_Pgp+fent y118/Vent18),

PSax18 = (PSpass_a18+ PSpgp18),

CL18 = Vmax_3A4 Arel_3A4_18 /(Km_3A4+fent y118/Vent18)/(1+(fent_inh*y248/Vent18)/Ki_3A4),

Ppass_lum_a19 = P_invivo (1+10^(pH_Caco2-pKa_acid)+10^(pKa_base-pH_Caco2))/(1+10^(pH_lum19-pKa_acid)+10^(pKa_base-pH_lum19)),

PSpass_a19 = P_invivo ME Sent19,

PSpass_b19 = P_invivo Sent19,

PSpass_lum_a19 = Ppass_lum_a19 ME Sent19,

PSap19 = PSpass_lum_a19,

PSbp19 = PSpass_b19,

PSbx19 = PSpass_b19,

PSpgp19 = psf_Pgp Vmax_Pgp Arel_Pgp19 /(Km_Pgp+fent y119/Vent19),

PSax19 = (PSpass_a19+ PSpgp19),

CL19 =   Vmax_3A4 Arel_3A4_19 /(Km_3A4+fent y119/Vent19)/(1+(fent_inh*y249/Vent19)/Ki_3A4),

Ppass_lum_a20 = P_invivo (1+10^(pH_Caco2-pKa_acid)+10^(pKa_base-pH_Caco2))/(1+10^(pH_lum20-pKa_acid)+10^(pKa_base-pH_lum20)),

PSpass_a20 = P_invivo ME Sent20,

PSpass_b20 = P_invivo Sent20,

PSpass_lum_a20 = Ppass_lum_a20 ME Sent20,

PSap20 = PSpass_lum_a20,

PSbp20 = PSpass_b20,

PSbx20 = PSpass_b20,

PSpgp20 = psf_Pgp Vmax_Pgp Arel_Pgp20 /(Km_Pgp+fent y120/Vent20),

PSax20 = (PSpass_a20+ PSpgp20),

CL20 =   Vmax_3A4 Arel_3A4_20 /(Km_3A4+fent y120/Vent20)/(1+(fent_inh*y250/Vent20)/Ki_3A4),

Ppass_lum_a21 = P_invivo (1+10^(pH_Caco2-pKa_acid)+10^(pKa_base-pH_Caco2))/(1+10^(pH_lum21-pKa_acid)+10^(pKa_base-pH_lum21)),

PSpass_a21 = P_invivo ME Sent21,

PSpass_b21 = P_invivo Sent21,

PSpass_lum_a21 = Ppass_lum_a21 ME Sent21,

PSap21 = PSpass_lum_a21,

PSbp21 = PSpass_b21,

PSbx21 = PSpass_b21,

PSpgp21 = psf_Pgp Vmax_Pgp Arel_Pgp21 /(Km_Pgp+fent y121/Vent21),

PSax21 = (PSpass_a21+ PSpgp21),

CL21 = Vmax_3A4 Arel_3A4_21 /(Km_3A4+fent y121/Vent21)/(1+(fent_inh*y251/Vent21)/Ki_3A4),

Ppass_lum_a22 = P_invivo (1+10^(pH_Caco2-pKa_acid)+10^(pKa_base-pH_Caco2))/(1+10^(pH_lum22-pKa_acid)+10^(pKa_base-pH_lum22)),

PSpass_a22 = P_invivo ME Sent22,

PSpass_b22 = P_invivo Sent22,

PSpass_lum_a22 = Ppass_lum_a22 ME Sent22,

PSap22 = PSpass_lum_a22,

PSbp22 = PSpass_b22,

PSbx22 = PSpass_b22,

PSpgp22 = psf_Pgp Vmax_Pgp Arel_Pgp22 /(Km_Pgp+fent y122/Vent22),

PSax22 = (PSpass_a22+ PSpgp22),

CL22 = Vmax_3A4 Arel_3A4_22 /(Km_3A4+fent y122/Vent22)/(1+(fent_inh*y252/Vent22)/Ki_3A4),

Ppass_lum_a23 = P_invivo (1+10^(pH_Caco2-pKa_acid)+10^(pKa_base-pH_Caco2))/(1+10^(pH_lum23-pKa_acid)+10^(pKa_base-pH_lum23)),

PSpass_a23 = P_invivo ME Sent23,

PSpass_b23 = P_invivo Sent23,

PSpass_lum_a23 = Ppass_lum_a23 ME Sent23,

PSap23 = PSpass_lum_a23,

PSbp23 = PSpass_b23,

PSbx23 = PSpass_b23,

PSpgp23 = psf_Pgp Vmax_Pgp Arel_Pgp23 /(Km_Pgp+fent y123/Vent23),

PSax23 = (PSpass_a23+ PSpgp23),

CL23 = Vmax_3A4 Arel_3A4_23 /(Km_3A4+fent y123/Vent23)/(1+(fent_inh*y253/Vent23)/Ki_3A4),

Ppass_lum_a24 = P_invivo (1+10^(pH_Caco2-pKa_acid)+10^(pKa_base-pH_Caco2))/(1+10^(pH_lum24-pKa_acid)+10^(pKa_base-pH_lum24)),

PSpass_a24 = P_invivo ME Sent24,

PSpass_b24 = P_invivo Sent24,

PSpass_lum_a24 = Ppass_lum_a24 ME Sent24,

PSap24 = PSpass_lum_a24,

PSbp24 = PSpass_b24,

PSbx24 = PSpass_b24,

PSpgp24 = psf_Pgp Vmax_Pgp Arel_Pgp24 /(Km_Pgp+fent y124/Vent24),

PSax24 = (PSpass_a24+ PSpgp24),

CL24 = Vmax_3A4 Arel_3A4_24 /(Km_3A4+fent y124/Vent24)/(1+(fent_inh*y254/Vent24)/Ki_3A4),

Ppass_lum_a25 = P_invivo (1+10^(pH_Caco2-pKa_acid)+10^(pKa_base-pH_Caco2))/(1+10^(pH_lum25-pKa_acid)+10^(pKa_base-pH_lum25)),

PSpass_a25 = P_invivo ME Sent25,

PSpass_b25 = P_invivo Sent25,

PSpass_lum_a25 = Ppass_lum_a25 ME Sent25,

PSap25 = PSpass_lum_a25,

PSbp25 = PSpass_b25,

PSbx25 = PSpass_b25,

PSpgp25 = psf_Pgp Vmax_Pgp Arel_Pgp25 /(Km_Pgp+fent y125/Vent25),

PSax25 = (PSpass_a25+ PSpgp25),

CL25 = Vmax_3A4 Arel_3A4_25 /(Km_3A4+fent y125/Vent25)/(1+(fent_inh*y255/Vent25)/Ki_3A4),

Ppass_lum_a26 = P_invivo (1+10^(pH_Caco2-pKa_acid)+10^(pKa_base-pH_Caco2))/(1+10^(pH_lum26-pKa_acid)+10^(pKa_base-pH_lum26)),

PSpass_a26 = P_invivo ME Sent26,

PSpass_b26 = P_invivo Sent26,

PSpass_lum_a26 = Ppass_lum_a26 ME Sent26,

PSap26 = PSpass_lum_a26,

PSbp26 = PSpass_b26,

PSbx26 = PSpass_b26,

PSpgp26 = psf_Pgp Vmax_Pgp Arel_Pgp26 /(Km_Pgp+fent y126/Vent26),

PSax26 = (PSpass_a26+ PSpgp26),

CL26 = Vmax_3A4 Arel_3A4_26 /(Km_3A4+fent y126/Vent26)/(1+(fent_inh*y256/Vent26)/Ki_3A4),

Ppass_lum_a27 = P_invivo (1+10^(pH_Caco2-pKa_acid)+10^(pKa_base-pH_Caco2))/(1+10^(pH_lum27-pKa_acid)+10^(pKa_base-pH_lum27)),

PSpass_a27 = P_invivo ME Sent27,

PSpass_b27 = P_invivo Sent27,

PSpass_lum_a27 = Ppass_lum_a27 ME Sent27,

PSap27 = PSpass_lum_a27,

PSbp27 = PSpass_b27,

PSbx27 = PSpass_b27,

PSpgp27 = psf_Pgp Vmax_Pgp Arel_Pgp27 /(Km_Pgp+fent y127/Vent27),

PSax27 = (PSpass_a27+ PSpgp27),

CL27 =   Vmax_3A4 Arel_3A4_27 /(Km_3A4+fent

y127/Vent27)/(1+(fent_inh*y257/Vent27)/Ki_3A4),

Ppass_lum_a28 = P_invivo (1+10^(pH_Caco2-pKa_acid)+10^(pKa_base-

pH_Caco2))/(1+10^(pH_lum28-pKa_acid)+10^(pKa_base-pH_lum28)),

PSpass_a28 = P_invivo ME Sent28,

PSpass_b28 = P_invivo Sent28,

PSpass_lum_a28 = Ppass_lum_a28 ME Sent28,

PSap28 = PSpass_lum_a28,

PSbp28 = PSpass_b28,

PSbx28 = PSpass_b28,

PSpgp28 = psf_Pgp Vmax_Pgp Arel_Pgp28 /(Km_Pgp+fent y128/Vent28),

PSax28 = (PSpass_a28+ PSpgp28),

CL28 =   Vmax_3A4 Arel_3A4_28 /(Km_3A4+fent

y128/Vent28)/(1+(fent_inh*y258/Vent28)/Ki_3A4),

Ppass_lum_a29 = P_invivo (1+10^(pH_Caco2-pKa_acid)+10^(pKa_base-

pH_Caco2))/(1+10^(pH_lum29-pKa_acid)+10^(pKa_base-pH_lum29)),

PSpass_a29 = P_invivo ME Sent29,

PSpass_b29 = P_invivo Sent29,

PSpass_lum_a29 = Ppass_lum_a29 ME Sent29,

PSap29 = PSpass_lum_a29,

PSbp29 = PSpass_b29,

PSbx29 = PSpass_b29,

PSpgp29 = psf_Pgp Vmax_Pgp Arel_Pgp29 /(Km_Pgp+fent y129/Vent29),

PSax29 = (PSpass_a29+ PSpgp29),

CL29 = Vmax_3A4 Arel_3A4_29 /(Km_3A4+fent y129/Vent29)/(1+(fent_inh*y259/Vent29)/Ki_3A4),

Ppass_lum_a30 = P_invivo (1+10^(pH_Caco2-pKa_acid)+10^(pKa_base-pH_Caco2))/(1+10^(pH_lum30-pKa_acid)+10^(pKa_base-pH_lum30)),

PSpass_a30 = P_invivo ME Sent30,

PSpass_b30 = P_invivo Sent30,

PSpass_lum_a30 = Ppass_lum_a30 ME Sent30,

PSap30 = PSpass_lum_a30,

PSbp30 = PSpass_b30,

PSbx30 = PSpass_b30,

PSpgp30 = psf_Pgp Vmax_Pgp Arel_Pgp30 /(Km_Pgp+fent y130/Vent30),

PSax30 = (PSpass_a30+ PSpgp30),

CL30 = Vmax_3A4 Arel_3A4_30 /(Km_3A4+fent y130/Vent30)/(1+(fent_inh*y260/Vent30)/Ki_3A4),

Ppass_lum_a31 = P_invivo (1+10^(pH_Caco2-pKa_acid)+10^(pKa_base-pH_Caco2))/(1+10^(pH_lum31-pKa_acid)+10^(pKa_base-pH_lum31)),

PSpass_a31 = P_invivo ME Sent31,

PSpass_b31 = P_invivo Sent31,

PSpass_lum_a31 = Ppass_lum_a31 ME Sent31,

PSap31 = PSpass_lum_a31,

PSbp31 = PSpass_b31,

PSbx31 = PSpass_b31,

PSpgp31 = psf_Pgp Vmax_Pgp Arel_Pgp31 /(Km_Pgp+fent y131/Vent31),

PSax31 = (PSpass_a31+ PSpgp31),

CL31 = Vmax_3A4 Arel_3A4_31 /(Km_3A4+fent y131/Vent31)/(1+(fent_inh*y261/Vent31)/Ki_3A4),

Ppass_lum_a32 = P_invivo (1+10^(pH_Caco2-pKa_acid)+10^(pKa_base-pH_Caco2))/(1+10^(pH_lum32-pKa_acid)+10^(pKa_base-pH_lum32)),

PSpass_a32 = P_invivo ME Sent32,

PSpass_b32 = P_invivo Sent32,

PSpass_lum_a32 = Ppass_lum_a32 ME Sent32,

PSap32 = PSpass_lum_a32,

PSbp32 = PSpass_b32,

PSbx32 = PSpass_b32,

PSpgp32 = psf_Pgp Vmax_Pgp Arel_Pgp32 /(Km_Pgp+fent y132/Vent32),

PSax32 = (PSpass_a32+ PSpgp32),

CL32 = Vmax_3A4 Arel_3A4_32 /(Km_3A4+fent y132/Vent32)/(1+(fent_inh*y262/Vent32)/Ki_3A4),

Ppass_lum_a33 = P_invivo (1+10^(pH_Caco2-pKa_acid)+10^(pKa_base-pH_Caco2))/(1+10^(pH_lum33-pKa_acid)+10^(pKa_base-pH_lum33)),

PSpass_a33 = P_invivo ME Sent33,

PSpass_b33 = P_invivo Sent33,

PSpass_lum_a33 = Ppass_lum_a33 ME Sent33,

PSap33 = PSpass_lum_a33,

PSbp33 = PSpass_b33,

PSbx33 = PSpass_b33,

PSpgp33 = psf_Pgp Vmax_Pgp Arel_Pgp33 /(Km_Pgp+fent y133/Vent33),

PSax33 = (PSpass_a33+ PSpgp33),

CL33 = Vmax_3A4 Arel_3A4_33 /(Km_3A4+fent y133/Vent33)/(1+(fent_inh*y263/Vent33)/Ki_3A4),

Ppass_lum_a34 = P_invivo (1+10^(pH_Caco2-pKa_acid)+10^(pKa_base-pH_Caco2))/(1+10^(pH_lum34-pKa_acid)+10^(pKa_base-pH_lum34)),

PSpass_a34 = P_invivo ME Sent34,

PSpass_b34 = P_invivo Sent34,

PSpass_lum_a34 = Ppass_lum_a34 ME Sent34,

PSap34 = PSpass_lum_a34,

PSbp34 = PSpass_b34,

PSbx34 = PSpass_b34,

PSpgp34 = psf_Pgp Vmax_Pgp Arel_Pgp34 /(Km_Pgp+fent y134/Vent34),

PSax34 = (PSpass_a34+ PSpgp34),

CL34 = Vmax_3A4 Arel_3A4_34 /(Km_3A4+fent y134/Vent34)/(1+(fent_inh*y264/Vent34)/Ki_3A4),

Ppass_lum_a35 = P_invivo (1+10^(pH_Caco2-pKa_acid)+10^(pKa_base-pH_Caco2))/(1+10^(pH_lum35-pKa_acid)+10^(pKa_base-pH_lum35)),

PSpass_a35 = P_invivo ME Sent35,

PSpass_b35 = P_invivo Sent35,

PSpass_lum_a35 = Ppass_lum_a35 ME Sent35,

PSap35 = PSpass_lum_a35,

PSbp35 = PSpass_b35,

PSbx35 = PSpass_b35,

PSpgp35 = psf_Pgp Vmax_Pgp Arel_Pgp35 /(Km_Pgp+fent y135/Vent35),

PSax35 = (PSpass_a35+ PSpgp35),

CL35 = Vmax_3A4 Arel_3A4_35 /(Km_3A4+fent y135/Vent35)/(1+(fent_inh*y265/Vent35)/Ki_3A4),

Ppass_lum_a36 = P_invivo (1+10^(pH_Caco2-pKa_acid)+10^(pKa_base-pH_Caco2))/(1+10^(pH_lum36-pKa_acid)+10^(pKa_base-pH_lum36)),

PSpass_a36 = P_invivo ME Sent36,

PSpass_b36 = P_invivo Sent36,

PSpass_lum_a36 = Ppass_lum_a36 ME Sent36,

PSap36 = PSpass_lum_a36,

PSbp36 = PSpass_b36,

PSbx36 = PSpass_b36,

PSpgp36 = psf_Pgp Vmax_Pgp Arel_Pgp36 /(Km_Pgp+fent y136/Vent36),

PSax36 = (PSpass_a36+ PSpgp36),

CL36 = Vmax_3A4 Arel_3A4_36 /(Km_3A4+fent y136/Vent36)/(1+(fent_inh*y266/Vent36)/Ki_3A4),

Ppass_lum_a37 = P_invivo (1+10^(pH_Caco2-pKa_acid)+10^(pKa_base-pH_Caco2))/(1+10^(pH_lum37-pKa_acid)+10^(pKa_base-pH_lum37)),

PSpass_a37 = P_invivo ME Sent37,

PSpass_b37 = P_invivo Sent37,

PSpass_lum_a37 = Ppass_lum_a37 ME Sent37,

PSap37 = PSpass_lum_a37,

PSbp37 = PSpass_b37,

PSbx37 = PSpass_b37,

PSpgp37 = psf_Pgp Vmax_Pgp Arel_Pgp37 /(Km_Pgp+fent y137/Vent37),

PSax37 = (PSpass_a37+ PSpgp37),

CL37 = Vmax_3A4 Arel_3A4_37 /(Km_3A4+fent y137/Vent37)/(1+(fent_inh*y267/Vent37)/Ki_3A4),

Ppass_lum_a38 = P_invivo (1+10^(pH_Caco2-pKa_acid)+10^(pKa_base-pH_Caco2))/(1+10^(pH_lum38-pKa_acid)+10^(pKa_base-pH_lum38)),

PSpass_a38 = P_invivo ME Sent38,

PSpass_b38 = P_invivo Sent38,

PSpass_lum_a38 = Ppass_lum_a38 ME Sent38,

PSap38 = PSpass_lum_a38,

PSbp38 = PSpass_b38,

PSbx38 = PSpass_b38,

PSpgp38 = psf_Pgp Vmax_Pgp Arel_Pgp38 /(Km_Pgp+fent y138/Vent38),

PSax38 = (PSpass_a38+ PSpgp38),

CL38 = Vmax_3A4 Arel_3A4_38 /(Km_3A4+fent y138/Vent38)/(1+(fent_inh*y268/Vent38)/Ki_3A4),

Ppass_lum_a39 = P_invivo (1+10^(pH_Caco2-pKa_acid)+10^(pKa_base-pH_Caco2))/(1+10^(pH_lum39-pKa_acid)+10^(pKa_base-pH_lum39)),

PSpass_a39 = P_invivo ME Sent39,

PSpass_b39 = P_invivo Sent39,

PSpass_lum_a39 = Ppass_lum_a39 ME Sent39,

PSap39 = PSpass_lum_a39,

PSbp39 = PSpass_b39,

PSbx39 = PSpass_b39,

PSpgp39 = psf_Pgp Vmax_Pgp Arel_Pgp39 /(Km_Pgp+fent y139/Vent39),

PSax39 = (PSpass_a39+ PSpgp39),

CL39 = Vmax_3A4 Arel_3A4_39 /(Km_3A4+fent y139/Vent39)/(1+(fent_inh*y269/Vent39)/Ki_3A4),

Ppass_lum_a40 = P_invivo (1+10^(pH_Caco2-pKa_acid)+10^(pKa_base-pH_Caco2))/(1+10^(pH_lum40-pKa_acid)+10^(pKa_base-pH_lum40)),

PSpass_a40 = P_invivo ME Sent40,

PSpass_b40 = P_invivo Sent40,

PSpass_lum_a40 = Ppass_lum_a40 ME Sent40,

PSap40 = PSpass_lum_a40,

PSbp40 = PSpass_b40,

PSbx40 = PSpass_b40,

PSpgp40 = psf_Pgp Vmax_Pgp Arel_Pgp40 /(Km_Pgp+fent y140/Vent40),

PSax40 = (PSpass_a40+ PSpgp40),

CL40 = Vmax_3A4 Arel_3A4_40 /(Km_3A4+fent

y140/Vent40)/(1+(fent_inh*y270/Vent40)/Ki_3A4),

; Water volume in the small intetstine at each location (substrate)

y1' = (kg * y43) Vg div/ V + (c3a_1-kw_1)*y1 + c4a_2*y2 + c5_3*y3+sw_1,

y2' = c2a_1*y1 + c3_2_kw*y2 + c4_3*y3 + c5_4*y4+sw_2,

y3' = c1_1*y1 + c2_2*y2 + c3_3_kw*y3 + c4_4*y4 + c5_5*y5+sw_3,

y4' = c1_2*y2 + c2_3*y3 + c3_4_kw*y4 + c4_5*y5 + c5_6*y6+sw_4,

y5' = c1_3*y3 + c2_4*y4 + c3_5_kw*y5 + c4_6*y6 + c5_7*y7+sw_5,

y6' = c1_4*y4 + c2_5*y5 + c3_6_kw*y6 + c4_7*y7 + c5_8*y8+sw_6,

y7' = c1_5*y5 + c2_6*y6 + c3_7_kw*y7 + c4_8*y8 + c5_9*y9+sw_7,

y8' = c1_6*y6 + c2_7*y7 + c3_8_kw*y8 + c4_9*y9 + c5_10*y10+sw_8,

y9' = c1_7*y7 + c2_8*y8 + c3_9_kw*y9 + c4_10*y10 + c5_11*y11+sw_9,

y10' = c1_8*y8 + c2_9*y9 + c3_10_kw*y10 + c4_11*y11 + c5_12*y12+sw_10,

y11' = c1_9*y9 + c2_10*y10 + c3_11_kw*y11 + c4_12*y12 + c5_13*y13+sw_11,

y12' = c1_10*y10 + c2_11*y11 + c3_12_kw*y12 + c4_13*y13 + c5_14*y14+sw_12,

y13' = c1_11*y11 + c2_12*y12 + c3_13_kw*y13 + c4_14*y14 + c5_15*y15+sw_13,

y14' = c1_12*y12 + c2_13*y13 + c3_14_kw*y14 + c4_15*y15 + c5_16*y16+sw_14,

y15' = c1_13*y13 + c2_14*y14 + c3_15_kw*y15 + c4_16*y16 + c5_17*y17+sw_15,

y16' = c1_14*y14 + c2_15*y15 + c3_16_kw*y16 + c4_17*y17 + c5_18*y18+sw_16,

y17' = c1_15*y15 + c2_16*y16 + c3_17_kw*y17 + c4_18*y18 + c5_19*y19+sw_17,

y18' = c1_16*y16 + c2_17*y17 + c3_18_kw*y18 + c4_19*y19 + c5_20*y20+sw_18,

y19' = c1_17*y17 + c2_18*y18 + c3_19_kw*y19 + c4_20*y20 + c5_21*y21+sw_19,

y20' = c1_18*y18 + c2_19*y19 + c3_20_kw*y20 + c4_21*y21 + c5_22*y22+sw_20,

y21' = c1_19*y19 + c2_20*y20 + c3_21_kw*y21 + c4_22*y22 + c5_23*y23+sw_21, y22' = c1_20*y20 + c2_21*y21 + c3_22_kw*y22 + c4_23*y23 + c5_24*y24+sw_22,

y23' = c1_21*y21 + c2_22*y22 + c3_23_kw*y23 + c4_24*y24 + c5_25*y25+sw_23,

y24' = c1_22*y22 + c2_23*y23 + c3_24_kw*y24 + c4_25*y25 + c5_26*y26+sw_24,

y25' = c1_23*y23 + c2_24*y24 + c3_25_kw*y25 + c4_26*y26 + c5_27*y27+sw_25,

y26' = c1_24*y24 + c2_25*y25 + c3_26_kw*y26 + c4_27*y27 + c5_28*y28+sw_26,

y27' = c1_25*y25 + c2_26*y26 + c3_27_kw*y27 + c4_28*y28 + c5_29*y29+sw_27,

y28' = c1_26*y26 + c2_27*y27 + c3_28_kw*y28 + c4_29*y29 + c5_30*y30+sw_28,

y29' = c1_27*y27 + c2_28*y28 + c3_29_kw*y29 + c4_30*y30 + c5_31*y31+sw_29,

y30' = c1_28*y28 + c2_29*y29 + c3_30_kw*y30 + c4_31*y31 + c5_32*y32+sw_30,

y31' = c1_29*y29 + c2_30*y30 + c3_31_kw*y31 + c4_32*y32 + c5_33*y33+sw_31,

y32' = c1_30*y30 + c2_31*y31 + c3_32_kw*y32 + c4_33*y33 + c5_34*y34+sw_32,

y33' = c1_31*y31 + c2_32*y32 + c3_33_kw*y33 + c4_34*y34 + c5_35*y35+sw_33,

y34' = c1_32*y32 + c2_33*y33 + c3_34_kw*y34 + c4_35*y35 + c5_36*y36+sw_34,

y35' = c1_33*y33 + c2_34*y34 + c3_35_kw*y35 + c4_36*y36 + c5_37*y37+sw_35,

y36' = c1_34*y34 + c2_35*y35 + c3_36_kw*y36 + c4_37*y37 + c5_38*y38+sw_36,

y37' = c1_35*y35 + c2_36*y36 + c3_37_kw*y37 + c4_38*y38 + c5_39*y39+sw_37,

y38' = c1_36*y36 + c2_37*y37 + c3_38_kw*y38 + c4_39*y39 + c5_40*y40+sw_38,

y39' = c1_37*y37 + c2_38*y38 + c3_39_kw*y39 + c4a_40*y40+sw_39,

y40' = c1_38*y38 + c2b_39*y39 + (c3b_40-kw_40)*y40+sw_40,

; Water volume in the caecum/colon

y41' = ((9.0 y40 - y39) / 8.0) Q - (kw_col+krec) * y41+sw_col,

; Water volume in feces (assumed to be 0)

y42' = krec*y41,

; Water volume in stomach

y43' = ka*y50-(kg+kw_gut) * y43+sw_gut,

; Water volume in the upper small intestine (not used in this study)

y44=(y1+y2+y3+y4+y5+y6+y7+y8+y9+y10+y11+y12+y13+y14+y15+y16+y17+y18+y19+y20+y21+y22+y23+y24),

; Water volume in the lower small intestine (not used in this study)

y45=(y25+y26+y27+y28+y29+y30+y31+y32+y33+y34+y35+y36+y37+y38+y39+y40),

; Water volume in the whole small intestine

y46 = y1+y2+y3+y4+y5+y6+y7+y8+y9+y10+y11+y12+y13+y14+y15+y16+y17+y18+y19+y20+y21+y22+y23+y24+y25+y26+y27+y28+y29+y30+y31+y32+y33+y34+y35+y36+y37+y38+y39+y40,

; Water volume in distal jejunum and proximal ileum（not used in this study）

y48 = (y12+y13+y14+y15+y16+y17+y18+y19+y20+y21+y22+y23+y24+y25+y26+y27+y28+y29+y30),

; Water volume in distal ileum（not used in this study）

y49 = (y31+y32+y33+y34+y35+y36+y37+y38+y39+y40),

```
; Water volume in the esophagus）

y50'    = -ka*y50,


; Following is the codes about a substrate

; Drug concentration in the small intestine

y51' = (kg * y93) * Vg div / V + c3a_1*y51 + c4a_2*y52 + c5_3*y53-

PSap1*y51/y1+PSax1*fent*y101/Vent1/(V/div),

if y51 < 0 then y51=0 endif,

y52' = c2a_1*y51 + c3_2*y52 + c4_3*y53 + c5_4*y54-

PSap2*y52/y2+PSax2*fent*y102/Vent2/(V/div),

if y52 < 0 then y52=0 endif,

y53' = c1_1*y51 + c2_2*y52 + c3_3*y53 + c4_4*y54 + c5_5*y55-

PSap3*y53/y3+PSax3*fent*y103/Vent3/(V/div),

if y53 < 0 then y53=0 endif,

y54' = c1_2*y52 + c2_3*y53 + c3_4*y54 + c4_5*y55 + c5_6*y56-

PSap4*y54/y4+PSax4*fent*y104/Vent4/(V/div),

if y54 < 0 then y54=0 endif,

y55' = c1_3*y53 + c2_4*y54 + c3_5*y55 + c4_6*y56 + c5_7*y57-

PSap5*y55/y5+PSax5*fent*y105/Vent5/(V/div),

if y55 < 0 then y55=0 endif,

y56' = c1_4*y54 + c2_5*y55 + c3_6*y56 + c4_7*y57 + c5_8*y58-

PSap6*y56/y6+PSax6*fent*y106/Vent6/(V/div),

if y56 < 0 then y56=0 endif,

y57' = c1_5*y55 + c2_6*y56 + c3_7*y57 + c4_8*y58 + c5_9*y59-

PSap7*y57/y7+PSax7*fent*y107/Vent7/(V/div),
```

```
if y57 < 0 then y57=0 endif,

y58' = c1_6*y56 + c2_7*y57 + c3_8*y58 + c4_9*y59 + c5_10*y60-

PSap8*y58/y8+PSax8*fent*y108/Vent8/(V/div),

if y58 < 0 then y58=0 endif,

y59' = c1_7*y57 + c2_8*y58 + c3_9*y59 + c4_10*y60 + c5_11*y61-

PSap9*y59/y9+PSax9*fent*y109/Vent9/(V/div),

if y59 < 0 then y59=0 endif,

y60' = c1_8*y58 + c2_9*y59 + c3_10*y60 + c4_11*y61 + c5_12*y62-

PSap10*y60/y10+PSax10*fent*y110/Vent10/(V/div),

if y60 < 0 then y60=0 endif,

y61' = c1_9*y59 + c2_10*y60 + c3_11*y61 + c4_12*y62 + c5_13*y63-

PSap11*y61/y11+PSax11*fent*y111/Vent11/(V/div),

if y61 < 0 then y61=0 endif,

y62' = c1_10*y60 + c2_11*y61 + c3_12*y62 + c4_13*y63 + c5_14*y64-

PSap12*y62/y12+PSax12*fent*y112/Vent12/(V/div),

if y62 < 0 then y62=0 endif,

y63' = c1_11*y61 + c2_12*y62 + c3_13*y63 + c4_14*y64 + c5_15*y65-

PSap13*y63/y13+PSax13*fent*y113/Vent13/(V/div),

if y63 < 0 then y63=0 endif,

y64' = c1_12*y62 + c2_13*y63 + c3_14*y64 + c4_15*y65 + c5_16*y66-

PSap14*y64/y14+PSax14*fent*y114/Vent14/(V/div),

if y64 < 0 then y64=0 endif,

y65' = c1_13*y63 + c2_14*y64 + c3_15*y65 + c4_16*y66 + c5_17*y67-

PSap15*y65/y15+PSax15*fent*y115/Vent15/(V/div),

if y65 < 0 then y65=0 endif,
```

```
y66' = c1_14*y64 + c2_15*y65 + c3_16*y66 + c4_17*y67 + c5_18*y68-
PSap16*y66/y16+PSax16*fent*y116/Vent16/(V/div),
if y66 < 0 then y66=0 endif,
y67' = c1_15*y65 + c2_16*y66 + c3_17*y67 + c4_18*y68 + c5_19*y69-
PSap17*y67/y17+PSax17*fent*y117/Vent17/(V/div),
if y67 < 0 then y67=0 endif,
y68' = c1_16*y66 + c2_17*y67 + c3_18*y68 + c4_19*y69 + c5_20*y70-
PSap18*y68/y18+PSax18*fent*y118/Vent18/(V/div),
if y68 < 0 then y68=0 endif,
y69' = c1_17*y67 + c2_18*y68 + c3_19*y69 + c4_20*y70 + c5_21*y71-
PSap19*y69/y19+PSax19*fent*y119/Vent19/(V/div),
if y69 < 0 then y69=0 endif,
y70' = c1_18*y68 + c2_19*y69 + c3_20*y70 + c4_21*y71 + c5_22*y72-
PSap20*y70/y20+PSax20*fent*y120/Vent20/(V/div),
if y70 < 0 then y70=0 endif,
y71' = c1_19*y69 + c2_20*y70 + c3_21*y71 + c4_22*y72 + c5_23*y73-
PSap21*y71/y21+PSax21*fent*y121/Vent21/(V/div),
if y71 < 0 then y71=0 endif,
y72' = c1_20*y70 + c2_21*y71 + c3_22*y72 + c4_23*y73 + c5_24*y74-
PSap22*y72/y22+PSax22*fent*y122/Vent22/(V/div),
if y72 < 0 then y72=0 endif,
y73' = c1_21*y71 + c2_22*y72 + c3_23*y73 + c4_24*y74 + c5_25*y75-
PSap23*y73/y23+PSax23*fent*y123/Vent23/(V/div),
if y73 < 0 then y73=0 endif,
```

y74' = c1_22*y72 + c2_23*y73 + c3_24*y74 + c4_25*y75 + c5_26*y76-

PSap24*y74/y24+PSax24*fent*y124/Vent24/(V/div),

if y74 < 0 then y74=0 endif,

y75' = c1_23*y73 + c2_24*y74 + c3_25*y75 + c4_26*y76 + c5_27*y77-

PSap25*y75/y25+PSax25*fent*y125/Vent25/(V/div),

if y75 < 0 then y75=0 endif,

y76' = c1_24*y74 + c2_25*y75 + c3_26*y76 + c4_27*y77 + c5_28*y78-

PSap26*y76/y26+PSax26*fent*y126/Vent26/(V/div),

if y76 < 0 then y76=0 endif,

y77' = c1_25*y75 + c2_26*y76 + c3_27*y77 + c4_28*y78 + c5_29*y79-

PSap27*y77/y27+PSax27*fent*y127/Vent27/(V/div),

if y77 < 0 then y77=0 endif,

y78' = c1_26*y76 + c2_27*y77 + c3_28*y78 + c4_29*y79 + c5_30*y80-

PSap28*y78/y28+PSax28*fent*y128/Vent28/(V/div),

if y78 < 0 then y78=0 endif,

y79' = c1_27*y77 + c2_28*y78 + c3_29*y79 + c4_30*y80 + c5_31*y81-

PSap29*y79/y29+PSax29*fent*y129/Vent29/(V/div),

if y79 < 0 then y79=0 endif,

y80' = c1_28*y78 + c2_29*y79 + c3_30*y80 + c4_31*y81 + c5_32*y82-

PSap30*y80/y30+PSax30*fent*y130/Vent30/(V/div),

if y80 < 0 then y80=0 endif,

y81' = c1_29*y79 + c2_30*y80 + c3_31*y81 + c4_32*y82 + c5_33*y83-

PSap31*y81/y31+PSax31*fent*y131/Vent31/(V/div),

if y81 < 0 then y81=0 endif,

```
y82' = c1_30*y80 + c2_31*y81 + c3_32*y82 + c4_33*y83 + c5_34*y84-
PSap32*y82/y32+PSax32*fent*y132/Vent32/(V/div),
if y82 < 0 then y82=0 endif,
y83' = c1_31*y81 + c2_32*y82 + c3_33*y83 + c4_34*y84 + c5_35*y85-
PSap33*y83/y33+PSax33*fent*y133/Vent33/(V/div),
if y83 < 0 then y83=0 endif,
y84' = c1_32*y82 + c2_33*y83 + c3_34*y84 + c4_35*y85 + c5_36*y86-
PSap34*y84/y34+PSax34*fent*y134/Vent34/(V/div),
if y84 < 0 then y84=0 endif,
y85' = c1_33*y83 + c2_34*y84 + c3_35*y85 + c4_36*y86 + c5_37*y87-
PSap35*y85/y35+PSax35*fent*y135/Vent35/(V/div),
if y85 < 0 then y85=0 endif,
y86' = c1_34*y84 + c2_35*y85 + c3_36*y86 + c4_37*y87 + c5_38*y88-
PSap36*y86/y36+PSax36*fent*y136/Vent36/(V/div),
if y86 < 0 then y86=0 endif,
y87' = c1_35*y85 + c2_36*y86 + c3_37*y87 + c4_38*y88 + c5_39*y89-
PSap37*y87/y37+PSax37*fent*y137/Vent37/(V/div),
if y87 < 0 then y87=0 endif,
y88' = c1_36*y86 + c2_37*y87 + c3_38*y88 + c4_39*y89 + c5_40*y90-
PSap38*y88/y38+PSax38*fent*y138/Vent38/(V/div),
if y88 < 0 then y88=0 endif,
y89' = c1_37*y87 + c2_38*y88 + c3_39*y89 + c4a_40*y90-
PSap39*y89/y39+PSax39*fent*y139/Vent39/(V/div),
if y89 < 0 then y89=0 endif,
```

y90' = c1_38*y88 + c2b_39*y89 + c3b_40*y90-

PSap40*y90/y40+PSax40*fent*y140/Vent40/(V/div),

if y90 < 0 then y90=0 endif,

; Drug amount in the colon

y91' = ((9.0 y90 - y89) / 8.0) Q   - krec * y91,

; Drug amount in the feces

y92' = krec*y91 * Vcae_col,

; Drug concentration in the stomach

y93' = ka*y100*Ves/Vg-kg*y93,

; % of dose in stomach (used in the analysis of ^{99m}Tc-DTPA)

y94 = y93 Vg / dose*100,

; % of dose in jejunum (used in the analysis of ^{99m}Tc-DTPA)

y95=(y51+y52+y53+y54+y55+y56+y57+y58+y59+y60+y61+y62+y63+y64+y65+y66+y67+

y68+y69+y70) V/div/dose*100,

; % of dose in ileum (used in the analysis of ^{99m}Tc-DTPA)

y96=(y71+y72+y73+y74+y75+y76+y77+y78+y79+y80+y81+y82+y83+y84+y85+y86+y87+

y88+y89+y90) V/div/dose*100,

; % of dose in colon (used in the analysis of ^{99m}Tc-DTPA)

```
y97 = y91 Vc / dose * 100,

; % of dose in whole lumen (not used in this study)
y98 = y95 + y96 + y97,

; Drug amount in the gastrointestinal tract (not used in this study)
y99 = y94+y95+y96+y97,

; Drug concentration in the esophagus
y100'=-ka*y100,

; Drug amount in the enterocytes
y101'=PSap1*y51*(V/div)/y1-(PSax1+CL1+PSbp1)*fent*y101/Vent1+PSbx1*y141/Vlam1,
if y101 < 0 then y101=0 endif,
y102'=PSap2*y52*(V/div)/y2-(PSax2+CL2+PSbp2)*fent*y102/Vent2+PSbx2*y142/Vlam2,
if y102 < 0 then y102=0 endif,
y103'=PSap3*y53*(V/div)/y3-(PSax3+CL3+PSbp3)*fent*y103/Vent3+PSbx3*y143/Vlam3,
if y103 < 0 then y103=0 endif,
y104'=PSap4*y54*(V/div)/y4-(PSax4+CL4+PSbp4)*fent*y104/Vent4+PSbx4*y144/Vlam4,
if y104 < 0 then y104=0 endif,
y105'=PSap5*y55*(V/div)/y5-(PSax5+CL5+PSbp5)*fent*y105/Vent5+PSbx5*y145/Vlam5,
if y105 < 0 then y105=0 endif,
y106'=PSap6*y56*(V/div)/y6-(PSax6+CL6+PSbp6)*fent*y106/Vent6+PSbx6*y146/Vlam6,
if y106 < 0 then y106=0 endif,
y107'=PSap7*y57*(V/div)/y7-(PSax7+CL7+PSbp7)*fent*y107/Vent7+PSbx7*y147/Vlam7,
```

```
if y107 < 0 then y107=0 endif,
y108'=PSap8*y58*(V/div)/y8-(PSax8+CL8+PSbp8)*fent*y108/Vent8+PSbx8*y148/Vlam8,
if y108 < 0 then y108=0 endif,
y109'=PSap9*y59*(V/div)/y9-(PSax9+CL9+PSbp9)*fent*y109/Vent9+PSbx9*y149/Vlam9,
if y109 < 0 then y109=0 endif,
y110'=PSap10*y60*(V/div)/y10-
(PSax10+CL10+PSbp10)*fent*y110/Vent10+PSbx10*y150/Vlam10,
if y110 < 0 then y110=0 endif,
y111'=PSap11*y61*(V/div)/y11-
(PSax11+CL11+PSbp11)*fent*y111/Vent11+PSbx11*y151/Vlam11,
if y111 < 0 then y111=0 endif,
y112'=PSap12*y62*(V/div)/y12-
(PSax12+CL12+PSbp12)*fent*y112/Vent12+PSbx12*y152/Vlam12,
if y112 < 0 then y112=0 endif,
y113'=PSap13*y63*(V/div)/y13-
(PSax13+CL13+PSbp13)*fent*y113/Vent13+PSbx13*y153/Vlam13,
if y113 < 0 then y113=0 endif,
y114'=PSap14*y64*(V/div)/y14-
(PSax14+CL14+PSbp14)*fent*y114/Vent14+PSbx14*y154/Vlam14,
if y114 < 0 then y114=0 endif,
y115'=PSap15*y65*(V/div)/y15-
(PSax15+CL15+PSbp15)*fent*y115/Vent15+PSbx15*y155/Vlam15,
if y115 < 0 then y115=0 endif,
y116'=PSap16*y66*(V/div)/y16-
(PSax16+CL16+PSbp16)*fent*y116/Vent16+PSbx16*y156/Vlam16,
```

```
if y116 < 0 then y116=0 endif,

y117'=PSap17*y67*(V/div)/y17-

(PSax17+CL17+PSbp17)*fent*y117/Vent17+PSbx17*y157/Vlam17,

if y117 < 0 then y117=0 endif,

y118'=PSap18*y68*(V/div)/y18-

(PSax18+CL18+PSbp18)*fent*y118/Vent18+PSbx18*y158/Vlam18,

if y118 < 0 then y118=0 endif,

y119'=PSap19*y69*(V/div)/y19-

(PSax19+CL19+PSbp19)*fent*y119/Vent19+PSbx19*y159/Vlam19,

if y119 < 0 then y119=0 endif,

y120'=PSap20*y70*(V/div)/y20-

(PSax20+CL20+PSbp20)*fent*y120/Vent20+PSbx20*y160/Vlam20,

if y120 < 0 then y120=0 endif,

y121'=PSap21*y71*(V/div)/y21-

(PSax21+CL21+PSbp21)*fent*y121/Vent21+PSbx21*y161/Vlam21,

if y121 < 0 then y121=0 endif,

y122'=PSap22*y72*(V/div)/y22-

(PSax22+CL22+PSbp22)*fent*y122/Vent22+PSbx22*y162/Vlam22,

if y122 < 0 then y122=0 endif,

y123'=PSap23*y73*(V/div)/y23-

(PSax23+CL23+PSbp23)*fent*y123/Vent23+PSbx23*y163/Vlam23,

if y123 < 0 then y123=0 endif,

y124'=PSap24*y74*(V/div)/y24-

(PSax24+CL24+PSbp24)*fent*y124/Vent24+PSbx24*y164/Vlam24,

if y124 < 0 then y124=0 endif,
```

```
y125'=PSap25*y75*(V/div)/y25-
(PSax25+CL25+PSbp25)*fent*y125/Vent25+PSbx25*y165/Vlam25,
if y125 < 0 then y125=0 endif,
y126'=PSap26*y76*(V/div)/y26-
(PSax26+CL26+PSbp26)*fent*y126/Vent26+PSbx26*y166/Vlam26,
if y126 < 0 then y126=0 endif,
y127'=PSap27*y77*(V/div)/y27-
(PSax27+CL27+PSbp27)*fent*y127/Vent27+PSbx27*y167/Vlam27,
if y127 < 0 then y127=0 endif,
y128'=PSap28*y78*(V/div)/y28-
(PSax28+CL28+PSbp28)*fent*y128/Vent28+PSbx28*y168/Vlam28,
if y128 < 0 then y128=0 endif,
y129'=PSap29*y79*(V/div)/y29-
(PSax29+CL29+PSbp29)*fent*y129/Vent29+PSbx29*y169/Vlam29,
if y129 < 0 then y129=0 endif,
y130'=PSap30*y80*(V/div)/y30-
(PSax30+CL30+PSbp30)*fent*y130/Vent30+PSbx30*y170/Vlam30,
if y130 < 0 then y130=0 endif,
y131'=PSap31*y81*(V/div)/y31-
(PSax31+CL31+PSbp31)*fent*y131/Vent31+PSbx31*y171/Vlam31,
if y131 < 0 then y131=0 endif,
y132'=PSap32*y82*(V/div)/y32-
(PSax32+CL32+PSbp32)*fent*y132/Vent32+PSbx32*y172/Vlam32,
if y132 < 0 then y132=0 endif,
```

y133'=PSap33*y83*(V/div)/y33-

(PSax33+CL33+PSbp33)*fent*y133/Vent33+PSbx33*y173/Vlam33,

if y133 < 0 then y133=0 endif,

y134'=PSap34*y84*(V/div)/y34-

(PSax34+CL34+PSbp34)*fent*y134/Vent34+PSbx34*y174/Vlam34,

if y134 < 0 then y134=0 endif,

y135'=PSap35*y85*(V/div)/y35-

(PSax35+CL35+PSbp35)*fent*y135/Vent35+PSbx35*y175/Vlam35,

if y135 < 0 then y135=0 endif,

y136'=PSap36*y86*(V/div)/y36-

(PSax36+CL36+PSbp36)*fent*y136/Vent36+PSbx36*y176/Vlam36,

if y136 < 0 then y136=0 endif,

y137'=PSap37*y87*(V/div)/y37-

(PSax37+CL37+PSbp37)*fent*y137/Vent37+PSbx37*y177/Vlam37,

if y137 < 0 then y137=0 endif,

y138'=PSap38*y88*(V/div)/y38-

(PSax38+CL38+PSbp38)*fent*y138/Vent38+PSbx38*y178/Vlam38,

if y138 < 0 then y138=0 endif,

y139'=PSap39*y89*(V/div)/y39-

(PSax39+CL39+PSbp39)*fent*y139/Vent39+PSbx39*y179/Vlam39,

if y139 < 0 then y139=0 endif,

y140'=PSap40*y90*(V/div)/y40-

(PSax40+CL40+PSbp40)*fent*y140/Vent40+PSbx40*y180/Vlam40,

if y140 < 0 then y140=0 endif,

```
; Drug amount in the lamina propria

y141'= PSbp1*fent*y101/Vent1- (Qlam1/fb+PSbx1)*y141/Vlam1,

if y141 < 0 then y141=0 endif,

y142'= PSbp2*fent*y102/Vent2- (Qlam2/fb+PSbx2)*y142/Vlam2,

if y142 < 0 then y142=0 endif,

y143'= PSbp3*fent*y103/Vent3- (Qlam3/fb+PSbx3)*y143/Vlam3,

if y143 < 0 then y143=0 endif,

y144'= PSbp4*fent*y104/Vent4- (Qlam4/fb+PSbx4)*y144/Vlam4,

if y144 < 0 then y144=0 endif,

y145'= PSbp5*fent*y105/Vent5- (Qlam5/fb+PSbx5)*y145/Vlam5,

if y145 < 0 then y145=0 endif,

y146'= PSbp6*fent*y106/Vent6- (Qlam6/fb+PSbx6)*y146/Vlam6,

if y146 < 0 then y146=0 endif,

y147'= PSbp7*fent*y107/Vent7- (Qlam7/fb+PSbx7)*y147/Vlam7,

if y147 < 0 then y147=0 endif,

y148'= PSbp8*fent*y108/Vent8- (Qlam8/fb+PSbx8)*y148/Vlam8,

if y148 < 0 then y148=0 endif,

y149'= PSbp9*fent*y109/Vent9- (Qlam9/fb+PSbx9)*y149/Vlam9,

if y149 < 0 then y149=0 endif,

y150'= PSbp10*fent*y110/Vent10- (Qlam10/fb+PSbx10)*y150/Vlam10,

if y150 < 0 then y150=0 endif,

y151'= PSbp11*fent*y111/Vent11- (Qlam11/fb+PSbx11)*y151/Vlam11,

if y151 < 0 then y151=0 endif,

y152'= PSbp12*fent*y112/Vent12- (Qlam12/fb+PSbx12)*y152/Vlam12,

if y152 < 0 then y152=0 endif,
```

```
y153'= PSbp13*fent*y113/Vent13- (Qlam13/fb+PSbx13)*y153/Vlam13,

if y153 < 0 then y153=0 endif,

y154'= PSbp14*fent*y114/Vent14- (Qlam14/fb+PSbx14)*y154/Vlam14,

if y154 < 0 then y154=0 endif,

y155'= PSbp15*fent*y115/Vent15- (Qlam15/fb+PSbx15)*y155/Vlam15,

if y155 < 0 then y155=0 endif,

y156'= PSbp16*fent*y116/Vent16- (Qlam16/fb+PSbx16)*y156/Vlam16,

if y156 < 0 then y156=0 endif,

y157'= PSbp17*fent*y117/Vent17- (Qlam17/fb+PSbx17)*y157/Vlam17,

if y157 < 0 then y157=0 endif,

y158'= PSbp18*fent*y118/Vent18- (Qlam18/fb+PSbx18)*y158/Vlam18,

if y158 < 0 then y158=0 endif,

y159'= PSbp19*fent*y119/Vent19- (Qlam19/fb+PSbx19)*y159/Vlam19,

if y159 < 0 then y159=0 endif,

y160'= PSbp20*fent*y120/Vent20- (Qlam20/fb+PSbx20)*y160/Vlam20,

if y160 < 0 then y160=0 endif,

y161'= PSbp21*fent*y121/Vent21- (Qlam21/fb+PSbx21)*y161/Vlam21,

if y161 < 0 then y161=0 endif,

y162'= PSbp22*fent*y122/Vent22- (Qlam22/fb+PSbx22)*y162/Vlam22,

if y162 < 0 then y162=0 endif,

y163'= PSbp23*fent*y123/Vent23- (Qlam23/fb+PSbx23)*y163/Vlam23,

if y163 < 0 then y163=0 endif,

y164'= PSbp24*fent*y124/Vent24- (Qlam24/fb+PSbx24)*y164/Vlam24,

if y164 < 0 then y164=0 endif,

y165'= PSbp25*fent*y125/Vent25- (Qlam25/fb+PSbx25)*y165/Vlam25,
```

```
if y165 < 0 then y165=0 endif,

y166'= PSbp26*fent*y126/Vent26- (Qlam26/fb+PSbx26)*y166/Vlam26,

if y166 < 0 then y166=0 endif,

y167'= PSbp27*fent*y127/Vent27- (Qlam27/fb+PSbx27)*y167/Vlam27,

if y167 < 0 then y167=0 endif,

y168'= PSbp28*fent*y128/Vent28- (Qlam28/fb+PSbx28)*y168/Vlam28,

if y168 < 0 then y168=0 endif,

y169'= PSbp29*fent*y129/Vent29- (Qlam29/fb+PSbx29)*y169/Vlam29,

if y169 < 0 then y169=0 endif,

y170'= PSbp30*fent*y130/Vent30- (Qlam30/fb+PSbx30)*y170/Vlam30,

if y170 < 0 then y170=0 endif,

y171'= PSbp31*fent*y131/Vent31- (Qlam31/fb+PSbx31)*y171/Vlam31,

if y171 < 0 then y171=0 endif,

y172'= PSbp32*fent*y132/Vent32- (Qlam32/fb+PSbx32)*y172/Vlam32,

if y172 < 0 then y172=0 endif,

y173'= PSbp33*fent*y133/Vent33- (Qlam33/fb+PSbx33)*y173/Vlam33,

if y173 < 0 then y173=0 endif,

y174'= PSbp34*fent*y134/Vent34- (Qlam34/fb+PSbx34)*y174/Vlam34,

if y174 < 0 then y174=0 endif,

y175'= PSbp35*fent*y135/Vent35- (Qlam35/fb+PSbx35)*y175/Vlam35,

if y175 < 0 then y175=0 endif,

y176'= PSbp36*fent*y136/Vent36- (Qlam36/fb+PSbx36)*y176/Vlam36,

if y176 < 0 then y176=0 endif,

y177'= PSbp37*fent*y137/Vent37- (Qlam37/fb+PSbx37)*y177/Vlam37,

if y177 < 0 then y177=0 endif,
```

y178'= PSbp38*fent*y138/Vent38- (Qlam38/fb+PSbx38)*y178/Vlam38,

if y178 < 0 then y178=0 endif,

y179'= PSbp39*fent*y139/Vent39- (Qlam39/fb+PSbx39)*y179/Vlam39,

if y179 < 0 then y179=0 endif,

y180'= PSbp40*fent*y140/Vent40- (Qlam40/fb+PSbx40)*y180/Vlam40,

if y180 < 0 then y180=0 endif,

; Drug accumulated amount in the portal vein

y181' =

(y141/Vlam1*Qlam1+y142/Vlam2*Qlam2+y143/Vlam3*Qlam3+y144/Vlam4*Qlam4+y145/Vlam5*Qlam5+y146/Vlam6*Qlam6+y147/Vlam7*Qlam7+y148/Vlam8*Qlam8+y149/Vlam9*Qlam9+y150/Vlam10*Qlam10+y151/Vlam11*Qlam11+y152/Vlam12*Qlam12+y153/Vlam13*Qlam13+y154/Vlam14*Qlam14+y155/Vlam15*Qlam15+y156/Vlam16*Qlam16+y157/Vlam17*Qlam17+y158/Vlam18*Qlam18+y159/Vlam19*Qlam19+y160/Vlam20*Qlam20+y161/Vlam21*Qlam21+y162/Vlam22*Qlam22+y163/Vlam23*Qlam23+y164/Vlam24*Qlam24+y165/Vlam25*Qlam25+y166/Vlam26*Qlam26+y167/Vlam27*Qlam27+y168/Vlam28*Qlam28+y169/Vlam29*Qlam29+y170/Vlam30*Qlam30+y171/Vlam31*Qlam31+y172/Vlam32*Qlam32+y173/Vlam33*Qlam33+y174/Vlam34*Qlam34+y175/Vlam35*Qlam35+y176/Vlam36*Qlam36+y177/Vlam37*Qlam37+y178/Vlam38*Qlam38+y179/Vlam39*Qlam39+y180/Vlam40*Qlam40)/fb,

; F_A of a substrate

y182 = 1-y91/dose,

; F_AF_G of a substrate

y183=y181/dose,

; F_G of a substrate

y184=y183/y182,

; Intestinal clearance amount (not used in this study)

y185'=CL1*y101/Vent1+CL2*y102/Vent2+CL3*y103/Vent3+CL4*y104/Vent4+CL5*y105/Vent5+CL6*y106/Vent6+CL7*y107/Vent7+CL8*y108/Vent8+CL9*y109/Vent9+CL10*y110/Vent10+CL11*y111/Vent11+CL12*y112/Vent12+CL13*y113/Vent13+CL14*y114/Vent14+CL15*y115/Vent15+CL16*y116/Vent16+CL17*y117/Vent17+CL18*y118/Vent18+CL19*y119/Vent19+CL20*y120/Vent20+CL21*y121/Vent21+CL22*y122/Vent22+CL23*y123/Vent23+CL24*y124/Vent24+CL25*y125/Vent25+CL26*y126/Vent26+CL27*y127/Vent27+CL28*y128/Vent28+CL29*y129/Vent29+CL30*y130/Vent30+CL31*y131/Vent31+CL32*y132/Vent32+CL33*y133/Vent33+CL34*y134/Vent34+CL35*y135/Vent35+CL36*y136/Vent36+CL37*y137/Vent37+CL38*y138/Vent38+CL39*y139/Vent39+CL40*y140/Vent40,

; Drug amount in the portal vein

y186' =

(y141/Vlam1*Qlam1+y142/Vlam2*Qlam2+y143/Vlam3*Qlam3+y144/Vlam4*Qlam4+y145/Vlam5*Qlam5+y146/Vlam6*Qlam6+y147/Vlam7*Qlam7+y148/Vlam8*Qlam8+y149/Vlam9*Qlam9+y150/Vlam10*Qlam10+y151/Vlam11*Qlam11+y152/Vlam12*Qlam12+y153/Vlam13*Qlam13+y154/Vlam14*Qlam14+y155/Vlam15*Qlam15+y156/Vlam16*Qlam16+y157/Vlam17*Qlam17+y158/Vlam18*Qlam18+y159/Vlam19*Qlam19+y160/Vlam20*Qlam20+y161/Vlam21*Qlam21+y162/Vlam22*Qlam22+y163/Vlam23*Qlam23+y164/Vlam24*Qlam24+y165/Vlam25*Qlam25+y166/Vlam26*Qlam26+y167/Vlam27*Qlam27+y168/Vlam28

```
*Qlam28+y169/Vlam29*Qlam29+y170/Vlam30*Qlam30+y171/Vlam31*Qlam31+y172/Vla
m32*Qlam32+y173/Vlam33*Qlam33+y174/Vlam34*Qlam34+y175/Vlam35*Qlam35+y176
/Vlam36*Qlam36+y177/Vlam37*Qlam37+y178/Vlam38*Qlam38+y179/Vlam39*Qlam39+
y180/Vlam40*Qlam40)/fb-Qpv*y186/Vpv,

; Drug concentration in the liver
y187'=(Qpv*y186/Vpv-Qh*y187/Kp_liver*Rb-
fb*Rb/Kp_liver*CLint_h/(1+fb_inh*y330/Ki_3A4)*y187+Qha*y188)/Vliver,

; Drug concentration in the blood
y188'=(Qh*y187/Kp_liver*Rb-Qha*y188-k12*y188*Vb+k21*y189)/Vb,

; Drug amount in the peripheral compartment 1
; The number of compartments can be increased as necessary
y189'=k12*y188*Vb-k21*y189,

; Drug concentration in the plasma (unit: umol/L)
y190=y188/MW/Rb*1000,

; Following is the codes about an inhibitor
; Membrane permeability of an inhibitor
Ppass_lum_a1_inh = P_invivo_inh (1+10^(pH_Caco2-pKa_acid_inh)+10^(pKa_base_inh-
pH_Caco2))/(1+10^(pH_lum1-pKa_acid_inh)
+10^(pKa_base_inh-pH_lum1)),
PSpass_lum_a1_inh= Ppass_lum_a1_inh ME Sent1,
```

PSpass_a1_inh = P_invivo_inh ME Sent1,

PSpass_b1_inh = P_invivo_inh Sent1,

PSap1_inh = PSpass_lum_a1_inh,

PSbp1_inh = PSpass_b1_inh,

PSbx1_inh = PSpass_b1_inh,

PSpgp1_inh = psf_Pgp*Vmax_Pgp_inh*Arel_Pgp1 /(Km_Pgp_inh+fent_inh*y231/Vent1),

PSax1_inh = (PSpass_a1_inh+ PSpgp1_inh),

CL1_inh = Vmax_3A4_inh*Arel_3A4_1 /(Km_3A4_inh+fent_inh*y231/Vent1),

Ppass_lum_a2_inh = P_invivo_inh (1+10^(pH_Caco2-pKa_acid_inh)+10^(pKa_base_inh-pH_Caco2))/(1+10^(pH_lum2-pKa_acid_inh)
+10^(pKa_base_inh-pH_lum2)),

PSpass_lum_a2_inh= Ppass_lum_a2_inh ME Sent2,

PSpass_a2_inh = P_invivo_inh ME Sent2,

PSpass_b2_inh = P_invivo_inh Sent2,

PSap2_inh = PSpass_lum_a2_inh,

PSbp2_inh = PSpass_b2_inh,

PSbx2_inh = PSpass_b2_inh,

PSpgp2_inh = psf_Pgp*Vmax_Pgp_inh*Arel_Pgp2 /(Km_Pgp_inh+fent_inh*y232/Vent2),

PSax2_inh = (PSpass_a2_inh+ PSpgp2_inh),

CL2_inh = Vmax_3A4_inh*Arel_3A4_2 /(Km_3A4_inh+fent_inh*y232/Vent2),

Ppass_lum_a3_inh = P_invivo_inh (1+10^(pH_Caco2-pKa_acid_inh)+10^(pKa_base_inh-pH_Caco2))/(1+10^(pH_lum3-pKa_acid_inh)
+10^(pKa_base_inh-pH_lum3)),

PSpass_lum_a3_inh= Ppass_lum_a3_inh ME Sent3,

PSpass_a3_inh = P_invivo_inh ME Sent3,

PSpass_b3_inh = P_invivo_inh Sent3,

PSap3_inh = PSpass_lum_a3_inh,

PSbp3_inh = PSpass_b3_inh,

PSbx3_inh = PSpass_b3_inh,

PSpgp3_inh = psf_Pgp*Vmax_Pgp_inh*Arel_Pgp3 /(Km_Pgp_inh+fent_inh*y233/Vent3),

PSax3_inh = (PSpass_a3_inh+ PSpgp3_inh),

CL3_inh = Vmax_3A4_inh*Arel_3A4_3 /(Km_3A4_inh+fent_inh*y233/Vent3),

Ppass_lum_a4_inh = P_invivo_inh (1+10^(pH_Caco2-pKa_acid_inh)+10^(pKa_base_inh-pH_Caco2))/(1+10^(pH_lum4-pKa_acid_inh)

+10^(pKa_base_inh-pH_lum4)),

PSpass_lum_a4_inh= Ppass_lum_a4_inh ME Sent4,

PSpass_a4_inh = P_invivo_inh ME Sent4,

PSpass_b4_inh = P_invivo_inh Sent4,

PSap4_inh = PSpass_lum_a4_inh,

PSbp4_inh = PSpass_b4_inh,

PSbx4_inh = PSpass_b4_inh,

PSpgp4_inh = psf_Pgp*Vmax_Pgp_inh*Arel_Pgp4 /(Km_Pgp_inh+fent_inh*y234/Vent4),

PSax4_inh = (PSpass_a4_inh+ PSpgp4_inh),

CL4_inh = Vmax_3A4_inh*Arel_3A4_4 /(Km_3A4_inh+fent_inh*y234/Vent4),

Ppass_lum_a5_inh = P_invivo_inh (1+10^(pH_Caco2-pKa_acid_inh)+10^(pKa_base_inh-pH_Caco2))/(1+10^(pH_lum5-pKa_acid_inh)

+10^(pKa_base_inh-pH_lum5)),

PSpass_lum_a5_inh= Ppass_lum_a5_inh ME Sent5,

PSpass_a5_inh = P_invivo_inh ME Sent5,

PSpass_b5_inh = P_invivo_inh Sent5,

PSap5_inh = PSpass_lum_a5_inh,

PSbp5_inh = PSpass_b5_inh,

PSbx5_inh = PSpass_b5_inh,

PSpgp5_inh = psf_Pgp*Vmax_Pgp_inh*Arel_Pgp5 /(Km_Pgp_inh+fent_inh*y235/Vent5),

PSax5_inh = (PSpass_a5_inh+ PSpgp5_inh),

CL5_inh =   Vmax_3A4_inh*Arel_3A4_5 /(Km_3A4_inh+fent_inh*y235/Vent5),

Ppass_lum_a6_inh = P_invivo_inh (1+10^(pH_Caco2-pKa_acid_inh)+10^(pKa_base_inh-pH_Caco2))/(1+10^(pH_lum6-pKa_acid_inh)

+10^(pKa_base_inh-pH_lum6)),

PSpass_lum_a6_inh= Ppass_lum_a6_inh ME Sent6,

PSpass_a6_inh = P_invivo_inh ME Sent6,

PSpass_b6_inh = P_invivo_inh Sent6,

PSap6_inh = PSpass_lum_a6_inh,

PSbp6_inh = PSpass_b6_inh,

PSbx6_inh = PSpass_b6_inh,

PSpgp6_inh = psf_Pgp*Vmax_Pgp_inh*Arel_Pgp6 /(Km_Pgp_inh+fent_inh*y236/Vent6),

PSax6_inh = (PSpass_a6_inh+ PSpgp6_inh),

CL6_inh =   Vmax_3A4_inh*Arel_3A4_6 /(Km_3A4_inh+fent_inh*y236/Vent6),

Ppass_lum_a7_inh = P_invivo_inh (1+10^(pH_Caco2-pKa_acid_inh)+10^(pKa_base_inh-pH_Caco2))/(1+10^(pH_lum7-pKa_acid_inh)

+10^(pKa_base_inh-pH_lum7)),

PSpass_lum_a7_inh= Ppass_lum_a7_inh ME Sent7,

PSpass_a7_inh = P_invivo_inh ME Sent7,

PSpass_b7_inh = P_invivo_inh Sent7,

PSap7_inh = PSpass_lum_a7_inh,

PSbp7_inh = PSpass_b7_inh,

PSbx7_inh = PSpass_b7_inh,

PSpgp7_inh = psf_Pgp*Vmax_Pgp_inh*Arel_Pgp7 /(Km_Pgp_inh+fent_inh*y237/Vent7),

PSax7_inh = (PSpass_a7_inh+ PSpgp7_inh),

CL7_inh = Vmax_3A4_inh*Arel_3A4_7 /(Km_3A4_inh+fent_inh*y237/Vent7),

Ppass_lum_a8_inh = P_invivo_inh (1+10^(pH_Caco2-pKa_acid_inh)+10^(pKa_base_inh-pH_Caco2))/(1+10^(pH_lum8-pKa_acid_inh)

+10^(pKa_base_inh-pH_lum8)),

PSpass_lum_a8_inh= Ppass_lum_a8_inh ME Sent8,

PSpass_a8_inh = P_invivo_inh ME Sent8,

PSpass_b8_inh = P_invivo_inh Sent8,

PSap8_inh = PSpass_lum_a8_inh,

PSbp8_inh = PSpass_b8_inh,

PSbx8_inh = PSpass_b8_inh,

PSpgp8_inh = psf_Pgp*Vmax_Pgp_inh*Arel_Pgp8 /(Km_Pgp_inh+fent_inh*y238/Vent8),

PSax8_inh = (PSpass_a8_inh+ PSpgp8_inh),

CL8_inh = Vmax_3A4_inh*Arel_3A4_8 /(Km_3A4_inh+fent_inh*y238/Vent8),

Ppass_lum_a9_inh = P_invivo_inh (1+10^(pH_Caco2-pKa_acid_inh)+10^(pKa_base_inh-pH_Caco2))/(1+10^(pH_lum9-pKa_acid_inh)

+10^(pKa_base_inh-pH_lum9)),

PSpass_lum_a9_inh= Ppass_lum_a9_inh ME Sent9,

PSpass_a9_inh = P_invivo_inh ME Sent9,

PSpass_b9_inh = P_invivo_inh Sent9,

PSap9_inh = PSpass_lum_a9_inh,

PSbp9_inh = PSpass_b9_inh,

PSbx9_inh = PSpass_b9_inh,

PSpgp9_inh = psf_Pgp*Vmax_Pgp_inh*Arel_Pgp9 /(Km_Pgp_inh+fent_inh*y239/Vent9),

PSax9_inh = (PSpass_a9_inh+ PSpgp9_inh),

CL9_inh = Vmax_3A4_inh*Arel_3A4_9 /(Km_3A4_inh+fent_inh*y239/Vent9),

Ppass_lum_a10_inh = P_invivo_inh (1+10^(pH_Caco2-pKa_acid_inh)+10^(pKa_base_inh-pH_Caco2))/(1+10^(pH_lum10-pKa_acid_inh)

+10^(pKa_base_inh-pH_lum10)),

PSpass_lum_a10_inh= Ppass_lum_a10_inh ME Sent10,

PSpass_a10_inh = P_invivo_inh ME Sent10,

PSpass_b10_inh = P_invivo_inh Sent10,

PSap10_inh = PSpass_lum_a10_inh,

PSbp10_inh = PSpass_b10_inh,

PSbx10_inh = PSpass_b10_inh,

PSpgp10_inh = psf_Pgp*Vmax_Pgp_inh*Arel_Pgp10 /(Km_Pgp_inh+fent_inh*y240/Vent10),

PSax10_inh = (PSpass_a10_inh+ PSpgp10_inh),

CL10_inh =   Vmax_3A4_inh*Arel_3A4_10 /(Km_3A4_inh+fent_inh*y240/Vent10),

Ppass_lum_a11_inh = P_invivo_inh (1+10^(pH_Caco2-pKa_acid_inh)+10^(pKa_base_inh-pH_Caco2))/(1+10^(pH_lum11-pKa_acid_inh) +10^(pKa_base_inh-pH_lum11)),

PSpass_lum_a11_inh= Ppass_lum_a11_inh ME Sent11,

PSpass_a11_inh = P_invivo_inh ME Sent11,

PSpass_b11_inh = P_invivo_inh Sent11,

PSap11_inh = PSpass_lum_a11_inh,

PSbp11_inh = PSpass_b11_inh,

PSbx11_inh = PSpass_b11_inh,

PSpgp11_inh = psf_Pgp*Vmax_Pgp_inh*Arel_Pgp11 /(Km_Pgp_inh+fent_inh*y241/Vent11),

PSax11_inh = (PSpass_a11_inh+ PSpgp11_inh),

CL11_inh =   Vmax_3A4_inh*Arel_3A4_11 /(Km_3A4_inh+fent_inh*y241/Vent11),

Ppass_lum_a12_inh = P_invivo_inh (1+10^(pH_Caco2-pKa_acid_inh)+10^(pKa_base_inh-pH_Caco2))/(1+10^(pH_lum12-pKa_acid_inh) +10^(pKa_base_inh-pH_lum12)),

PSpass_lum_a12_inh= Ppass_lum_a12_inh ME Sent12,

PSpass_a12_inh = P_invivo_inh ME Sent12,

PSpass_b12_inh = P_invivo_inh Sent12,

PSap12_inh = PSpass_lum_a12_inh,

PSbp12_inh = PSpass_b12_inh,

PSbx12_inh = PSpass_b12_inh,

PSpgp12_inh = psf_Pgp*Vmax_Pgp_inh*Arel_Pgp12

/(Km_Pgp_inh+fent_inh*y242/Vent12),

PSax12_inh = (PSpass_a12_inh+ PSpgp12_inh),

CL12_inh =   Vmax_3A4_inh*Arel_3A4_12 /(Km_3A4_inh+fent_inh*y242/Vent12),

Ppass_lum_a13_inh = P_invivo_inh (1+10^(pH_Caco2-pKa_acid_inh)+10^(pKa_base_inh-pH_Caco2))/(1+10^(pH_lum13-pKa_acid_inh)

+10^(pKa_base_inh-pH_lum13)),

PSpass_lum_a13_inh= Ppass_lum_a13_inh ME Sent13,

PSpass_a13_inh = P_invivo_inh ME Sent13,

PSpass_b13_inh = P_invivo_inh Sent13,

PSap13_inh = PSpass_lum_a13_inh,

PSbp13_inh = PSpass_b13_inh,

PSbx13_inh = PSpass_b13_inh,

PSpgp13_inh = psf_Pgp*Vmax_Pgp_inh*Arel_Pgp13

/(Km_Pgp_inh+fent_inh*y243/Vent13),

PSax13_inh = (PSpass_a13_inh+ PSpgp13_inh),

CL13_inh =   Vmax_3A4_inh*Arel_3A4_13 /(Km_3A4_inh+fent_inh*y243/Vent13),

Ppass_lum_a14_inh = P_invivo_inh (1+10^(pH_Caco2-pKa_acid_inh)+10^(pKa_base_inh-pH_Caco2))/(1+10^(pH_lum14-pKa_acid_inh)

+10^(pKa_base_inh-pH_lum14)),

PSpass_lum_a14_inh= Ppass_lum_a14_inh ME Sent14,

PSpass_a14_inh = P_invivo_inh ME Sent14,

PSpass_b14_inh = P_invivo_inh Sent14,

PSap14_inh = PSpass_lum_a14_inh,

PSbp14_inh = PSpass_b14_inh,

PSbx14_inh = PSpass_b14_inh,

PSpgp14_inh = psf_Pgp*Vmax_Pgp_inh*Arel_Pgp14

/(Km_Pgp_inh+fent_inh*y244/Vent14),

PSax14_inh = (PSpass_a14_inh+ PSpgp14_inh),

CL14_inh = Vmax_3A4_inh*Arel_3A4_14 /(Km_3A4_inh+fent_inh*y244/Vent14),

Ppass_lum_a15_inh = P_invivo_inh (1+10^(pH_Caco2-pKa_acid_inh)+10^(pKa_base_inh-pH_Caco2))/(1+10^(pH_lum15-pKa_acid_inh)

+10^(pKa_base_inh-pH_lum15)),

PSpass_lum_a15_inh= Ppass_lum_a15_inh ME Sent15,

PSpass_a15_inh = P_invivo_inh ME Sent15,

PSpass_b15_inh = P_invivo_inh Sent15,

PSap15_inh = PSpass_lum_a15_inh,

PSbp15_inh = PSpass_b15_inh,

PSbx15_inh = PSpass_b15_inh,

PSpgp15_inh = psf_Pgp*Vmax_Pgp_inh*Arel_Pgp15

/(Km_Pgp_inh+fent_inh*y245/Vent15),

PSax15_inh = (PSpass_a15_inh+ PSpgp15_inh),

CL15_inh = Vmax_3A4_inh*Arel_3A4_15 /(Km_3A4_inh+fent_inh*y245/Vent15),

Ppass_lum_a16_inh = P_invivo_inh (1+10^(pH_Caco2-pKa_acid_inh)+10^(pKa_base_inh-pH_Caco2))/(1+10^(pH_lum16-pKa_acid_inh)

+10^(pKa_base_inh-pH_lum16)),

PSpass_lum_a16_inh= Ppass_lum_a16_inh ME Sent16,

PSpass_a16_inh = P_invivo_inh ME Sent16,

PSpass_b16_inh = P_invivo_inh Sent16,

PSap16_inh = PSpass_lum_a16_inh,

PSbp16_inh = PSpass_b16_inh,

PSbx16_inh = PSpass_b16_inh,

PSpgp16_inh = psf_Pgp*Vmax_Pgp_inh*Arel_Pgp16

/(Km_Pgp_inh+fent_inh*y246/Vent16),

PSax16_inh = (PSpass_a16_inh+ PSpgp16_inh),

CL16_inh = Vmax_3A4_inh*Arel_3A4_16 /(Km_3A4_inh+fent_inh*y246/Vent16),

Ppass_lum_a17_inh = P_invivo_inh (1+10^(pH_Caco2-pKa_acid_inh)+10^(pKa_base_inh-pH_Caco2))/(1+10^(pH_lum17-pKa_acid_inh)

+10^(pKa_base_inh-pH_lum17)),

PSpass_lum_a17_inh= Ppass_lum_a17_inh ME Sent17,

PSpass_a17_inh = P_invivo_inh ME Sent17,

PSpass_b17_inh = P_invivo_inh Sent17,

PSap17_inh = PSpass_lum_a17_inh,

PSbp17_inh = PSpass_b17_inh,

PSbx17_inh = PSpass_b17_inh,

PSpgp17_inh = psf_Pgp*Vmax_Pgp_inh*Arel_Pgp17

/(Km_Pgp_inh+fent_inh*y247/Vent17),

PSax17_inh = (PSpass_a17_inh+ PSpgp17_inh),

CL17_inh = Vmax_3A4_inh*Arel_3A4_17 /(Km_3A4_inh+fent_inh*y247/Vent17),

Ppass_lum_a18_inh = P_invivo_inh (1+10^(pH_Caco2-pKa_acid_inh)+10^(pKa_base_inh-pH_Caco2))/(1+10^(pH_lum18-pKa_acid_inh)

+10^(pKa_base_inh-pH_lum18)),

PSpass_lum_a18_inh= Ppass_lum_a18_inh ME Sent18,

PSpass_a18_inh = P_invivo_inh ME Sent18,

PSpass_b18_inh = P_invivo_inh Sent18,

PSap18_inh = PSpass_lum_a18_inh,

PSbp18_inh = PSpass_b18_inh,

PSbx18_inh = PSpass_b18_inh,

PSpgp18_inh = psf_Pgp*Vmax_Pgp_inh*Arel_Pgp18

/(Km_Pgp_inh+fent_inh*y248/Vent18),

PSax18_inh = (PSpass_a18_inh+ PSpgp18_inh),

CL18_inh = Vmax_3A4_inh*Arel_3A4_18 /(Km_3A4_inh+fent_inh*y248/Vent18),

Ppass_lum_a19_inh = P_invivo_inh (1+10^(pH_Caco2-pKa_acid_inh)+10^(pKa_base_inh-pH_Caco2))/(1+10^(pH_lum19-pKa_acid_inh)

+10^(pKa_base_inh-pH_lum19)),

PSpass_lum_a19_inh= Ppass_lum_a19_inh ME Sent19,

PSpass_a19_inh = P_invivo_inh ME Sent19,

PSpass_b19_inh = P_invivo_inh Sent19,

PSap19_inh = PSpass_lum_a19_inh,

PSbp19_inh = PSpass_b19_inh,

PSbx19_inh = PSpass_b19_inh,

PSpgp19_inh = psf_Pgp*Vmax_Pgp_inh*Arel_Pgp19

/(Km_Pgp_inh+fent_inh*y249/Vent19),

PSax19_inh = (PSpass_a19_inh+ PSpgp19_inh),

CL19_inh = Vmax_3A4_inh*Arel_3A4_19 /(Km_3A4_inh+fent_inh*y249/Vent19),

Ppass_lum_a20_inh = P_invivo_inh (1+10^(pH_Caco2-pKa_acid_inh)+10^(pKa_base_inh-pH_Caco2))/(1+10^(pH_lum20-pKa_acid_inh)

+10^(pKa_base_inh-pH_lum20)),

PSpass_lum_a20_inh= Ppass_lum_a20_inh ME Sent20,

PSpass_a20_inh = P_invivo_inh ME Sent20,

PSpass_b20_inh = P_invivo_inh Sent20,

PSap20_inh = PSpass_lum_a20_inh,

PSbp20_inh = PSpass_b20_inh,

PSbx20_inh = PSpass_b20_inh,

PSpgp20_inh = psf_Pgp*Vmax_Pgp_inh*Arel_Pgp20

/(Km_Pgp_inh+fent_inh*y250/Vent20),

PSax20_inh = (PSpass_a20_inh+ PSpgp20_inh),

CL20_inh = Vmax_3A4_inh*Arel_3A4_20 /(Km_3A4_inh+fent_inh*y250/Vent20),

Ppass_lum_a21_inh = P_invivo_inh (1+10^(pH_Caco2-pKa_acid_inh)+10^(pKa_base_inh-pH_Caco2))/(1+10^(pH_lum21-pKa_acid_inh)

+10^(pKa_base_inh-pH_lum21)),

PSpass_lum_a21_inh= Ppass_lum_a21_inh ME Sent21,

PSpass_a21_inh = P_invivo_inh ME Sent21,

PSpass_b21_inh = P_invivo_inh Sent21,

PSap21_inh = PSpass_lum_a21_inh,

PSbp21_inh = PSpass_b21_inh,

PSbx21_inh = PSpass_b21_inh,

PSpgp21_inh = psf_Pgp*Vmax_Pgp_inh*Arel_Pgp21

/(Km_Pgp_inh+fent_inh*y251/Vent21),

PSax21_inh = (PSpass_a21_inh+ PSpgp21_inh),

CL21_inh = Vmax_3A4_inh*Arel_3A4_21 /(Km_3A4_inh+fent_inh*y251/Vent21),

Ppass_lum_a22_inh = P_invivo_inh (1+10^(pH_Caco2-pKa_acid_inh)+10^(pKa_base_inh-pH_Caco2))/(1+10^(pH_lum22-pKa_acid_inh)

+10^(pKa_base_inh-pH_lum22)),

PSpass_lum_a22_inh= Ppass_lum_a22_inh ME Sent22,

PSpass_a22_inh = P_invivo_inh ME Sent22,

PSpass_b22_inh = P_invivo_inh Sent22,

PSap22_inh = PSpass_lum_a22_inh,

PSbp22_inh = PSpass_b22_inh,

PSbx22_inh = PSpass_b22_inh,

PSpgp22_inh = psf_Pgp*Vmax_Pgp_inh*Arel_Pgp22

/(Km_Pgp_inh+fent_inh*y252/Vent22),

PSax22_inh = (PSpass_a22_inh+ PSpgp22_inh),

CL22_inh = Vmax_3A4_inh*Arel_3A4_22 /(Km_3A4_inh+fent_inh*y252/Vent22),

Ppass_lum_a23_inh = P_invivo_inh (1+10^(pH_Caco2-pKa_acid_inh)+10^(pKa_base_inh-pH_Caco2))/(1+10^(pH_lum23-pKa_acid_inh)

+10^(pKa_base_inh-pH_lum23)),

PSpass_lum_a23_inh= Ppass_lum_a23_inh ME Sent23,

PSpass_a23_inh = P_invivo_inh ME Sent23,

PSpass_b23_inh = P_invivo_inh Sent23,

PSap23_inh = PSpass_lum_a23_inh,

PSbp23_inh = PSpass_b23_inh,

PSbx23_inh = PSpass_b23_inh,

PSpgp23_inh = psf_Pgp*Vmax_Pgp_inh*Arel_Pgp23

/(Km_Pgp_inh+fent_inh*y253/Vent23),

PSax23_inh = (PSpass_a23_inh+ PSpgp23_inh),

CL23_inh = Vmax_3A4_inh*Arel_3A4_23 /(Km_3A4_inh+fent_inh*y253/Vent23),

Ppass_lum_a24_inh = P_invivo_inh (1+10^(pH_Caco2-pKa_acid_inh)+10^(pKa_base_inh-pH_Caco2))/(1+10^(pH_lum24-pKa_acid_inh)

+10^(pKa_base_inh-pH_lum24)),

PSpass_lum_a24_inh= Ppass_lum_a24_inh ME Sent24,

PSpass_a24_inh = P_invivo_inh ME Sent24,

PSpass_b24_inh = P_invivo_inh Sent24,

PSap24_inh = PSpass_lum_a24_inh,

PSbp24_inh = PSpass_b24_inh,

PSbx24_inh = PSpass_b24_inh,

PSpgp24_inh = psf_Pgp*Vmax_Pgp_inh*Arel_Pgp24

/(Km_Pgp_inh+fent_inh*y254/Vent24),

PSax24_inh = (PSpass_a24_inh+ PSpgp24_inh),

CL24_inh = Vmax_3A4_inh*Arel_3A4_24 /(Km_3A4_inh+fent_inh*y254/Vent24),

Ppass_lum_a25_inh = P_invivo_inh (1+10^(pH_Caco2-pKa_acid_inh)+10^(pKa_base_inh-pH_Caco2))/(1+10^(pH_lum25-pKa_acid_inh)

+10^(pKa_base_inh-pH_lum25)),

PSpass_lum_a25_inh= Ppass_lum_a25_inh ME Sent25,

PSpass_a25_inh = P_invivo_inh ME Sent25,

PSpass_b25_inh = P_invivo_inh Sent25,

PSap25_inh = PSpass_lum_a25_inh,

PSbp25_inh = PSpass_b25_inh,

PSbx25_inh = PSpass_b25_inh,

PSpgp25_inh = psf_Pgp*Vmax_Pgp_inh*Arel_Pgp25

/(Km_Pgp_inh+fent_inh*y255/Vent25),

PSax25_inh = (PSpass_a25_inh+ PSpgp25_inh),

CL25_inh = Vmax_3A4_inh*Arel_3A4_25 /(Km_3A4_inh+fent_inh*y255/Vent25),

Ppass_lum_a26_inh = P_invivo_inh (1+10^(pH_Caco2-pKa_acid_inh)+10^(pKa_base_inh-pH_Caco2))/(1+10^(pH_lum26-pKa_acid_inh)

+10^(pKa_base_inh-pH_lum26)),

PSpass_lum_a26_inh= Ppass_lum_a26_inh ME Sent26,

PSpass_a26_inh = P_invivo_inh ME Sent26,

PSpass_b26_inh = P_invivo_inh Sent26,

PSap26_inh = PSpass_lum_a26_inh,

PSbp26_inh = PSpass_b26_inh,

PSbx26_inh = PSpass_b26_inh,

PSpgp26_inh = psf_Pgp*Vmax_Pgp_inh*Arel_Pgp26

/(Km_Pgp_inh+fent_inh*y256/Vent26),

PSax26_inh = (PSpass_a26_inh+ PSpgp26_inh),

CL26_inh = Vmax_3A4_inh*Arel_3A4_26 /(Km_3A4_inh+fent_inh*y256/Vent26),

Ppass_lum_a27_inh = P_invivo_inh (1+10^(pH_Caco2-pKa_acid_inh)+10^(pKa_base_inh-pH_Caco2))/(1+10^(pH_lum27-pKa_acid_inh)

+10^(pKa_base_inh-pH_lum27)),

PSpass_lum_a27_inh= Ppass_lum_a27_inh ME Sent27,

PSpass_a27_inh = P_invivo_inh ME Sent27,

PSpass_b27_inh = P_invivo_inh Sent27,

PSap27_inh = PSpass_lum_a27_inh,

PSbp27_inh = PSpass_b27_inh,

PSbx27_inh = PSpass_b27_inh,

PSpgp27_inh = psf_Pgp*Vmax_Pgp_inh*Arel_Pgp27

/(Km_Pgp_inh+fent_inh*y257/Vent27),

PSax27_inh = (PSpass_a27_inh+ PSpgp27_inh),

CL27_inh = Vmax_3A4_inh*Arel_3A4_27 /(Km_3A4_inh+fent_inh*y257/Vent27),

Ppass_lum_a28_inh = P_invivo_inh (1+10^(pH_Caco2-pKa_acid_inh)+10^(pKa_base_inh-pH_Caco2))/(1+10^(pH_lum28-pKa_acid_inh)

+10^(pKa_base_inh-pH_lum28)),

PSpass_lum_a28_inh= Ppass_lum_a28_inh ME Sent28,

PSpass_a28_inh = P_invivo_inh ME Sent28,

PSpass_b28_inh = P_invivo_inh Sent28,

PSap28_inh = PSpass_lum_a28_inh,

PSbp28_inh = PSpass_b28_inh,

PSbx28_inh = PSpass_b28_inh,

PSpgp28_inh = psf_Pgp*Vmax_Pgp_inh*Arel_Pgp28 /(Km_Pgp_inh+fent*y258/Vent28),

PSax28_inh = (PSpass_a28_inh+ PSpgp28_inh),

CL28_inh =   Vmax_3A4_inh*Arel_3A4_28 /(Km_3A4_inh+fent_inh*y258/Vent28),

Ppass_lum_a29_inh = P_invivo_inh (1+10^(pH_Caco2-pKa_acid_inh)+10^(pKa_base_inh-pH_Caco2))/(1+10^(pH_lum29-pKa_acid_inh)

+10^(pKa_base_inh-pH_lum29)),

PSpass_lum_a29_inh= Ppass_lum_a29_inh ME Sent29,

PSpass_a29_inh = P_invivo_inh ME Sent29,

PSpass_b29_inh = P_invivo_inh Sent29,

PSap29_inh = PSpass_lum_a29_inh,

PSbp29_inh = PSpass_b29_inh,

PSbx29_inh = PSpass_b29_inh,

PSpgp29_inh = psf_Pgp*Vmax_Pgp_inh*Arel_Pgp29 /(Km_Pgp_inh+fent*y259/Vent29),

PSax29_inh = (PSpass_a29_inh+ PSpgp29_inh),

CL29_inh =   Vmax_3A4_inh*Arel_3A4_29 /(Km_3A4_inh+fent_inh*y259/Vent29),

Ppass_lum_a30_inh = P_invivo_inh (1+10^(pH_Caco2-pKa_acid_inh)+10^(pKa_base_inh-pH_Caco2))/(1+10^(pH_lum30-pKa_acid_inh)

+10^(pKa_base_inh-pH_lum30)),

PSpass_lum_a30_inh= Ppass_lum_a30_inh ME Sent30,

PSpass_a30_inh = P_invivo_inh ME Sent30,

PSpass_b30_inh = P_invivo_inh Sent30,

PSap30_inh = PSpass_lum_a30_inh,

PSbp30_inh = PSpass_b30_inh,

PSbx30_inh = PSpass_b30_inh,

PSpgp30_inh = psf_Pgp*Vmax_Pgp_inh*Arel_Pgp30

/(Km_Pgp_inh+fent_inh*y260/Vent30),

PSax30_inh = (PSpass_a30_inh+ PSpgp30_inh),

CL30_inh = Vmax_3A4_inh*Arel_3A4_30 /(Km_3A4_inh+fent_inh*y260/Vent30),

Ppass_lum_a31_inh = P_invivo_inh (1+10^(pH_Caco2-pKa_acid_inh)+10^(pKa_base_inh-pH_Caco2))/(1+10^(pH_lum31-pKa_acid_inh)

+10^(pKa_base_inh-pH_lum31)),

PSpass_lum_a31_inh= Ppass_lum_a31_inh ME Sent31,

PSpass_a31_inh = P_invivo_inh ME Sent31,

PSpass_b31_inh = P_invivo_inh Sent31,

PSap31_inh = PSpass_lum_a31_inh,

PSbp31_inh = PSpass_b31_inh,

PSbx31_inh = PSpass_b31_inh,

PSpgp31_inh = psf_Pgp*Vmax_Pgp_inh*Arel_Pgp31

/(Km_Pgp_inh+fent_inh*y261/Vent31),

PSax31_inh = (PSpass_a31_inh+ PSpgp31_inh),

CL31_inh = Vmax_3A4_inh*Arel_3A4_31 /(Km_3A4_inh+fent_inh*y261/Vent31),

Ppass_lum_a32_inh = P_invivo_inh (1+10^(pH_Caco2-pKa_acid_inh)+10^(pKa_base_inh-pH_Caco2))/(1+10^(pH_lum32-pKa_acid_inh)

+10^(pKa_base_inh-pH_lum32)),

PSpass_lum_a32_inh= Ppass_lum_a32_inh ME Sent32,

PSpass_a32_inh = P_invivo_inh ME Sent32,

PSpass_b32_inh = P_invivo_inh Sent32,

PSap32_inh = PSpass_lum_a32_inh,

PSbp32_inh = PSpass_b32_inh,

PSbx32_inh = PSpass_b32_inh,

PSpgp32_inh = psf_Pgp*Vmax_Pgp_inh*Arel_Pgp32

/(Km_Pgp_inh+fent_inh*y262/Vent32),

PSax32_inh = (PSpass_a32_inh+ PSpgp32_inh),

CL32_inh = Vmax_3A4_inh*Arel_3A4_32 /(Km_3A4_inh+fent_inh*y262/Vent32),

Ppass_lum_a33_inh = P_invivo_inh (1+10^(pH_Caco2-pKa_acid_inh)+10^(pKa_base_inh-pH_Caco2))/(1+10^(pH_lum33-pKa_acid_inh)

+10^(pKa_base_inh-pH_lum33)),

PSpass_lum_a33_inh= Ppass_lum_a33_inh ME Sent33,

PSpass_a33_inh = P_invivo_inh ME Sent33,

PSpass_b33_inh = P_invivo_inh Sent33,

PSap33_inh = PSpass_lum_a33_inh,

PSbp33_inh = PSpass_b33_inh,

PSbx33_inh = PSpass_b33_inh,

PSpgp33_inh = psf_Pgp*Vmax_Pgp_inh*Arel_Pgp33

/(Km_Pgp_inh+fent_inh*y263/Vent33),

PSax33_inh = (PSpass_a33_inh+ PSpgp33_inh),

CL33_inh = Vmax_3A4_inh*Arel_3A4_33 /(Km_3A4_inh+fent_inh*y263/Vent33),

Ppass_lum_a34_inh = P_invivo_inh (1+10^(pH_Caco2-pKa_acid_inh)+10^(pKa_base_inh-pH_Caco2))/(1+10^(pH_lum34-pKa_acid_inh)
+10^(pKa_base_inh-pH_lum34)),

PSpass_lum_a34_inh= Ppass_lum_a34_inh ME Sent34,

PSpass_a34_inh = P_invivo_inh ME Sent34,

PSpass_b34_inh = P_invivo_inh Sent34,

PSap34_inh = PSpass_lum_a34_inh,

PSbp34_inh = PSpass_b34_inh,

PSbx34_inh = PSpass_b34_inh,

PSpgp34_inh = psf_Pgp*Vmax_Pgp_inh*Arel_Pgp34
/(Km_Pgp_inh+fent_inh*y264/Vent34),

PSax34_inh = (PSpass_a34_inh+ PSpgp34_inh),

CL34_inh = Vmax_3A4_inh*Arel_3A4_34 /(Km_3A4_inh+fent_inh*y264/Vent34),

Ppass_lum_a35_inh = P_invivo_inh (1+10^(pH_Caco2-pKa_acid_inh)+10^(pKa_base_inh-pH_Caco2))/(1+10^(pH_lum35-pKa_acid_inh)
+10^(pKa_base_inh-pH_lum35)),

PSpass_lum_a35_inh= Ppass_lum_a35_inh ME Sent35,

PSpass_a35_inh = P_invivo_inh ME Sent35,

PSpass_b35_inh = P_invivo_inh Sent35,

PSap35_inh = PSpass_lum_a35_inh,

PSbp35_inh = PSpass_b35_inh,

PSbx35_inh = PSpass_b35_inh,

PSpgp35_inh = psf_Pgp*Vmax_Pgp_inh*Arel_Pgp35
/(Km_Pgp_inh+fent_inh*y265/Vent35),

PSax35_inh = (PSpass_a35_inh+ PSpgp35_inh),

CL35_inh =   Vmax_3A4_inh*Arel_3A4_35 /(Km_3A4_inh+fent_inh*y265/Vent35),

Ppass_lum_a36_inh = P_invivo_inh (1+10^(pH_Caco2-pKa_acid_inh)+10^(pKa_base_inh-pH_Caco2))/(1+10^(pH_lum36-pKa_acid_inh)
+10^(pKa_base_inh-pH_lum36)),

PSpass_lum_a36_inh= Ppass_lum_a36_inh ME Sent36,

PSpass_a36_inh = P_invivo_inh ME Sent36,

PSpass_b36_inh = P_invivo_inh Sent36,

PSap36_inh = PSpass_lum_a36_inh,

PSbp36_inh = PSpass_b36_inh,

PSbx36_inh = PSpass_b36_inh,

PSpgp36_inh = psf_Pgp*Vmax_Pgp_inh*Arel_Pgp36
/(Km_Pgp_inh+fent_inh*y266/Vent36),

PSax36_inh = (PSpass_a36_inh+ PSpgp36_inh),

CL36_inh =   Vmax_3A4_inh*Arel_3A4_36 /(Km_3A4_inh+fent_inh*y266/Vent36),

Ppass_lum_a37_inh = P_invivo_inh (1+10^(pH_Caco2-pKa_acid_inh)+10^(pKa_base_inh-pH_Caco2))/(1+10^(pH_lum37-pKa_acid_inh)
+10^(pKa_base_inh-pH_lum37)),

PSpass_lum_a37_inh= Ppass_lum_a37_inh ME Sent37,

PSpass_a37_inh = P_invivo_inh ME Sent37,

PSpass_b37_inh = P_invivo_inh Sent37,

PSap37_inh = PSpass_lum_a37_inh,

PSbp37_inh = PSpass_b37_inh,

PSbx37_inh = PSpass_b37_inh,

PSpgp37_inh = psf_Pgp*Vmax_Pgp_inh*Arel_Pgp37

/(Km_Pgp_inh+fent_inh*y267/Vent37),

PSax37_inh = (PSpass_a37_inh+ PSpgp37_inh),

CL37_inh = Vmax_3A4_inh*Arel_3A4_37 /(Km_3A4_inh+fent_inh*y267/Vent37),

Ppass_lum_a38_inh = P_invivo_inh (1+10^(pH_Caco2-pKa_acid_inh)+10^(pKa_base_inh-pH_Caco2))/(1+10^(pH_lum38-pKa_acid_inh)

+10^(pKa_base_inh-pH_lum38)),

PSpass_lum_a38_inh= Ppass_lum_a38_inh ME Sent38,

PSpass_a38_inh = P_invivo_inh ME Sent38,

PSpass_b38_inh = P_invivo_inh Sent38,

PSap38_inh = PSpass_lum_a38_inh,

PSbp38_inh = PSpass_b38_inh,

PSbx38_inh = PSpass_b38_inh,

PSpgp38_inh = psf_Pgp*Vmax_Pgp_inh*Arel_Pgp38

/(Km_Pgp_inh+fent_inh*y268/Vent38),

PSax38_inh = (PSpass_a38_inh+ PSpgp38_inh),

CL38_inh = Vmax_3A4_inh*Arel_3A4_38 /(Km_3A4_inh+fent_inh*y268/Vent38),

Ppass_lum_a39_inh = P_invivo_inh (1+10^(pH_Caco2-pKa_acid_inh)+10^(pKa_base_inh-pH_Caco2))/(1+10^(pH_lum39-pKa_acid_inh)

+10^(pKa_base_inh-pH_lum39)),

PSpass_lum_a39_inh= Ppass_lum_a39_inh ME Sent39,

PSpass_a39_inh = P_invivo_inh ME Sent39,

PSpass_b39_inh = P_invivo_inh Sent39,

PSap39_inh = PSpass_lum_a39_inh,

PSbp39_inh = PSpass_b39_inh,

PSbx39_inh = PSpass_b39_inh,

PSpgp39_inh = psf_Pgp*Vmax_Pgp_inh*Arel_Pgp39

/(Km_Pgp_inh+fent_inh*y269/Vent39),

PSax39_inh = (PSpass_a39_inh+ PSpgp39_inh),

CL39_inh = Vmax_3A4_inh*Arel_3A4_39 /(Km_3A4_inh+fent_inh*y269/Vent39),

Ppass_lum_a40_inh = P_invivo_inh (1+10^(pH_Caco2-pKa_acid_inh)+10^(pKa_base_inh-pH_Caco2))/(1+10^(pH_lum40-pKa_acid_inh)

+10^(pKa_base_inh-pH_lum40)),

PSpass_lum_a40_inh= Ppass_lum_a40_inh ME Sent40,

PSpass_a40_inh = P_invivo_inh ME Sent40,

PSpass_b40_inh = P_invivo_inh Sent40,

PSap40_inh = PSpass_lum_a40_inh,

PSbp40_inh = PSpass_b40_inh,

PSbx40_inh = PSpass_b40_inh,

PSpgp40_inh = psf_Pgp*Vmax_Pgp_inh*Arel_Pgp40

/(Km_Pgp_inh+fent_inh*y270/Vent40),

PSax40_inh = (PSpass_a40_inh+ PSpgp40_inh),

CL40_inh = Vmax_3A4_inh*Arel_3A4_40 /(Km_3A4_inh+fent_inh*y270/Vent40),

; Drug concentration in the lumen

```
y191' = (kg * y313) * Vg div / V + c3a_1*y191 + c4a_2*y192 + c5_3*y193-
PSap1_inh*y191/y1+PSax1_inh*fent_inh*y231/Vent1/(V/div),
if y191 < 0 then y191=0 endif,
y192' = c2a_1*y191 + c3_2*y192 + c4_3*y193 + c5_4*y194-
PSap2_inh*y192/y2+PSax2_inh*fent_inh*y232/Vent2/(V/div),
if y192 < 0 then y192=0 endif,
y193' = c1_1*y191 + c2_2*y192 + c3_3*y193 + c4_4*y194 + c5_5*y195-
PSap3_inh*y193/y3+PSax3_inh*fent_inh*y233/Vent3/(V/div),
if y193 < 0 then y193=0 endif,
y194' = c1_2*y192 + c2_3*y193 + c3_4*y194 + c4_5*y195 + c5_6*y196-
PSap4_inh*y194/y4+PSax4_inh*fent_inh*y234/Vent4/(V/div),
if y194 < 0 then y194=0 endif,
y195' = c1_3*y193 + c2_4*y194 + c3_5*y195 + c4_6*y196 + c5_7*y197-
PSap5_inh*y195/y5+PSax5_inh*fent_inh*y235/Vent5/(V/div),
if y195 < 0 then y195=0 endif,
y196' = c1_4*y194 + c2_5*y195 + c3_6*y196 + c4_7*y197 + c5_8*y198-
PSap6_inh*y196/y6+PSax6_inh*fent_inh*y236/Vent6/(V/div),
if y196 < 0 then y196=0 endif,
y197' = c1_5*y195 + c2_6*y196 + c3_7*y197 + c4_8*y198 + c5_9*y199-
PSap7_inh*y197/y7+PSax7_inh*fent_inh*y237/Vent7/(V/div),
if y197 < 0 then y197=0 endif,
y198' = c1_6*y196 + c2_7*y197 + c3_8*y198 + c4_9*y199 + c5_10*y200-
PSap8_inh*y198/y8+PSax8_inh*fent_inh*y238/Vent8/(V/div),
if y198 < 0 then y198=0 endif,
```

```
y199' = c1_7*y197 + c2_8*y198 + c3_9*y199 + c4_10*y200 + c5_11*y201-
PSap9_inh*y199/y9+PSax9_inh*fent_inh*y239/Vent9/(V/div),
if y199 < 0 then y199=0 endif,
y200' = c1_8*y198 + c2_9*y199 + c3_10*y200 + c4_11*y201 + c5_12*y202-
PSap10_inh*y200/y10+PSax10_inh*fent_inh*y240/Vent10/(V/div),
if y200 < 0 then y200=0 endif,
y201' = c1_9*y199 + c2_10*y200 + c3_11*y201 + c4_12*y202 + c5_13*y203-
PSap11_inh*y201/y11+PSax11_inh*fent_inh*y241/Vent11/(V/div),
if y201 < 0 then y201=0 endif,
y202' = c1_10*y200 + c2_11*y201 + c3_12*y202 + c4_13*y203 + c5_14*y204-
PSap12_inh*y202/y12+PSax12_inh*fent_inh*y242/Vent12/(V/div),
if y202 < 0 then y202=0 endif,
y203' = c1_11*y201 + c2_12*y202 + c3_13*y203 + c4_14*y204 + c5_15*y205-
PSap13_inh*y203/y13+PSax13_inh*fent_inh*y243/Vent13/(V/div),
if y203 < 0 then y203=0 endif,
y204' = c1_12*y202 + c2_13*y203 + c3_14*y204 + c4_15*y205 + c5_16*y206-
PSap14_inh*y204/y14+PSax14_inh*fent_inh*y244/Vent14/(V/div),
if y204 < 0 then y204=0 endif,
y205' = c1_13*y203 + c2_14*y204 + c3_15*y205 + c4_16*y206 + c5_17*y207-
PSap15_inh*y205/y15+PSax15_inh*fent_inh*y245/Vent15/(V/div),
if y205 < 0 then y205=0 endif,
y206' = c1_14*y204 + c2_15*y205 + c3_16*y206 + c4_17*y207 + c5_18*y208-
PSap16_inh*y206/y16+PSax16_inh*fent_inh*y246/Vent16/(V/div),
if y206 < 0 then y206=0 endif,
```

y207' = c1_15*y205 + c2_16*y206 + c3_17*y207 + c4_18*y208 + c5_19*y209-

PSap17_inh*y207/y17+PSax17_inh*fent_inh*y247/Vent17/(V/div),

if y207 < 0 then y207=0 endif,

y208' = c1_16*y206 + c2_17*y207 + c3_18*y208 + c4_19*y209 + c5_20*y210-

PSap18_inh*y208/y18+PSax18_inh*fent_inh*y248/Vent18/(V/div),

if y208 < 0 then y208=0 endif,

y209' = c1_17*y207 + c2_18*y208 + c3_19*y209 + c4_20*y210 + c5_21*y211-

PSap19_inh*y209/y19+PSax19_inh*fent_inh*y249/Vent19/(V/div),

if y209 < 0 then y209=0 endif,

y210' = c1_18*y208 + c2_19*y209 + c3_20*y210 + c4_21*y211 + c5_22*y212-

PSap20_inh*y210/y20+PSax20_inh*fent_inh*y250/Vent20/(V/div),

if y210 < 0 then y210=0 endif,

y211' = c1_19*y209 + c2_20*y210 + c3_21*y211 + c4_22*y212 + c5_23*y213-

PSap21_inh*y211/y21+PSax21_inh*fent_inh*y251/Vent21/(V/div),

if y211 < 0 then y211=0 endif,

y212' = c1_20*y210 + c2_21*y211 + c3_22*y212 + c4_23*y213 + c5_24*y214-

PSap22_inh*y212/y22+PSax22_inh*fent_inh*y252/Vent22/(V/div),

if y212 < 0 then y212=0 endif,

y213' = c1_21*y211 + c2_22*y212 + c3_23*y213 + c4_24*y214 + c5_25*y215-

PSap23_inh*y213/y23+PSax23_inh*fent_inh*y253/Vent23/(V/div),

if y213 < 0 then y213=0 endif,

y214' = c1_22*y212 + c2_23*y213 + c3_24*y214 + c4_25*y215 + c5_26*y216-

PSap24_inh*y214/y24+PSax24_inh*fent_inh*y254/Vent24/(V/div),

if y214 < 0 then y214=0 endif,

```
y215' = c1_23*y213 + c2_24*y214 + c3_25*y215 + c4_26*y216 + c5_27*y217-
PSap25_inh*y215/y25+PSax25_inh*fent_inh*y255/Vent25/(V/div),
if y215 < 0 then y215=0 endif,
y216' = c1_24*y214 + c2_25*y215 + c3_26*y216 + c4_27*y217 + c5_28*y218-
PSap26_inh*y216/y26+PSax26_inh*fent_inh*y256/Vent26/(V/div),
if y216 < 0 then y216=0 endif,
y217' = c1_25*y215 + c2_26*y216 + c3_27*y217 + c4_28*y218 + c5_29*y219-
PSap27_inh*y217/y27+PSax27_inh*fent_inh*y257/Vent27/(V/div),
if y217 < 0 then y217=0 endif,
y218' = c1_26*y216 + c2_27*y217 + c3_28*y218 + c4_29*y219 + c5_30*y220-
PSap28_inh*y218/y28+PSax28_inh*fent_inh*y258/Vent28/(V/div),
if y218 < 0 then y218=0 endif,
y219' = c1_27*y217 + c2_28*y218 + c3_29*y219 + c4_30*y220 + c5_31*y221-
PSap29_inh*y219/y29+PSax29_inh*fent_inh*y259/Vent29/(V/div),
if y219 < 0 then y219=0 endif,
y220' = c1_28*y218 + c2_29*y219 + c3_30*y220 + c4_31*y221 + c5_32*y222-
PSap30_inh*y220/y30+PSax30_inh*fent_inh*y260/Vent30/(V/div),
if y220 < 0 then y220=0 endif,
y221' = c1_29*y219 + c2_30*y220 + c3_31*y221 + c4_32*y222 + c5_33*y223-
PSap31_inh*y221/y31+PSax31_inh*fent_inh*y261/Vent31/(V/div),
if y221 < 0 then y221=0 endif,
y222' = c1_30*y220 + c2_31*y221 + c3_32*y222 + c4_33*y223 + c5_34*y224-
PSap32_inh*y222/y32+PSax32_inh*fent_inh*y262/Vent32/(V/div),
if y222 < 0 then y222=0 endif,
```

```
y223' = c1_31*y221 + c2_32*y222 + c3_33*y223 + c4_34*y224 + c5_35*y225-
PSap33_inh*y223/y33+PSax33_inh*fent_inh*y263/Vent33/(V/div),
if y223 < 0 then y223=0 endif,
y224' = c1_32*y222 + c2_33*y223 + c3_34*y224 + c4_35*y225 + c5_36*y226-
PSap34_inh*y224/y34+PSax34_inh*fent_inh*y264/Vent34/(V/div),
if y224 < 0 then y224=0 endif,
y225' = c1_33*y223 + c2_34*y224 + c3_35*y225 + c4_36*y226 + c5_37*y227-
PSap35_inh*y225/y35+PSax35_inh*fent_inh*y265/Vent35/(V/div),
if y225 < 0 then y225=0 endif,
y226' = c1_34*y224 + c2_35*y225 + c3_36*y226 + c4_37*y227 + c5_38*y228-
PSap36_inh*y226/y36+PSax36_inh*fent_inh*y266/Vent36/(V/div),
if y226 < 0 then y226=0 endif,
y227' = c1_35*y225 + c2_36*y226 + c3_37*y227 + c4_38*y228 + c5_39*y229-
PSap37_inh*y227/y37+PSax37_inh*fent_inh*y267/Vent37/(V/div),
if y227 < 0 then y227=0 endif,
y228' = c1_36*y226 + c2_37*y227 + c3_38*y228 + c4_39*y229 + c5_40*y230-
PSap38_inh*y228/y38+PSax38_inh*fent_inh*y268/Vent38/(V/div),
if y228 < 0 then y228=0 endif,
y229' = c1_37*y227 + c2_38*y228 + c3_39*y229 + c4a_40*y230-
PSap39_inh*y229/y39+PSax39_inh*fent_inh*y269/Vent39/(V/div),
if y229 < 0 then y229=0 endif,
y230' = c1_38*y228 + c2b_39*y229 + c3b_40*y230-
PSap40_inh*y230/y40+PSax40_inh*fent_inh*y270/Vent40/(V/div),
if y230 < 0 then y230=0 endif,
```

```
; Drug amount in the enterocytes
y231'=PSap1_inh*y191*(V/div)/y1-
(PSax1_inh+CL1_inh+PSbp1_inh)*fent_inh*y231/Vent1+PSbx1_inh*y271/Vlam1,
if y231 < 0 then y231=0 endif,
y232'=PSap2_inh*y192*(V/div)/y2-
(PSax2_inh+CL2_inh+PSbp2_inh)*fent_inh*y232/Vent2+PSbx2_inh*y272/Vlam2,
if y232 < 0 then y232=0 endif,
y233'=PSap3_inh*y193*(V/div)/y3-
(PSax3_inh+CL3_inh+PSbp3_inh)*fent_inh*y233/Vent3+PSbx3_inh*y273/Vlam3,
if y233 < 0 then y233=0 endif,
y234'=PSap4_inh*y194*(V/div)/y4-
(PSax4_inh+CL4_inh+PSbp4_inh)*fent_inh*y234/Vent4+PSbx4_inh*y274/Vlam4,
if y234 < 0 then y234=0 endif,
y235'=PSap5_inh*y195*(V/div)/y5-
(PSax5_inh+CL5_inh+PSbp5_inh)*fent_inh*y235/Vent5+PSbx5_inh*y275/Vlam5,
if y235 < 0 then y235=0 endif,
y236'=PSap6_inh*y196*(V/div)/y6-
(PSax6_inh+CL6_inh+PSbp6_inh)*fent_inh*y236/Vent6+PSbx6_inh*y276/Vlam6,
if y236 < 0 then y236=0 endif,
y237'=PSap7_inh*y197*(V/div)/y7-
(PSax7_inh+CL7_inh+PSbp7_inh)*fent_inh*y237/Vent7+PSbx7_inh*y277/Vlam7,
if y237 < 0 then y237=0 endif,
y238'=PSap8_inh*y198*(V/div)/y8-
(PSax8_inh+CL8_inh+PSbp8_inh)*fent_inh*y238/Vent8+PSbx8_inh*y278/Vlam8,
if y238 < 0 then y238=0 endif,
```

```
y239'=PSap9_inh*y199*(V/div)/y9-
(PSax9_inh+CL9_inh+PSbp9_inh)*fent_inh*y239/Vent9+PSbx9_inh*y279/Vlam9,
if y239 < 0 then y239=0 endif,
y240'=PSap10_inh*y200*(V/div)/y10-
(PSax10_inh+CL10_inh+PSbp10_inh)*fent_inh*y240/Vent10+PSbx10_inh*y280/Vlam10,
if y240 < 0 then y240=0 endif,
y241'=PSap11_inh*y201*(V/div)/y11-
(PSax11_inh+CL11_inh+PSbp11_inh)*fent_inh*y241/Vent11+PSbx11_inh*y281/Vlam11,
if y241 < 0 then y241=0 endif,
y242'=PSap12_inh*y202*(V/div)/y12-
(PSax12_inh+CL12_inh+PSbp12_inh)*fent_inh*y242/Vent12+PSbx12_inh*y282/Vlam12,
if y242 < 0 then y242=0 endif,
y243'=PSap13_inh*y203*(V/div)/y13-
(PSax13_inh+CL13_inh+PSbp13_inh)*fent_inh*y243/Vent13+PSbx13_inh*y283/Vlam13,
if y243 < 0 then y243=0 endif,
y244'=PSap14_inh*y204*(V/div)/y14-
(PSax14_inh+CL14_inh+PSbp14_inh)*fent_inh*y244/Vent14+PSbx14_inh*y284/Vlam14,
if y244 < 0 then y244=0 endif,
y245'=PSap15_inh*y205*(V/div)/y15-
(PSax15_inh+CL15_inh+PSbp15_inh)*fent_inh*y245/Vent15+PSbx15_inh*y285/Vlam15,
if y245 < 0 then y245=0 endif,
y246'=PSap16_inh*y206*(V/div)/y16-
(PSax16_inh+CL16_inh+PSbp16_inh)*fent_inh*y246/Vent16+PSbx16_inh*y286/Vlam16,
if y246 < 0 then y246=0 endif,
```

y247'=PSap17_inh*y207*(V/div)/y17-

(PSax17_inh+CL17_inh+PSbp17_inh)*fent_inh*y247/Vent17+PSbx17_inh*y287/Vlam17,

if y247 < 0 then y247=0 endif,

y248'=PSap18_inh*y208*(V/div)/y18-

(PSax18_inh+CL18_inh+PSbp18_inh)*fent_inh*y248/Vent18+PSbx18_inh*y288/Vlam18,

if y248 < 0 then y248=0 endif,

y249'=PSap19_inh*y209*(V/div)/y19-

(PSax19_inh+CL19_inh+PSbp19_inh)*fent_inh*y249/Vent19+PSbx19_inh*y289/Vlam19,

if y249 < 0 then y249=0 endif,

y250'=PSap20_inh*y210*(V/div)/y20-

(PSax20_inh+CL20_inh+PSbp20_inh)*fent_inh*y250/Vent20+PSbx20_inh*y290/Vlam20,

if y250 < 0 then y250=0 endif,

y251'=PSap21_inh*y211*(V/div)/y21-

(PSax21_inh+CL21_inh+PSbp21_inh)*fent_inh*y251/Vent21+PSbx21_inh*y291/Vlam21,

if y251 < 0 then y251=0 endif,

y252'=PSap22_inh*y212*(V/div)/y22-

(PSax22_inh+CL22_inh+PSbp22_inh)*fent_inh*y252/Vent22+PSbx22_inh*y292/Vlam22,

if y252 < 0 then y252=0 endif,

y253'=PSap23_inh*y213*(V/div)/y23-

(PSax23_inh+CL23_inh+PSbp23_inh)*fent_inh*y253/Vent23+PSbx23_inh*y293/Vlam23,

if y253 < 0 then y253=0 endif,

y254'=PSap24_inh*y214*(V/div)/y24-

(PSax24_inh+CL24_inh+PSbp24_inh)*fent_inh*y254/Vent24+PSbx24_inh*y294/Vlam24,

if y254 < 0 then y254=0 endif,

y255'=PSap25_inh*y215*(V/div)/y25-

(PSax25_inh+CL25_inh+PSbp25_inh)*fent_inh*y255/Vent25+PSbx25_inh*y295/Vlam25,

if y255 < 0 then y255=0 endif,

y256'=PSap26_inh*y216*(V/div)/y26-

(PSax26_inh+CL26_inh+PSbp26_inh)*fent_inh*y256/Vent26+PSbx26_inh*y296/Vlam26,

if y256 < 0 then y256=0 endif,

y257'=PSap27_inh*y217*(V/div)/y27-

(PSax27_inh+CL27_inh+PSbp27_inh)*fent_inh*y257/Vent27+PSbx27_inh*y297/Vlam27,

if y257 < 0 then y257=0 endif,

y258'=PSap28_inh*y218*(V/div)/y28-

(PSax28_inh+CL28_inh+PSbp28_inh)*fent_inh*y258/Vent28+PSbx28_inh*y298/Vlam28,

if y258 < 0 then y258=0 endif,

y259'=PSap29_inh*y219*(V/div)/y29-

(PSax29_inh+CL29_inh+PSbp29_inh)*fent_inh*y259/Vent29+PSbx29_inh*y299/Vlam29,

if y259 < 0 then y259=0 endif,

y260'=PSap30_inh*y220*(V/div)/y30-

(PSax30_inh+CL30_inh+PSbp30_inh)*fent_inh*y260/Vent30+PSbx30_inh*y300/Vlam30,

if y260 < 0 then y260=0 endif,

y261'=PSap31_inh*y221*(V/div)/y31-

(PSax31_inh+CL31_inh+PSbp31_inh)*fent_inh*y261/Vent31+PSbx31_inh*y301/Vlam31,

if y261 < 0 then y261=0 endif,

y262'=PSap32_inh*y222*(V/div)/y32-

(PSax32_inh+CL32_inh+PSbp32_inh)*fent_inh*y262/Vent32+PSbx32_inh*y302/Vlam32,

if y262 < 0 then y262=0 endif,

y263'=PSap33_inh*y223*(V/div)/y33-

(PSax33_inh+CL33_inh+PSbp33_inh)*fent_inh*y263/Vent33+PSbx33_inh*y303/Vlam33,

if y263 < 0 then y263=0 endif,

y264'=PSap34_inh*y224*(V/div)/y34-

(PSax34_inh+CL34_inh+PSbp34_inh)*fent_inh*y264/Vent34+PSbx34_inh*y304/Vlam34,

if y264 < 0 then y264=0 endif,

y265'=PSap35_inh*y225*(V/div)/y35-

(PSax35_inh+CL35_inh+PSbp35_inh)*fent_inh*y265/Vent35+PSbx35_inh*y305/Vlam35,

if y265 < 0 then y265=0 endif,

y266'=PSap36_inh*y226*(V/div)/y36-

(PSax36_inh+CL36_inh+PSbp36_inh)*fent_inh*y266/Vent36+PSbx36_inh*y306/Vlam36,

if y266 < 0 then y266=0 endif,

y267'=PSap37_inh*y227*(V/div)/y37-

(PSax37_inh+CL37_inh+PSbp37_inh)*fent_inh*y267/Vent37+PSbx37_inh*y307/Vlam37,

if y267 < 0 then y267=0 endif,

y268'=PSap38_inh*y228*(V/div)/y38-

(PSax38_inh+CL38_inh+PSbp38_inh)*fent_inh*y268/Vent38+PSbx38_inh*y308/Vlam38,

if y268 < 0 then y268=0 endif,

y269'=PSap39_inh*y229*(V/div)/y39-

(PSax39_inh+CL39_inh+PSbp39_inh)*fent_inh*y269/Vent39+PSbx39_inh*y309/Vlam39,

if y269 < 0 then y269=0 endif,

y270'=PSap40_inh*y230*(V/div)/y40-

(PSax40_inh+CL40_inh+PSbp40_inh)*fent_inh*y270/Vent40+PSbx40_inh*y310/Vlam40,

if y270 < 0 then y270=0 endif,

```
; Drug amount in the lamina propria

y271'= PSbp1_inh*fent_inh*y231/Vent1- (Qlam1/fb_inh+PSbx1_inh)*y271/Vlam1,

if y271 < 0 then y271=0 endif,

y272'= PSbp2_inh*fent_inh*y232/Vent2- (Qlam2/fb_inh+PSbx2_inh)*y272/Vlam2,

if y272 < 0 then y272=0 endif,

y273'= PSbp3_inh*fent_inh*y233/Vent3- (Qlam3/fb_inh+PSbx3_inh)*y273/Vlam3,

if y273 < 0 then y273=0 endif,

y274'= PSbp4_inh*fent_inh*y234/Vent4- (Qlam4/fb_inh+PSbx4_inh)*y274/Vlam4,

if y274 < 0 then y274=0 endif,

y275'= PSbp5_inh*fent_inh*y235/Vent5- (Qlam5/fb_inh+PSbx5_inh)*y275/Vlam5,

if y275 < 0 then y275=0 endif,

y276'= PSbp6_inh*fent_inh*y236/Vent6- (Qlam6/fb_inh+PSbx6_inh)*y276/Vlam6,

if y276 < 0 then y276=0 endif,

y277'= PSbp7_inh*fent_inh*y237/Vent7- (Qlam7/fb_inh+PSbx7_inh)*y277/Vlam7,

if y277 < 0 then y277=0 endif,

y278'= PSbp8_inh*fent_inh*y238/Vent8- (Qlam8/fb_inh+PSbx8_inh)*y278/Vlam8,

if y278 < 0 then y278=0 endif,

y279'= PSbp9_inh*fent_inh*y239/Vent9- (Qlam9/fb_inh+PSbx9_inh)*y279/Vlam9,

if y279 < 0 then y279=0 endif,

y280'= PSbp10_inh*fent_inh*y240/Vent10- (Qlam10/fb_inh+PSbx10_inh)*y280/Vlam10,

if y280 < 0 then y280=0 endif,

y281'= PSbp11_inh*fent_inh*y241/Vent11- (Qlam11/fb_inh+PSbx11_inh)*y281/Vlam11,

if y281 < 0 then y281=0 endif,

y282'= PSbp12_inh*fent_inh*y242/Vent12- (Qlam12/fb_inh+PSbx12_inh)*y282/Vlam12,

if y282 < 0 then y282=0 endif,
```

y283'= PSbp13_inh*fent_inh*y243/Vent13- (Qlam13/fb_inh+PSbx13_inh)*y283/Vlam13,

if y283 < 0 then y283=0 endif,

y284'= PSbp14_inh*fent_inh*y244/Vent14- (Qlam14/fb_inh+PSbx14_inh)*y284/Vlam14,

if y284 < 0 then y284=0 endif,

y285'= PSbp15_inh*fent_inh*y245/Vent15- (Qlam15/fb_inh+PSbx15_inh)*y285/Vlam15,

if y285 < 0 then y285=0 endif,

y286'= PSbp16_inh*fent_inh*y246/Vent16- (Qlam16/fb_inh+PSbx16_inh)*y286/Vlam16,

if y286 < 0 then y286=0 endif,

y287'= PSbp17_inh*fent_inh*y247/Vent17- (Qlam17/fb_inh+PSbx17_inh)*y287/Vlam17,

if y287 < 0 then y287=0 endif,

y288'= PSbp18_inh*fent_inh*y248/Vent18- (Qlam18/fb_inh+PSbx18_inh)*y288/Vlam18,

if y288 < 0 then y288=0 endif,

y289'= PSbp19_inh*fent_inh*y249/Vent19- (Qlam19/fb_inh+PSbx19_inh)*y289/Vlam19,

if y289 < 0 then y289=0 endif,

y290'= PSbp20_inh*fent_inh*y250/Vent20- (Qlam20/fb_inh+PSbx20_inh)*y290/Vlam20,

if y290 < 0 then y290=0 endif,

y291'= PSbp21_inh*fent_inh*y251/Vent21- (Qlam21/fb_inh+PSbx21_inh)*y291/Vlam21,

if y291 < 0 then y291=0 endif,

y292'= PSbp22_inh*fent_inh*y252/Vent22- (Qlam22/fb_inh+PSbx22_inh)*y292/Vlam22,

if y292 < 0 then y292=0 endif,

y293'= PSbp23_inh*fent_inh*y253/Vent23- (Qlam23/fb_inh+PSbx23_inh)*y293/Vlam23,

if y293 < 0 then y293=0 endif,

y294'= PSbp24_inh*fent_inh*y254/Vent24- (Qlam24/fb_inh+PSbx24_inh)*y294/Vlam24,

if y294 < 0 then y294=0 endif,

y295'= PSbp25_inh*fent_inh*y255/Vent25- (Qlam25/fb_inh+PSbx25_inh)*y295/Vlam25,

```
if y295 < 0 then y295=0 endif,

y296'= PSbp26_inh*fent_inh*y256/Vent26- (Qlam26/fb_inh+PSbx26_inh)*y296/Vlam26,

if y296 < 0 then y296=0 endif,

y297'= PSbp27_inh*fent_inh*y257/Vent27- (Qlam27/fb_inh+PSbx27_inh)*y297/Vlam27,

if y297 < 0 then y297=0 endif,

y298'= PSbp28_inh*fent_inh*y258/Vent28- (Qlam28/fb_inh+PSbx28_inh)*y298/Vlam28,

if y298 < 0 then y298=0 endif,

y299'= PSbp29_inh*fent_inh*y259/Vent29- (Qlam29/fb_inh+PSbx29_inh)*y299/Vlam29,

if y299 < 0 then y299=0 endif,

y300'= PSbp30_inh*fent_inh*y260/Vent30- (Qlam30/fb_inh+PSbx30_inh)*y300/Vlam30,

if y300 < 0 then y300=0 endif,

y301'= PSbp31_inh*fent_inh*y261/Vent31- (Qlam31/fb_inh+PSbx31_inh)*y301/Vlam31,

if y301 < 0 then y301=0 endif,

y302'= PSbp32_inh*fent_inh*y262/Vent32- (Qlam32/fb_inh+PSbx32_inh)*y302/Vlam32,

if y302 < 0 then y302=0 endif,

y303'= PSbp33_inh*fent_inh*y263/Vent33- (Qlam33/fb_inh+PSbx33_inh)*y303/Vlam33,

if y303 < 0 then y303=0 endif,

y304'= PSbp34_inh*fent_inh*y264/Vent34- (Qlam34/fb_inh+PSbx34_inh)*y304/Vlam34,

if y304 < 0 then y304=0 endif,

y305'= PSbp35_inh*fent_inh*y265/Vent35- (Qlam35/fb_inh+PSbx35_inh)*y305/Vlam35,

if y305 < 0 then y305=0 endif,

y306'= PSbp36_inh*fent_inh*y266/Vent36- (Qlam36/fb_inh+PSbx36_inh)*y306/Vlam36,

if y306 < 0 then y306=0 endif,

y307'= PSbp37_inh*fent_inh*y267/Vent37- (Qlam37/fb_inh+PSbx37_inh)*y307/Vlam37,

if y307 < 0 then y307=0 endif,
```

y308'= PSbp38_inh*fent_inh*y268/Vent38- (Qlam38/fb_inh+PSbx38_inh)*y308/Vlam38,

if y308 < 0 then y308=0 endif,

y309'= PSbp39_inh*fent_inh*y269/Vent39- (Qlam39/fb_inh+PSbx39_inh)*y309/Vlam39,

if y309 < 0 then y309=0 endif,

y310'= PSbp40_inh*fent_inh*y270/Vent40- (Qlam40/fb_inh+PSbx40_inh)*y310/Vlam40,

if y310 < 0 then y310=0 endif,

; Drug amount in the colon

y311' = ((9.0 y230 - y229) / 8.0) Q - krec * y311,

; Drug amount in the feces

y312' = krec*y311 * Vc,

; Drug concentration in the stomach

y313' = ka*y320*Ves/Vg-kg*y313,

; % of dose in stomach (not used in this study)

y314 = y313 Vg / dose_inh*100,

; % of dose in jejunum (not used in this study)

y315=(y191+y192+y193+y194+y195+y196+y197+y198+y199+y200+y201+y202+y203+y204+y205+y206+y207+y208+y209+y210) V/div/dose_inh*100,

; % of dose in ileum (not used in this study) y316=(y211+y212+y213+y214+y215+y216+y217+y218+y219+y220+y221+y222+y223+y224+y225+y226+y227+y228+y229+y230) V/div/dose_inh*100,

; % of dose in colon(not used in this study)

y317 = y311 Vc / dose_inh * 100,

; % of dose in whole lumen (not used in this study)

y318 = y315 + y316 + y317,

; Drug amount in the gastrointestinal tract (not used in this study)

y319 = y314+y315+y316+y317,

; Drug concentration in the esophagus

y320'=-ka*y320,

; not used in this study

y321=y320

; Drug amount in the enterocytes

y322=(y231+y232+y233+y234+y235+y236+y237+y238+y239+y240+y241+y242+y243+y244+y245+y246+y247+y248+y249+y250+y251+y252+y253+y254+y255+y256+y257+y258+y259+y260+y261+y262+y263+y264+y265+y266+y267+y268+y269+y270),

; Drug amount in the lamina propria

y323=(y231+y232+y233+y234+y235+y236+y237+y238+y239+y240+y241+y242+y243+y244+y245+y246+y247+y248+y249+y250+y251+y252+y253+y254+y255+y256+y257+y258+y259+y260+y261+y262+y263+y264+y265+y266+y267+y268+y269+y270),

; Drug accumulated amount in the portal vein

y324' =

(y271/Vlam1*Qlam1+y272/Vlam2*Qlam2+y273/Vlam3*Qlam3+y274/Vlam4*Qlam4+y275/Vlam5*Qlam5+y276/Vlam6*Qlam6+y277/Vlam7*Qlam7+y278/Vlam8*Qlam8+y279/Vlam9*Qlam9+y280/Vlam10*Qlam10+y281/Vlam11*Qlam11+y282/Vlam12*Qlam12+y283/Vlam13*Qlam13+y284/Vlam14*Qlam14+y285/Vlam15*Qlam15+y286/Vlam16*Qlam16+y287/Vlam17*Qlam17+y288/Vlam18*Qlam18+y289/Vlam19*Qlam19+y290/Vlam20*Qlam20+y291/Vlam21*Qlam21+y292/Vlam22*Qlam22+y293/Vlam23*Qlam23+y294/Vlam24*Qlam24+y295/Vlam25*Qlam25+y296/Vlam26*Qlam26+y297/Vlam27*Qlam27+y298/Vlam28*Qlam28+y299/Vlam29*Qlam29+y300/Vlam30*Qlam30+y301/Vlam31*Qlam31+y302/Vlam32*Qlam32+y303/Vlam33*Qlam33+y304/Vlam34*Qlam34+y305/Vlam35*Qlam35+y306/Vlam36*Qlam36+y307/Vlam37*Qlam37+y308/Vlam38*Qlam38+y309/Vlam39*Qlam39+y310/Vlam40*Qlam40)/fb_inh,

; F_A of an inhbitor

y325 = 1-y311/dose_inh,

; F_AF_G of an inhibitor

y326=y324/dose_inh,

; F_G of an inhibitor

y327=y326/y325,

; Intestinal clearance amount

y328'=CL1_inh*y231/Vent1+CL2_inh*y232/Vent2+CL3_inh*y233/Vent3+CL4_inh*y234/Vent4+CL5_inh*y235/Vent5+CL6_inh*y236/Vent6+CL7_inh*y237/Vent7+CL8_inh*y238/Vent8+CL9_inh*y239/Vent9+CL10_inh*y240/Vent10+CL11_inh*y241/Vent11+CL12_inh*y242/Vent12+CL13_inh*y243/Vent13+CL14_inh*y244/Vent14+CL15_inh*y245/Vent15+CL16_inh*y246/Vent16+CL17_inh*y247/Vent17+CL18_inh*y248/Vent18+CL19_inh*y249/Vent19+CL20_inh*y250/Vent20+CL21_inh*y251/Vent21+CL22_inh*y252/Vent22+CL23_inh*y253/Vent23+CL24_inh*y254/Vent24+CL25_inh*y255/Vent25+CL26_inh*y256/Vent26+CL27_inh*y257/Vent27+CL28_inh*y258/Vent28+CL29_inh*y259/Vent29+CL30_inh*y260/Vent30+CL31_inh*y261/Vent31+CL32_inh*y262/Vent32+CL33_inh*y263/Vent33+CL34_inh*y264/Vent34+CL35_inh*y265/Vent35+CL36_inh*y266/Vent36+CL37_inh*y267/Vent37+CL38_inh*y268/Vent38+CL39_inh*y269/Vent39+CL40_inh*y270/Vent40,

; Drug amount in the portal vein

y329'

=(y271/Vlam1*Qlam1+y272/Vlam2*Qlam2+y273/Vlam3*Qlam3+y274/Vlam4*Qlam4+y275/Vlam5*Qlam5+y276/Vlam6*Qlam6+y277/Vlam7*Qlam7+y278/Vlam8*Qlam8+y279/Vlam9*Qlam9+y280/Vlam10*Qlam10+y281/Vlam11*Qlam11+y282/Vlam12*Qlam12+y283/Vlam13*Qlam13+y284/Vlam14*Qlam14+y285/Vlam15*Qlam15+y286/Vlam16*Qlam16+y287/Vlam17*Qlam17+y288/Vlam18*Qlam18+y289/Vlam19*Qlam19+y290/Vlam20*Qlam20+y291/Vlam21*Qlam21+y292/Vlam22*Qlam22+y293/Vlam23*Qlam23+y294/Vlam24*Qlam24+y295/Vlam25*Qlam25+y296/Vlam26*Qlam26+y297/Vlam27*Qlam27+y298/Vlam28*Qlam28+y299/Vlam29*Qlam29+y300/Vlam30*Qlam30+y301/Vlam31*Qlam31+y302/Vla m32*Qlam32+y303/Vlam33*Qlam33+y304/Vlam34*Qlam34+y305/Vlam35*Qlam35+y306/Vlam36*Qlam36+y307/Vlam37*Qlam37+y308/Vlam38*Qlam38+y309/Vlam39*Qlam39+y310/Vlam40*Qlam40)/fb_inh-Qpv*y329/Vpv,

; Drug concentration in the liver

y330'=(Qpv*y329/Vpv-Qh*y330/Kp_liver_inh*Rb_inh-fb_inh*Rb_inh/Kp_liver_inh*CLint_h_inh*y330+Qha*y331)/Vliver,

; Drug concentration in the blood

y331'=(Qh*y330/Kp_liver_inh*Rb_inh-Qha*y331-k12_inh*y331*Vb+k21_inh*y332)/Vb_inh,

; Drug concentration in the peripheral compartment 1

; The number of peripheral compartments can be increased as necessary.

y332'=k12_inh*y331*Vb_inh-k21*y332,

; Drug concentration in the blood (unit: ug/L)

y333=y331*1000,

; Whole drug concentration of a substrate in the enterocytes

y334 =

(y101+y102+y103+y104+y105+y106+y107+y108+y109+y110+y111+y112+y113+y114+y115+y116+y117+y118+y119+y120+y121+y122+y123+y124+y125+y126+y127+y128+y129+y130+y131+y132+y133+y134+y135+y136+y137+y138+y139+y140)/(Vent1+Vent2+Vent3+Vent4+Vent5+Vent6+Vent7+Vent8+Vent9+Vent10+Vent11+Vent12+Vent13+Vent14+Ve nt15+Vent16+Vent17+Vent18+Vent19+Vent20+Vent21+Vent22+Vent23+Vent24+Vent25+Vent26+Vent27+Vent28+Vent29+Vent30+Vent31+Vent32+Vent33+Vent34+Vent35+Vent36+Vent37+Vent38+Vent39+Vent40)

; Drug concentration of a substrate in each compartment of the enterocytes

y335 = y101/Vent1,

y336 = y102/Vent2,

y337 = y103/Vent3,

y338 = y104/Vent4,

y339 = y105/Vent5,

y340 = y106/Vent6,

y341 = y107/Vent7,

y342 = y108/Vent8,

y343 = y109/Vent9,

y344 = y110/Vent10,

y345 = y111/Vent11,

y346 = y112/Vent12,

y347 = y113/Vent13,

y348 = y114/Vent14,

y349 = y115/Vent15,

y350 = y116/Vent16,

y351 = y117/Vent17,

y352 = y118/Vent18,

y353 = y119/Vent19,

y354 = y120/Vent20,

y355 = y121/Vent21,

y356 = y122/Vent22,

y357 = y123/Vent23,

y358 = y124/Vent24,

y359 = y125/Vent25,

y360 = y126/Vent26,

y361 = y127/Vent27,

y362 = y128/Vent28,

y363 = y129/Vent29,

y364 = y130/Vent30,

y365 = y131/Vent31,

y366 = y132/Vent32,

y367 = y133/Vent33,

y368 = y134/Vent34,

y369 = y135/Vent35,

y370 = y136/Vent36,

y371 = y137/Vent37,

y372 = y138/Vent38,

y373 = y139/Vent39,

y374 = y140/Vent40,

; Drug accumulation of a substrate in each compartment of the portal vein

y375'=y141/Vlam1*Qlam1/fb/dose,

y376'=y142/Vlam2*Qlam2/fb/dose,

y377'=y143/Vlam3*Qlam3/fb/dose,

y378'=y144/Vlam4*Qlam4/fb/dose,

y379'=y145/Vlam5*Qlam5/fb/dose,

y380'=y146/Vlam6*Qlam6/fb/dose,

y381'=y147/Vlam7*Qlam7/fb/dose,

y382'=y148/Vlam8*Qlam8/fb/dose,

y383'=y149/Vlam9*Qlam9/fb/dose,

y384'=y150/Vlam10*Qlam10/fb/dose,

y385'=y151/Vlam11*Qlam11/fb/dose,

y386'=y152/Vlam12*Qlam12/fb/dose,

y387'=y153/Vlam13*Qlam13/fb/dose,

y388'=y154/Vlam14*Qlam14/fb/dose,

y389'=y155/Vlam15*Qlam15/fb/dose,

y390'=y156/Vlam16*Qlam16/fb/dose,

y391'=y157/Vlam17*Qlam17/fb/dose,

y392'=y158/Vlam18*Qlam18/fb/dose,

y393'=y159/Vlam19*Qlam19/fb/dose,

y394'=y160/Vlam20*Qlam20/fb/dose,

y395'=y161/Vlam21*Qlam21/fb/dose,

y396'=y162/Vlam22*Qlam22/fb/dose,

y397'=y163/Vlam23*Qlam23/fb/dose,

y398'=y164/Vlam24*Qlam24/fb/dose,

y399'=y165/Vlam25*Qlam25/fb/dose,

y400'=y166/Vlam26*Qlam26/fb/dose,

y401'=y167/Vlam27*Qlam27/fb/dose,

y402'=y168/Vlam28*Qlam28/fb/dose,

y403'=y169/Vlam29*Qlam29/fb/dose,

y404'=y170/Vlam30*Qlam30/fb/dose,

y405'=y171/Vlam31*Qlam31/fb/dose,

y406'=y172/Vlam32*Qlam32/fb/dose,

y407'=y173/Vlam33*Qlam33/fb/dose,

y408'=y174/Vlam34*Qlam34/fb/dose,

y409'=y175/Vlam35*Qlam35/fb/dose,

y410'=y176/Vlam36*Qlam36/fb/dose,

y411'=y177/Vlam37*Qlam37/fb/dose,

y412'=y178/Vlam38*Qlam38/fb/dose,

y413'=y179/Vlam39*Qlam39/fb/dose,

y414'=y180/Vlam40*Qlam40/fb/dose,

; ***************** Preparative Calculation ********************div = 40,

; 40 is number of segments

; in this model, dispersion is defined by volume not by length

b = Q div / V,

kwn=kw/div,

; section 1

Dsp_1 = A*exp(-B*x_1)+0.005,

a_1 = Dsp_1 Q div div / V,

c1_1= -a_1/12 - b/12,

c2_1= a_1 4/3 + b 2/3,

```
c3_1= -a_1 5/2, ; - ke,

c4_1= a_1 4/3 - b 2/3,

c5_1= -a_1/12 + b/12,

c3a_1 = -c1_1 + c3_1 + c4_1 + c5_1,

c4a_1 = c4_1 + c5_1,

c2a_1 = c1_1 + c2_1,

kw_1 = kw,

sw_1=sw,


; section 2

Dsp_2 = A*exp(-B*x_2)+0.005,

a_2 = Dsp_2 Q div div / V,


c1_2= -a_2/12 - b/12,

c2_2= a_2 4/3 + b 2/3,

c3_2= -a_2 5/2, ; - ke,

c4_2= a_2 4/3 - b 2/3,

c5_2= -a_2/12 + b/12,

c3a_2 = -c1_2 + c3_2 + c4_2 + c5_2,

c4a_2 = c4_2 + c5_2,

c2a_2 = c1_2 + c2_2,

c3_2_kw = c3_2-kw,

sw_2=sw,


; section 3
```

```
Dsp_3 = A*exp(-B*x_3)+0.005,

a_3 = Dsp_3 Q div div / V,


c1_3= -a_3/12 - b/12,

c2_3= a_3 4/3 + b 2/3,

c3_3= -a_3 5/2, ; - ke,

c4_3= a_3 4/3 - b 2/3,

c5_3= -a_3/12 + b/12,

c3_3_kw = c3_3-kw,

sw_3=sw,


; section 4

Dsp_4 = A*exp(-B*x_4)+0.005,

a_4 = Dsp_4 Q div div / V,


c1_4= -a_4/12 - b/12,

c2_4= a_4 4/3 + b 2/3,

c3_4= -a_4 5/2, ; - ke,

c4_4= a_4 4/3 - b 2/3,

c5_4= -a_4/12 + b/12,

c3_4_kw = c3_4-kw,

sw_4=sw,


; section 5

Dsp_5 = A*exp(-B*x_5)+0.005,
```

```
a_5 = Dsp_5 Q div div / V,


c1_5= -a_5/12 - b/12,

c2_5= a_5 4/3 + b 2/3,

c3_5= -a_5 5/2, ; - ke,

c4_5= a_5 4/3 - b 2/3,

c5_5= -a_5/12 + b/12,

c3_5_kw = c3_5-kw,

sw_5=sw,


; section 6

Dsp_6 = A*exp(-B*x_6)+0.005,

a_6 = Dsp_6 Q div div / V,


c1_6= -a_6/12 - b/12,

c2_6= a_6 4/3 + b 2/3,

c3_6= -a_6 5/2, ; - ke,

c4_6= a_6 4/3 - b 2/3,

c5_6= -a_6/12 + b/12,

c3_6_kw = c3_6-kw,

sw_6=sw,


; section 7

Dsp_7= A*exp(-B*x_7)+0.005,

a_7 = Dsp_7 Q div div / V,
```

```
c1_7= -a_7/12 - b/12,
c2_7= a_7 4/3 + b 2/3,
c3_7= -a_7 5/2, ; - ke,
c4_7= a_7 4/3 - b 2/3,
c5_7= -a_7/12 + b/12,
c3_7_kw = c3_7-kw,
sw_7=sw,

; section 8
Dsp_8= A*exp(-B*x_8)+0.005,
a_8 = Dsp_8 Q div div / V,

c1_8= -a_8/12 - b/12,
c2_8= a_8 4/3 + b 2/3,
c3_8= -a_8 5/2, ; - ke,
c4_8= a_8 4/3 - b 2/3,
c5_8= -a_8/12 + b/12,
c3_8_kw = c3_8-kw,
sw_8=sw,

; section 9
Dsp_9= A*exp(-B*x_9)+0.005,
a_9 = Dsp_9 Q div div / V,
```

```
c1_9= -a_9/12 - b/12,

c2_9= a_9 4/3 + b 2/3,

c3_9= -a_9 5/2, ; - ke,

c4_9= a_9 4/3 - b 2/3,

c5_9= -a_9/12 + b/12,

c3_9_kw = c3_9-kw,

sw_9=sw,


; section 10

Dsp_10= A*exp(-B*x_10)+0.005,

a_10 = Dsp_10 Q div div / V,


c1_10= -a_10/12 - b/12,

c2_10= a_10 4/3 + b 2/3,

c3_10= -a_10 5/2, ; - ke,

c4_10= a_10 4/3 - b 2/3,

c5_10= -a_10/12 + b/12,

c3_10_kw = c3_10-kw,

sw_10=sw,


; section 11

Dsp_11= A*exp(-B*x_11)+0.005,

a_11 = Dsp_11 Q div div / V,


c1_11= -a_11/12 - b/12,
```

```
c2_11= a_11 4/3 + b 2/3,
c3_11= -a_11 5/2, ; - ke,
c4_11= a_11 4/3 - b 2/3,
c5_11= -a_11/12 + b/12,
c3_11_kw = c3_11-kw,
sw_11=sw,

; section 12
Dsp_12= A*exp(-B*x_12)+0.005,
a_12 = Dsp_12 Q div div / V,

c1_12= -a_12/12 - b/12,
c2_12= a_12 4/3 + b 2/3,
c3_12= -a_12 5/2, ; - ke,
c4_12= a_12 4/3 - b 2/3,
c5_12= -a_12/12 + b/12,
c3_12_kw = c3_12-kw,
sw_12=sw,

; section 13
Dsp_13= A*exp(-B*x_13)+0.005,
a_13 = Dsp_13 Q div div / V,

c1_13= -a_13/12 - b/12,
c2_13= a_13 4/3 + b 2/3,
```

```
c3_13= -a_13 5/2, ; - ke,

c4_13= a_13 4/3 - b 2/3,

c5_13= -a_13/12 + b/12,

c3_13_kw = c3_13-kw,

sw_13=sw,


; section 14

Dsp_14= A*exp(-B*x_14)+0.005,

a_14 = Dsp_14 Q div div / V,


c1_14= -a_14/12 - b/12,

c2_14= a_14 4/3 + b 2/3,

c3_14= -a_14 5/2, ; - ke,

c4_14= a_14 4/3 - b 2/3,

c5_14= -a_14/12 + b/12,

c3_14_kw = c3_14-kw,

sw_14=sw,


; section 15

Dsp_15= A*exp(-B*x_15)+0.005,

a_15 = Dsp_15 Q div div / V,


c1_15= -a_15/12 - b/12,

c2_15= a_15 4/3 + b 2/3,

c3_15= -a_15 5/2, ; - ke,
```

```
c4_15= a_15 4/3 - b 2/3,

c5_15= -a_15/12 + b/12,

c3_15_kw = c3_15-kw,

sw_15=sw,


; section 16

Dsp_16= A*exp(-B*x_16)+0.005,

a_16 = Dsp_16 Q div div / V,


c1_16= -a_16/12 - b/12,

c2_16= a_16 4/3 + b 2/3,

c3_16= -a_16 5/2, ; - ke,

c4_16= a_16 4/3 - b 2/3,

c5_16= -a_16/12 + b/12,

c3_16_kw = c3_16-kw,

sw_16=sw,


; section 17

Dsp_17= A*exp(-B*x_17)+0.005,

a_17 = Dsp_17 Q div div / V,


c1_17= -a_17/12 - b/12,

c2_17= a_17 4/3 + b 2/3,

c3_17= -a_17 5/2, ; - ke,

c4_17= a_17 4/3 - b 2/3,
```

```
c5_17= -a_17/12 + b/12,

c3_17_kw = c3_17-kw,

sw_17=sw,


; section 18

Dsp_18= A*exp(-B*x_18)+0.005,

a_18 = Dsp_18 Q div div / V,


c1_18= -a_18/12 - b/12,

c2_18= a_18 4/3 + b 2/3,

c3_18= -a_18 5/2, ; - ke,

c4_18= a_18 4/3 - b 2/3,

c5_18= -a_18/12 + b/12,

c3_18_kw = c3_18-kw,

sw_18=sw,


; section 19

Dsp_19= A*exp(-B*x_19)+0.005,

a_19 = Dsp_19 Q div div / V,


c1_19= -a_19/12 - b/12,

c2_19= a_19 4/3 + b 2/3,

c3_19= -a_19 5/2, ; - ke,

c4_19= a_19 4/3 - b 2/3,

c5_19= -a_19/12 + b/12,
```

```
c3_19_kw = c3_19-kw,
sw_19=sw,

; section 20
Dsp_20=A*exp(-B*x_20)+0.005,
a_20 = Dsp_20 Q div div / V,

c1_20= -a_20/12 - b/12,
c2_20= a_20 4/3 + b 2/3,
c3_20= -a_20 5/2, ; - ke,
c4_20= a_20 4/3 - b 2/3,
c5_20= -a_20/12 + b/12,
c3_20_kw = c3_20-kw,
sw_20=sw,

; section 21
Dsp_21= A*exp(-B*x_21)+0.005,
a_21 = Dsp_21 Q div div / V,

c1_21= -a_21/12 - b/12,
c2_21= a_21 4/3 + b 2/3,
c3_21= -a_21 5/2, ; - ke,
c4_21= a_21 4/3 - b 2/3,
c5_21= -a_21/12 + b/12,
c3_21_kw = c3_21-kw,
```

```
sw_21=sw,

; section 22
Dsp_22= A*exp(-B*x_22)+0.005,
a_22 = Dsp_22 Q div div / V,

c1_22= -a_22/12 - b/12,
c2_22= a_22 4/3 + b 2/3,
c3_22= -a_22 5/2, ; - ke,
c4_22= a_22 4/3 - b 2/3,
c5_22= -a_22/12 + b/12,
c3_22_kw = c3_22-kw,
sw_22=sw,

; section 23
Dsp_23= A*exp(-B*x_23)+0.005,
a_23 = Dsp_23 Q div div / V,

c1_23= -a_23/12 - b/12,
c2_23= a_23 4/3 + b 2/3,
c3_23= -a_23 5/2, ; - ke,
c4_23= a_23 4/3 - b 2/3,
c5_23= -a_23/12 + b/12,
c3_23_kw = c3_23-kw,
sw_23=sw,
```

```
; section 24
Dsp_24= A*exp(-B*x_24)+0.005,
a_24 = Dsp_24 Q div div / V,

c1_24= -a_24/12 - b/12,
c2_24= a_24 4/3 + b 2/3,
c3_24= -a_24 5/2, ; - ke,
c4_24= a_24 4/3 - b 2/3,
c5_24= -a_24/12 + b/12,
c3_24_kw = c3_24-kw,
sw_24=sw,

; section 25
Dsp_25= A*exp(-B*x_25)+0.005,
a_25 = Dsp_25 Q div div / V,

c1_25= -a_25/12 - b/12,
c2_25= a_25 4/3 + b 2/3,
c3_25= -a_25 5/2, ; - ke,
c4_25= a_25 4/3 - b 2/3,
c5_25= -a_25/12 + b/12,
c3_25_kw = c3_25-kw,
sw_25=sw,
```

```
; section 26
Dsp_26= A*exp(-B*x_26)+0.005,
a_26 = Dsp_26 Q div div / V,

c1_26= -a_26/12 - b/12,
c2_26= a_26 4/3 + b 2/3,
c3_26= -a_26 5/2, ; - ke,
c4_26= a_26 4/3 - b 2/3,
c5_26= -a_26/12 + b/12,
c3_26_kw = c3_26-kw,
sw_26=sw,

; section 27
Dsp_27= A*exp(-B*x_27)+0.005,
a_27 = Dsp_27 Q div div / V,

c1_27= -a_27/12 - b/12,
c2_27= a_27 4/3 + b 2/3,
c3_27= -a_27 5/2, ; - ke,
c4_27= a_27 4/3 - b 2/3,
c5_27= -a_27/12 + b/12,
c3_27_kw = c3_27-kw,
sw_27=sw,

; section 28
```

```
Dsp_28 = A*exp(-B*x_28)+0.005,
a_28 = Dsp_28 Q div div / V,

c1_28= -a_28/12 - b/12,
c2_28= a_28 4/3 + b 2/3,
c3_28= -a_28 5/2, ; - ke,
c4_28= a_28 4/3 - b 2/3,
c5_28= -a_28/12 + b/12,
c3_28_kw = c3_28-kw,
sw_28=sw,

; section 29
Dsp_29 = A*exp(-B*x_29)+0.005,
a_29 = Dsp_29 Q div div / V,

c1_29= -a_29/12 - b/12,
c2_29= a_29 4/3 + b 2/3,
c3_29= -a_29 5/2, ; - ke,
c4_29= a_29 4/3 - b 2/3,
c5_29= -a_29/12 + b/12,
c3_29_kw = c3_29-kw,
sw_29=sw,

; section 30
Dsp_30 = A*exp(-B*x_30)+0.005,
```

```
a_30 = Dsp_30 Q div div / V,


c1_30= -a_30/12 - b/12,
c2_30= a_30 4/3 + b 2/3,
c3_30= -a_30 5/2, ; - ke,
c4_30= a_30 4/3 - b 2/3,
c5_30= -a_30/12 + b/12,
c3_30_kw = c3_30-kw,
sw_30=sw,


; section 31
Dsp_31 = A*exp(-B*x_31)+0.005,
a_31 = Dsp_31 Q div div / V,


c1_31= -a_31/12 - b/12,
c2_31= a_31 4/3 + b 2/3,
c3_31= -a_31 5/2, ; - ke,
c4_31= a_31 4/3 - b 2/3,
c5_31= -a_31/12 + b/12,
c3_31_kw = c3_31-kw,
sw_31=sw,


; section 32
Dsp_32 = A*exp(-B*x_32)+0.005,
a_32 = Dsp_32 Q div div / V,
```

```
c1_32= -a_32/12 - b/12,

c2_32= a_32 4/3 + b 2/3,

c3_32= -a_32 5/2, ; - ke,

c4_32= a_32 4/3 - b 2/3,

c5_32= -a_32/12 + b/12,

c3_32_kw = c3_32-kw,

sw_32=sw,


; section 33

Dsp_33 = A*exp(-B*x_33)+0.005,

a_33 = Dsp_33 Q div div / V,


c1_33= -a_33/12 - b/12,

c2_33= a_33 4/3 + b 2/3,

c3_33= -a_33 5/2, ; - ke,

c4_33= a_33 4/3 - b 2/3,

c5_33= -a_33/12 + b/12,

c3_33_kw = c3_33-kw,

sw_33=sw,


; section 34

Dsp_34 = A*exp(-B*x_34)+0.005,

a_34 = Dsp_34 Q div div / V,
```

```
c1_34= -a_34/12 - b/12,
c2_34= a_34 4/3 + b 2/3,
c3_34= -a_34 5/2, ; - ke,
c4_34= a_34 4/3 - b 2/3,
c5_34= -a_34/12 + b/12,
c3_34_kw = c3_34-kw,
sw_34=sw,

; section 35
Dsp_35 = A*exp(-B*x_35)+0.005,
a_35 = Dsp_35 Q div div / V,

c1_35= -a_35/12 - b/12,
c2_35= a_35 4/3 + b 2/3,
c3_35= -a_35 5/2, ; - ke,
c4_35= a_35 4/3 - b 2/3,
c5_35= -a_35/12 + b/12,
c3_35_kw = c3_35-kw,
sw_35=sw,

; section 36
Dsp_36 = A*exp(-B*x_36)+0.005,
a_36 = Dsp_36 Q div div / V,

c1_36= -a_36/12 - b/12,
```

```
c2_36= a_36 4/3 + b 2/3,

c3_36= -a_36 5/2, ; - ke,

c4_36= a_36 4/3 - b 2/3,

c5_36= -a_36/12 + b/12,

c3_36_kw = c3_36-kw,

sw_36=sw,


; section 37

Dsp_37 = A*exp(-B*x_37)+0.005,

a_37 = Dsp_37 Q div div / V,


c1_37= -a_37/12 - b/12,

c2_37= a_37 4/3 + b 2/3,

c3_37= -a_37 5/2, ; - ke,

c4_37= a_37 4/3 - b 2/3,

c5_37= -a_37/12 + b/12,

c3_37_kw = c3_37-kw,

sw_37=sw,


; section 38

Dsp_38 = A*exp(-B*x_38)+0.005,

a_38 = Dsp_38 Q div div / V,


c1_38= -a_38/12 - b/12,

c2_38= a_38 4/3 + b 2/3,
```

```
c3_38= -a_38 5/2, ; - ke,

c4_38= a_38 4/3 - b 2/3,

c5_38= -a_38/12 + b/12,

c3_38_kw = c3_38-kw,

sw_38=sw,


; section 39

Dsp_39 = A*exp(-B*x_39)+0.005,

a_39 = Dsp_39 Q div div / V,


c1_39= -a_39/12 - b/12,

c2_39= a_39 4/3 + b 2/3,

c3_39= -a_39 5/2, ; - ke,

c4_39= a_39 4/3 - b 2/3,

c5_39= -a_39/12 + b/12,

c4a_39 = c4_39 + c5_39,

c2b_39 = c2_39 + c5_39,

c3b_39 = c3_39 + c4_39,

c3_39_kw = c3_39-kw,

sw_39=sw,


; section 40

Dsp_40 = A*exp(-B*x_40)+0.005,

a_40 = Dsp_40 Q div div / V,
```

c1_40= -a_40/12 - b/12,

c2_40= a_40 4/3 + b 2/3,

c3_40= -a_40 5/2, ; - ke,

c4_40= a_40 4/3 - b 2/3,

c5_40= -a_40/12 + b/12,

c4a_40 = c4_40 + c5_40,

c2b_40 = c2_40 + c5_40,

c3b_40 = c3_40 + c4_40,

kw_40=kw,

sw_40=sw,

; Translation from Permeability in Caco-2 cells to in vivo permeability (Substrate)

P_Caco2 = (1+ME_Caco2)/ME_Caco2 Papp_Caco2,

P_invivo = P_Caco2 psf_passive,

; Translation from Permeability in Caco-2 cells to in vivo permeability (Perpetrator)

P_Caco2_inh = (1+ME_Caco2)/ME_Caco2 Papp_Caco2_inh,

P_invivo_inh = P_Caco2_inh psf_passive,

; ratio of blood flow in lamina propria at each cpmpartment

Qlam1 = Qlam*Sapi_ratio1,

Qlam2 = Qlam*Sapi_ratio2,

Qlam3 = Qlam*Sapi_ratio3,

Qlam4 = Qlam*Sapi_ratio4,

Qlam5 = Qlam*Sapi_ratio5,

Qlam6 = Qlam*Sapi_ratio6,

Qlam7 = Qlam*Sapi_ratio7,

Qlam8 = Qlam*Sapi_ratio8,

Qlam9 = Qlam*Sapi_ratio9,

Qlam10 = Qlam*Sapi_ratio10,

Qlam11 = Qlam*Sapi_ratio11,

Qlam12 = Qlam*Sapi_ratio12,

Qlam13 = Qlam*Sapi_ratio13,

Qlam14 = Qlam*Sapi_ratio14,

Qlam15 = Qlam*Sapi_ratio15,

Qlam16 = Qlam*Sapi_ratio16,

Qlam17 = Qlam*Sapi_ratio17,

Qlam18 = Qlam*Sapi_ratio18,

Qlam19 = Qlam*Sapi_ratio19,

Qlam20 = Qlam*Sapi_ratio20,

Qlam21 = Qlam*Sapi_ratio21,

Qlam22 = Qlam*Sapi_ratio22,

Qlam23 = Qlam*Sapi_ratio23,

Qlam24 = Qlam*Sapi_ratio24,

Qlam25 = Qlam*Sapi_ratio25,

Qlam26 = Qlam*Sapi_ratio26,

Qlam27 = Qlam*Sapi_ratio27,

Qlam28 = Qlam*Sapi_ratio28,

Qlam29 = Qlam*Sapi_ratio29,

Qlam30 = Qlam*Sapi_ratio30,

```
Qlam31 = Qlam*Sapi_ratio31,

Qlam32 = Qlam*Sapi_ratio32,

Qlam33 = Qlam*Sapi_ratio33,

Qlam34 = Qlam*Sapi_ratio34,

Qlam35 = Qlam*Sapi_ratio35,

Qlam36 = Qlam*Sapi_ratio36,

Qlam37 = Qlam*Sapi_ratio37,

Qlam38 = Qlam*Sapi_ratio38,

Qlam39 = Qlam*Sapi_ratio39,

Qlam40 = Qlam*Sapi_ratio40,


; Volume of caecum and colon

Vcae_col = Vcae + Vc,


; Relative Expression of P-gp in the small intestine

Arel_Pgp1=(1+1+x_1/Lsi)*2*Tot_Pgp/(3*Lsi)*x_1/2,

Arel_Pgp2=(1+x_1/Lsi+1+x_2/Lsi)*2*Tot_Pgp/(3*Lsi)*(x_2-x_1)/2,

Arel_Pgp3=(1+x_2/Lsi+1+x_3/Lsi)*2*Tot_Pgp/(3*Lsi)*(x_3-x_2)/2,

Arel_Pgp4=(1+x_3/Lsi+1+x_4/Lsi)*2*Tot_Pgp/(3*Lsi)*(x_4-x_3)/2,

Arel_Pgp5=(1+x_4/Lsi+1+x_5/Lsi)*2*Tot_Pgp/(3*Lsi)*(x_5-x_4)/2,

Arel_Pgp6=(1+x_5/Lsi+1+x_6/Lsi)*2*Tot_Pgp/(3*Lsi)*(x_6-x_5)/2,

Arel_Pgp7=(1+x_6/Lsi+1+x_7/Lsi)*2*Tot_Pgp/(3*Lsi)*(x_7-x_6)/2,

Arel_Pgp8=(1+x_7/Lsi+1+x_8/Lsi)*2*Tot_Pgp/(3*Lsi)*(x_8-x_7)/2,

Arel_Pgp9=(1+x_8/Lsi+1+x_9/Lsi)*2*Tot_Pgp/(3*Lsi)*(x_9-x_8)/2,

Arel_Pgp10=(1+x_9/Lsi+1+x_10/Lsi)*2*Tot_Pgp/(3*Lsi)*(x_10-x_9)/2,
```

Arel_Pgp11=(1+x_10/Lsi+1+x_11/Lsi)*2*Tot_Pgp/(3*Lsi)*(x_11-x_10)/2,

Arel_Pgp12=(1+x_11/Lsi+1+x_12/Lsi)*2*Tot_Pgp/(3*Lsi)*(x_12-x_11)/2,

Arel_Pgp13=(1+x_12/Lsi+1+x_13/Lsi)*2*Tot_Pgp/(3*Lsi)*(x_13-x_12)/2,

Arel_Pgp14=(1+x_13/Lsi+1+x_14/Lsi)*2*Tot_Pgp/(3*Lsi)*(x_14-x_13)/2,

Arel_Pgp15=(1+x_14/Lsi+1+x_15/Lsi)*2*Tot_Pgp/(3*Lsi)*(x_15-x_14)/2,

Arel_Pgp16=(1+x_15/Lsi+1+x_16/Lsi)*2*Tot_Pgp/(3*Lsi)*(x_16-x_15)/2,

Arel_Pgp17=(1+x_16/Lsi+1+x_17/Lsi)*2*Tot_Pgp/(3*Lsi)*(x_17-x_16)/2,

Arel_Pgp18=(1+x_17/Lsi+1+x_18/Lsi)*2*Tot_Pgp/(3*Lsi)*(x_18-x_17)/2,

Arel_Pgp19=(1+x_18/Lsi+1+x_19/Lsi)*2*Tot_Pgp/(3*Lsi)*(x_19-x_18)/2,

Arel_Pgp20=(1+x_19/Lsi+1+x_20/Lsi)*2*Tot_Pgp/(3*Lsi)*(x_20-x_19)/2,

Arel_Pgp21=(1+x_20/Lsi+1+x_21/Lsi)*2*Tot_Pgp/(3*Lsi)*(x_21-x_20)/2,

Arel_Pgp22=(1+x_21/Lsi+1+x_22/Lsi)*2*Tot_Pgp/(3*Lsi)*(x_22-x_21)/2,

Arel_Pgp23=(1+x_22/Lsi+1+x_23/Lsi)*2*Tot_Pgp/(3*Lsi)*(x_23-x_22)/2,

Arel_Pgp24=(1+x_23/Lsi+1+x_24/Lsi)*2*Tot_Pgp/(3*Lsi)*(x_24-x_23)/2,

Arel_Pgp25=(1+x_24/Lsi+1+x_25/Lsi)*2*Tot_Pgp/(3*Lsi)*(x_25-x_24)/2,

Arel_Pgp26=(1+x_25/Lsi+1+x_26/Lsi)*2*Tot_Pgp/(3*Lsi)*(x_26-x_25)/2,

Arel_Pgp27=(1+x_26/Lsi+1+x_27/Lsi)*2*Tot_Pgp/(3*Lsi)*(x_27-x_26)/2,

Arel_Pgp28=(1+x_27/Lsi+1+x_28/Lsi)*2*Tot_Pgp/(3*Lsi)*(x_28-x_27)/2,

Arel_Pgp29=(1+x_28/Lsi+1+x_29/Lsi)*2*Tot_Pgp/(3*Lsi)*(x_29-x_28)/2,

Arel_Pgp30=(1+x_29/Lsi+1+x_30/Lsi)*2*Tot_Pgp/(3*Lsi)*(x_30-x_29)/2,

Arel_Pgp31=(1+x_30/Lsi+1+x_31/Lsi)*2*Tot_Pgp/(3*Lsi)*(x_31-x_30)/2,

Arel_Pgp32=(1+x_31/Lsi+1+x_32/Lsi)*2*Tot_Pgp/(3*Lsi)*(x_32-x_31)/2,

Arel_Pgp33=(1+x_32/Lsi+1+x_33/Lsi)*2*Tot_Pgp/(3*Lsi)*(x_33-x_32)/2,

Arel_Pgp34=(1+x_33/Lsi+1+x_34/Lsi)*2*Tot_Pgp/(3*Lsi)*(x_34-x_33)/2,

Arel_Pgp35=(1+x_34/Lsi+1+x_35/Lsi)*2*Tot_Pgp/(3*Lsi)*(x_35-x_34)/2, Arel_Pgp36=(1+x_35/Lsi+1+x_36/Lsi)*2*Tot_Pgp/(3*Lsi)*(x_36-x_35)/2,

Arel_Pgp37=(1+x_36/Lsi+1+x_37/Lsi)*2*Tot_Pgp/(3*Lsi)*(x_37-x_36)/2,

Arel_Pgp38=(1+x_37/Lsi+1+x_38/Lsi)*2*Tot_Pgp/(3*Lsi)*(x_38-x_37)/2,

Arel_Pgp39=(1+x_38/Lsi+1+x_39/Lsi)*2*Tot_Pgp/(3*Lsi)*(x_39-x_38)/2,

Arel_Pgp40=(1+x_39/Lsi+1+x_40/Lsi)*2*Tot_Pgp/(3*Lsi)*(x_40-x_39)/2,

Supplementary Table

Supplemental Table S1 Optimized parameters for intestinal water movement in ATOM

Parameter	Value	Unit
k_{es}	114.41	/h
$k_{water,sto}$	0	/h
$Se_{water,sto}$	88.63	mL/h
$k_{water,abs}$	881.26	/h
$Se_{water,abs}$	1500.00	mL/h

k_{es}: transit rate of drug (or water) from esophagus to stomach, $k_{water,sto}$: water absorption rate in stomach, $Se_{water,sto}$: water secretion clearance in stomach, $k_{water,abs}$: water absorption rate in lumen, $Se_{water,abs}$: water secretion clearance in lumen

Supplemental Table S2 Optimized parameters for transit rate from stomach to intestine, dispersion constants and intestinal flow rates using ^{99m}Tc-DTPA distribution in the lumen in ATOM

Subject and fasted/fed	k_{sto} (h^{-1})	D_z (h^{-1})		M_t (h^{-1})			
		A	B	C	D	t_{lag}	E
Subject A fasted	4.27	816.59	0.082	11.34	0[a]	-	1[a]
Subject B fasted	5.23	584.19	0.044	15.00	0.92	1.05	1.01
Subject A fed	1.29	524.22	0.028	16.90	0.98	2.35	3.43
Subject B fed	0.89	201.76	0.031	12.50	0.91	2.12	1.82

These parameters were obtained by fitting analysis using ^{99m}Tc-DTPA distribution in the lumen reported by Haruta et al. .

a: Constant flow rate (D=0 and E=1) was adopted because AIC values were similar with the simulated results by ATOM using time-dependent flow rate.

k_{sto}: transit rate of drug or water from stomach to intestine, D_z: location-dependent dispersion number, M_t: time-dependent intestinal flow rate

Supplemental Table S3 Reported and optimized transit times in CAT using ^{99m}Tc-DTPA distribution in the lumen in both fasted and fed state.

Parameters	Value					Unit
	Reported	Optimized				
		Subject A fasted	Subject B fasted	Subject A fed	Subject B fed	
k_{sto}	4.00	4.17	3.45	1.11	0.77	/h
$k_{t,1}$	3.85	3.03	1.33	2.94	62.50	/h
$k_{t,2}$	1.08	3.03	208.33	357.14	2.33	/h
$k_{t,3}$	1.35	3.03	2.86	31.25	14.08	/h
$k_{t,4}$	1.72	0.81	1.64	9.09	0.65	/h
$k_{t,5}$	2.38	0.81	13.16	2.94	0.58	/h
$k_{t,6}$	3.45	0.81	0.68	0.20	58.82	/h

Each transit rate was calculated using the equation, Transit rate = 1/ Transit time. Reported transit times were referred from the report by Heikkinen et al. Optimized transit times were obtained by fitting analysis using observed distribution of ^{99m}Tc-DTPA in the lumen by Haruta et al.

k_{sto}: transit rate of drug or water from stomach to intestine, $k_{t,n}$: transit rate of drug or water from nth compartment in the lumen

Supplemental Table S4 Pharmacokinetic parameters of compounds

Parameter	Value	Unit	Reference and comment
midazolam			
$P_{app,Caco\text{-}2}$	0.117	cm/h	2
pKa	14 (acid), 4.57 (base)	-	ADMET Predictor® ver. 9.5
f_b	0.056	-	2
f_{ent}	0.056	-	Assumed to be equal with f_b
$V_{max,CYP3A}$	0.44	µg /h pmol CYP3A	2
$K_{m,CYP3A,u}$	1.08	µg/mL	2
$K_{p,liver}$	6.96	-	3
R_B	0.55	-	4
CL_{int}	587336	mL/h	5 Optimized using plasma concentration after iv dosing
CL_R	0	mL/h	Assumed to be 0
$V_{central}$	99888	mL	5 Optimized using plasma concentration after iv dosing
k_{12}	0.288	/h	5 Optimized using plasma concentration after iv dosing
k_{21}	0.0042	/h	5 Optimized using plasma concentration after iv dosing

k_{12}^{*}	0.288	/h	Assumed to be same with k_{12}
k_{21}^{*}	0.0042	/h	Assumed to be same with k_{21}
Digoxin			
$P_{app,Caco-2}$	0.00396	cm/h	6
pKa	14(acid), 1(base)	-	ADMET Predictor® ver. 9.5
f_p	0.75	-	Digoxin Elixir, Printed Labeling
f_b	0.697	-	Calculated as $f_b=f_p/R_B$
f_{ent}	0.697	-	Assumed to be equal with f_b
$V_{max,P-gp}$	1.0×10^7	µg /h pmol P-gp	7 Optimized to the range of reported F_A values
$K_{m,Pgp,u}$	57	µg/mL	8
$K_{p,liver}$	1.35	-	GastroPlus® ver. 9.7
R_B	1.08	-	ADMET Predictor® ver. 9.0
CL_{int}^{a}	4793	mL/h	9
$CL_{R,Pgp}$	4080	mL/h	10 Assumed from the CL_R change in P-gp inhibitor administration
$CL_{R,nonPgp}$	7560	mL/h	10 Assumed from the CL_R change in P-gp inhibitor administration
$V_{central}$	11800	mL	10

k_{12}	2	/h	10 Optimized using plasma concentration of digoxin in iv administration
k_{21}	0.029	/h	10 Optimized using plasma concentration of digoxin in iv administration
k_{13}	2	/h	10 Optimized using plasma concentration of digoxin in iv administration
k_{31}	0.432	/h	10 Optimized using plasma concentration of digoxin in iv administration
k_{12}^*	2	/h	Assumed to be same with k_{12}
k_{21}^*	0.029	/h	Assumed to be same with k_{21}
k_{13}^*	2	/h	Assumed to be same with k_{13}
k_{31}^*	0.432	/h	Assumed to be same with k_{31}
itraconazole			
$P_{app,Caco-2}$	0.0245	cm/h	12
pKa	14(acid), 4.57(base)	-	ADMET Predictor® ver. 9.5
f_b	0.0034	-	Calculated as $f_b=f_p/R_B$
f_p	0.002	-	13

f_{ent}	0.0034	-	Assumed to be equal with f_b
$V_{max,CYP3A}$	0.0114	µg /h pmol CYP3A	13
$K_{m,CYP3A,u}$	0.0313	µg/mL	13
$K_{p,liver}$	6.67	-	14
R_B	0.58	-	14
CL_{int}	14700000	mL/h	14
CL_R	0	mL/h	Assumed to be 0
$V_{central}$	59200	mL	14
$K_{i,CYP3A}$	0.212	µg/mL	35
clarithromycin			
$P_{app,Caco-2}$	0.0138	cm/h	15
pKa	13.1(acid), 8.2(base)	-	16
f_b	0.32	-	16
f_{ent}	0.32	-	Assumed to be equal with f_b
$V_{max,CYP3A}$	0.013	µg /h pmol CYP3A	24
$K_{m,CYP3A,u}$	36.43	µg/mL	17
LogP	2.3	-	18
R_B	0.74	-	16
CL_{int}	68504	mL/h	11 Optimized using plasma concentration of clarithromycin after po administration

CL_R	6000	mL/h	19
$V_{central}$	25193	mL	20 Optimized using plasma concentration of clarithromycin after iv administration
$K_{i,CYP3A}$	4.52	µg/mL	17
$K_{i,Pgp}$	324.61	µg/mL	32
k_{12}	8.91	/h	11 Optimized using plasma concentration of clarithromycin after po administration
k_{21}	2.51	/h	11 Optimized using plasma concentration of clarithromycin after po administration

a: The value was calculated using the number of hepatocytes (1.2×10^8 cells/g liver) and the weight of the liver (25.7 g liver/kg) (Watari et al., 2019)

Supplemental Table S5 Physiological parameters used in ATOM and CAT

Parameter	Value	Unit	Reference
Q_{pro}	18000	mL/h	2
Q_{pv}	37170	mL/h	3
Q_{h}	107100	mL/h	3
Q_{ha}	69930	mL/h	Calculated as $Q_{ha} = Q_{h} - Q_{pv}$
V_{es}	78.5	mL	Assumed a column with 1 cm radius and 25 cm length
V_{sto}	48.92	mL	GastroPlus® ver. 9.7
V_{pv}	70	mL	3
V_{liver}	1687	mL	3
V_{cae}	50.49	mL	GastroPlus® ver. 9.7
V_{col}	53.55	mL	GastroPlus® ver. 9.7
V_{si}	105	mL	31

Q_{pro}: blood flow of the blood capillaries in lamina propria, Q_{pv}: blood flow in the portal vein, Q_{h}: blood flow in the liver, Q_{ha}: arterial blood flow in the liver, V_{sto}: volume in the stomach, V_{pv}: volume in the portal vein, V_{liver}: volume in the liver, V_{cae}: volume in the caecum, V_{col}: volume in the colon, V_{si}: volume in the small intestine

Supplemental Table S6 Dataset for F_G prediction about CYP3A or P-gp/CYP3A substrates and predicted or reported F_G values

Compound	Dose	$K_{m,u}$		V_{max}		$P_{app,caco-2}$	f_b	pKa[a]		F_G		
		CYP3A	P-gp	CYP3A	P-gp			acid	base	ATOM	TLM	Reported
	nmol	μg/mL	μg/mL	μg /h pmol CYP3A	μg /h pmol P-gp	cm/h						
alfentanil	7220	9.51	-	0.542	0	0.105	0.137	-	6.72	0.76	0.72	0.60
alprazolam	1290	81.9	-	0.074	0	0.0918	0.341	-	3.01	0.99	0.99	0.99
buspirone	4150	3.08	-	0.401	0	0.0914	0.062	-	7.16	0.56	0.51	0.22
cisapride	16100	1.49	-	0.245	0	0.108	0.020	11.2	7.30	0.63	0.56	0.55
cyclosporin	474000	1.68	0.0682	0.040	1.66×10^6	0.0286	0.014	-	-	0.99	0.99	0.35

felodipine	26000	2.04	-	2.86	0	0.0151	0.068	10.95	0.51	0.02	0.02	0.53
lovastatin	49400	3.16	-	9.23	0	0.0522	0.030	-	-	0.04	0.04	0.09
midazolam	9200	1.08	-	0.440	0	0.117	0.056	-	4.57	0.39	0.36	0.48
nifedipine	28900	3.81	-	0.502	0	0.0846	0.066	11.06	1.28	0.63	0.60	0.74
nisoldipine	12900	0.815	-	3.75	0	0.072	0.003	11.2	0.68	0.03	0.03	0.11
rifabutin	177000	9.23	-	0.286	0	0.0342	0.483	6.92	8.12	0.94	0.85	0.21
saquinavir	1490000	0.201	0.579	0.731	1.66×10^{6}	0.0497	0.038	10.83	6.40	0.94	0.92	0.18
sildenafil	52600	7.13	-	0.480	0	0.0922	0.063	9.38	7.60	0.78	0.77	0.54
simvasatin	95500	1.42	-	5.95	0	0.0245	0.025	-	-	0.02	0.02	0.19
trazodone	202000	116	-	1.64	0	0.0871	0.070	-	7.15	0.93	0.90	0.83
triazolam	729	29.2	-	0.090	0	0.101	0.161	-	2.85	0.98	0.98	0.45

zolpidem	16300	43.0	-	0.057	0	0.115	0.105	-	4.99	0.99	0.99	0.81

Dataset of each compound, predicted (TLM) and reported F_G values were referred from the previous report by Ando et al.

a: Obtained from ADMET Predictor® version 9.5 (Simulations Plus Inc.)

Supplemental Table S7 Predictive performance of F_G values using ATOM and TLM compared with reported F_G values

Parameters	ATOM	TLM
Within ±0.3 (%)	65	71
AFE	1.06	1.10
RMSE	0.373	0.357

AFE: average fold error, RMSE: root mean square error

AFE and RMSE was calculated using the following equations. Parameter N represents the number of drugs.

$$\mathrm{AFE} = 10^{\Sigma \log(\mathrm{reported}/\mathrm{predicted})/\mathrm{N}}, \quad \mathrm{RMSE} = \sqrt{\frac{\Sigma[(\mathrm{predicted}-\mathrm{reported})^2]}{\mathrm{N}}}$$

Supplemental Table S8 Summary of AUCR ratio and F_G or F_A changes of digoxin and midazolam during DIs

midazolam[a]

Perpetrator	AUCR ratio (predicted AUCR / reported AUCR)	F_G changes ($F_{G,p}/F_{G,control}$)
50 mg itraconazole	1.19	2.15
200 mg itraconazole	0.63	2.50
400 mg itraconazole	0.58	2.58

digoxin[b]

Perpetrator	AUCR ratio (predicted AUCR / reported AUCR)	F_A changes ($F_{A,p}/F_{A,control}$)
250 mg clarithromycin	1.64	1.25

AUCR: AUC ratio, $F_{A,p}$: predicted F_A value of the substrate with the perpetrator, $F_{A,control}$: predicted F_A value of the substrate in the control, $F_{G,p}$: predicted F_G value of the substrate with the perpetrator, $F_{G,control}$: predicted F_G value of the substrate in the control

a: AUC_{inf} was used according to the report with the observed values by Templeton et al. (2010).

b: $AUC_{0\text{-}24}$ was used according to the report with the observed values by Rengelshausen et al. (2003).

Supplementary Figures

Supplemental Fig. 1

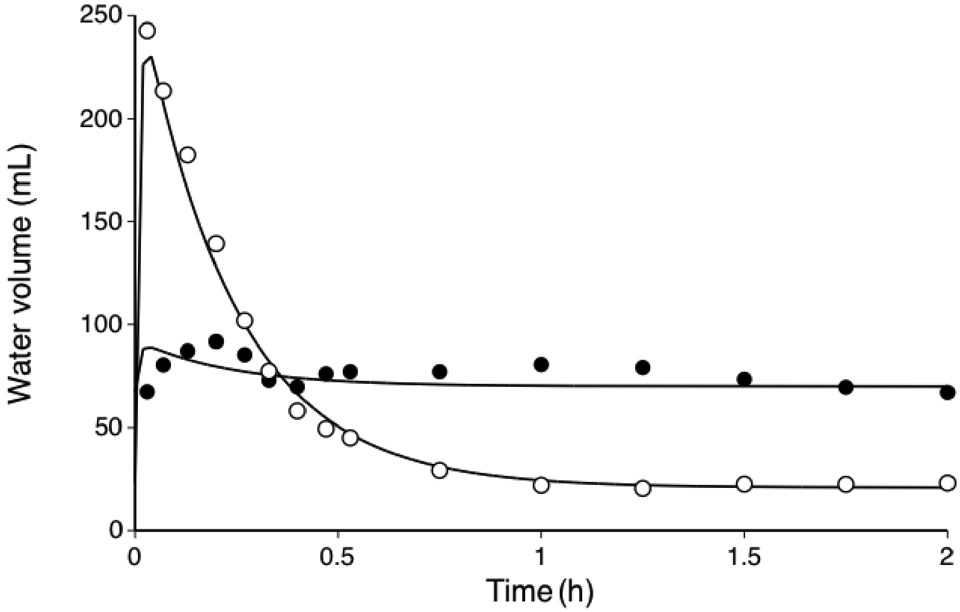

Supplemental Fig. 2

(A)

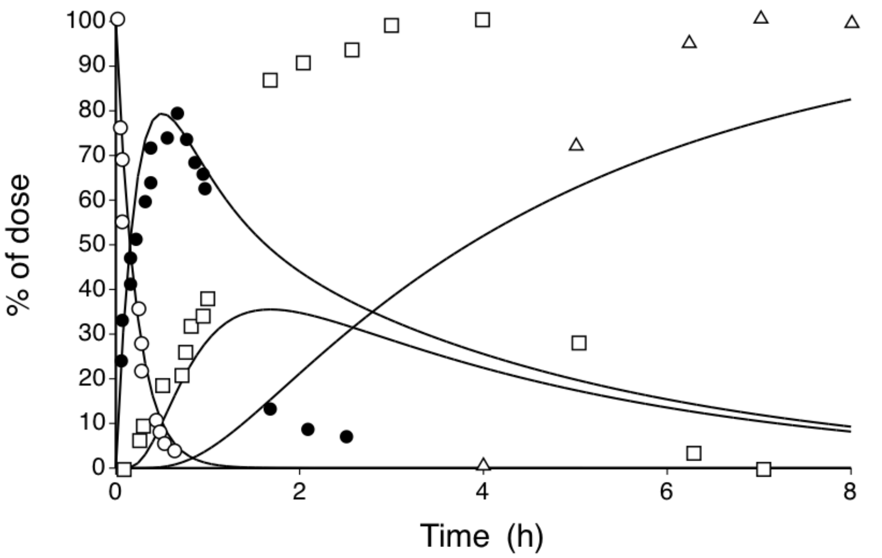

(B)

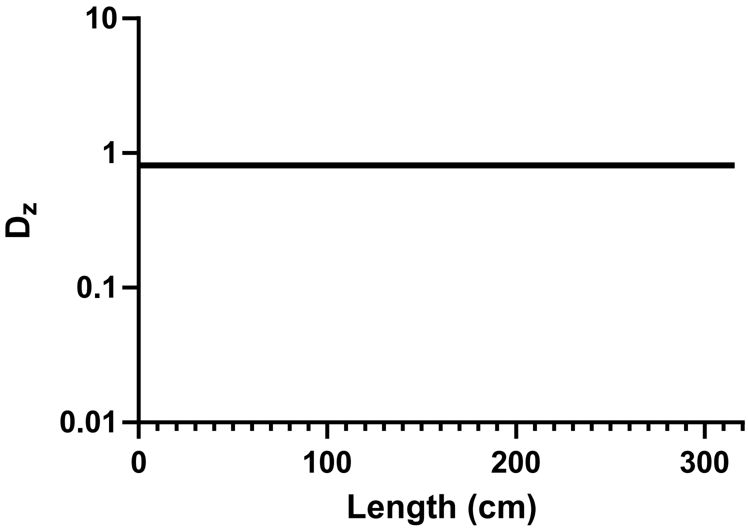

Supplemental Fig. 3

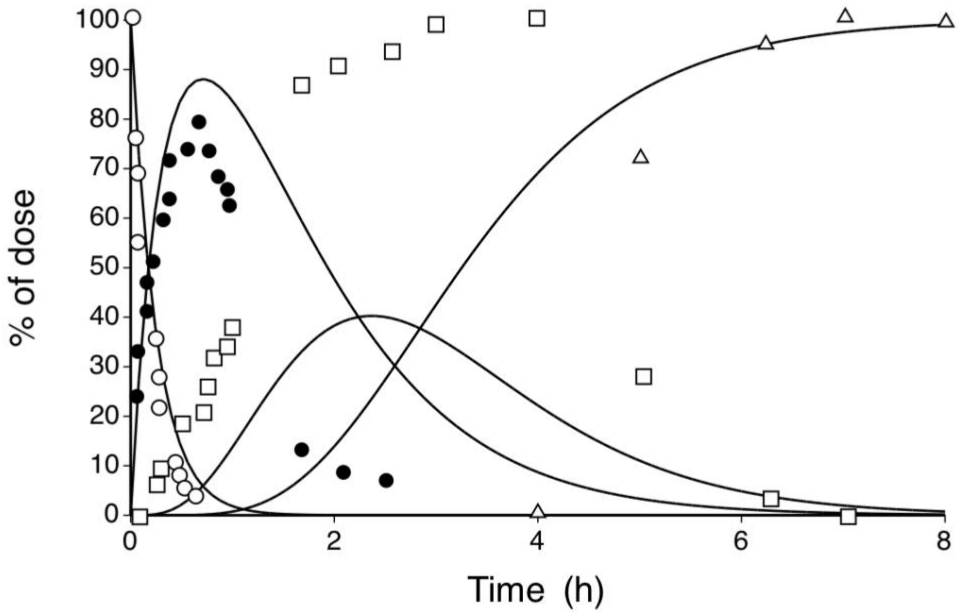

Supplemental Fig. 4

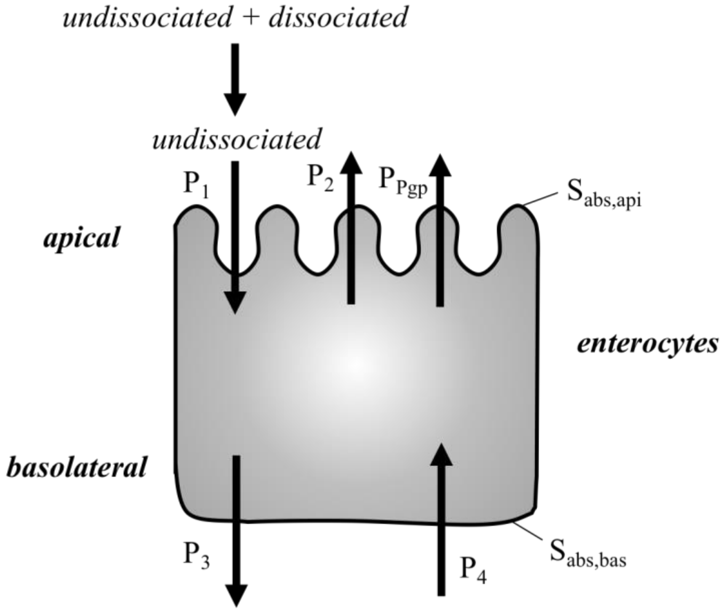

Supplemental Fig. 5

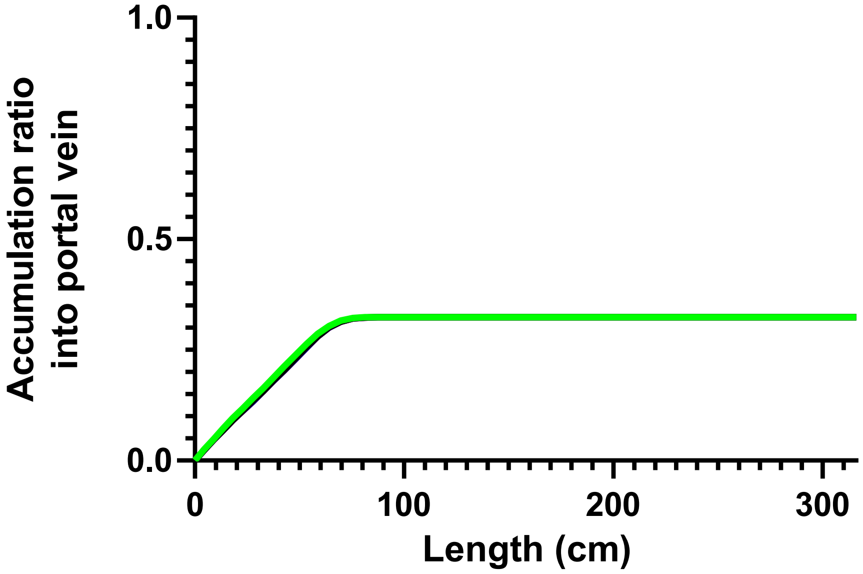

Supplemental Fig. 6

(A)

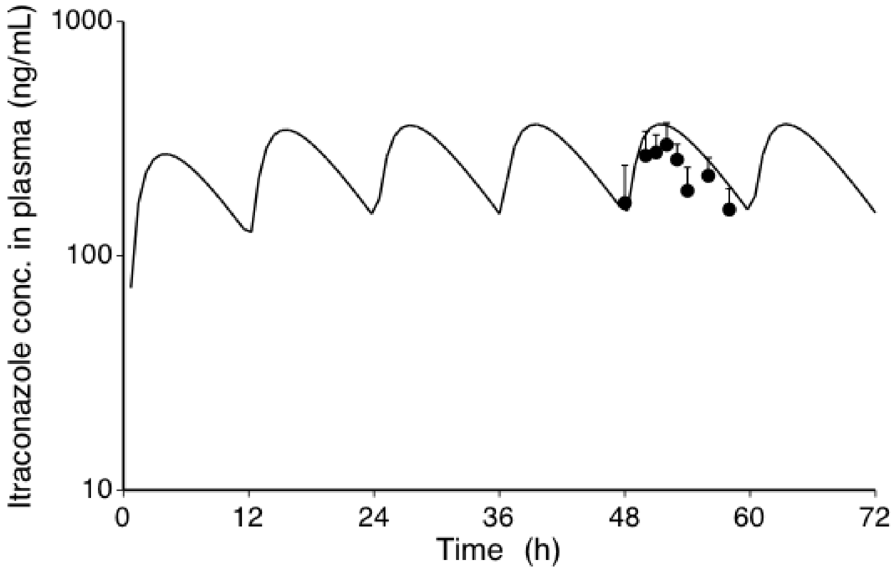

(B)